rt No. FHWA-RD-74-61

ELOPMENT OF PROCEDURES FOR RACTERIZATION OF UNTREATED GRANULAR E COURSE AND ASPHALT-TREATED E COURSE MATERIALS

W.S. Smith and K. Nair

October 1973

Final Report

Prepared for
FEDERAL HIGHWAY ADMINISTRATION
Offices of Research & Development
Washington, D.C. 20590

NOTICE

Technical Report Documentation Page

1. Report No.	2. Government Accession No.	3. Recipient's Catalog No.
FHWA-RD-74-61		

4. Title and Subtitle	5. Report Date
DEVELOPMENT OF PROCEDURES FOR CHARACTERIZATION OF UNTREATED GRANULAR BASE COURSE AND ASPHALT-TREATED BASE COURSE MATERIALS	October 1973
	6. Performing Organization Code
	8. Performing Orgonization Report No.

7. Author(s)	
W. S. Smith, and K. Nair	

9. Performing Organization Name and Address	10. Work Unit No. (TRAIS)
Materials Research & Development, Inc. A Division of Woodward-Lundgren & Associates 2730 Adeline Street Oakland, California 94607	11. Contract or Grant No. DOT-FH-7785
	13. Type of Report and Period Covered June 1971 - Sept. 1974 Final Report
12. Sponsoring Agency Name and Address U.S. Department of Transportation Federal Highway Administration, 400 - 7th Street, S.W. Washington, D.C. 20590	14. Sponsoring Agency Code

15. Supplementary Notes

FHWA Contract Manager - William J. Kenis

16. Abstract

The report describes a study on the characterization of untreated granular base course and asphalt-treated base course materials. The applicability of elastic and linear viscoelastic characterization have been evaluated.

A review of previous information and an experimental program which consisted of dynamic and creep triaxial tests at a variety of temperatures and stress states was conducted and the results analyzed.

A sensitivity study using a linear elastic model, together with a fatigue mode of failure, was conducted to evaluate the significance of material characterization relative to other factors as they influence pavement performance.

17. Key Words	18. Distribution Statement
pavements, materials characterization, paving materials, testing materials	No restrictions. This document is available to the public through the National Technical Information Service, Springfield, Virginia 22151.

19. Security Classif. (of this report)	20. Security Classif. (of this page)	21. No. of Pages	22. Price
Unclassified	Unclassified	204	

Form DOT F 1700.7 (8-72) Reproduction of completed page authorized

FORM FHWA-121A (REV. 4-70)
UNITED STATES GOVERNMENT

Memorandum

U.S. DEPARTMENT OF TRANSPORTATION
FEDERAL HIGHWAY ADMINISTRATION

TO : Individual Researchers

DATE: December 5, 1974

In reply refer to: HRS-14

FROM : William J. Kenis
Project Manager, FCP Project 5C
New Methodology for Flexible Pavement Design

SUBJECT. Transmittal of Research Report No. FHWA-RD-74-61, "Development of Procedures for Characterization of Untreated Granular Base Course and Asphalt Treated Base Course Materials," Contract FH-11-7785

Distributed with this memorandum is the subject report intended primarily for research audiences. This report will be of interest to highway engineers concerned with the many aspects of material characterization for rational pavement design and analysis.

This report describes a study on the characterization of untreated granular base course and asphalt treated base course materials. The applicability of elastic and linear viscoelastic characterizations have been evaluated.

A review of previous information and an experimental program which consisted of dynamic and creep triaxial tests at a variety of temperatures and stresses was conducted and the results analyzed.

A sensitivity study using a linear elastic model, together with a fatigue mode of failure, was conducted to evaluate the significance of material characterization relative to other factors as they influence pavement performance.

One copy each of the report is being sent to the Region and Division offices for the individual Planning and Research Engineer (Field Project Adviser) and Field Technical Coordinator. In addition, an extra copy is being provided each Division office to be forwarded to the responsible flexible pavement research engineer in the State.

Additional copies are available from the National Technical Information Service (NTIS), Department of Commerce, 5285 Port Royal Road, Springfield, Virginia 22151. A small charge is imposed for copies provided by NTIS.

Attachment

ACKNOWLEDGMENT

The authors wish to acknowledge the cooperation and assistance received from the Federal Highway Administration; specifically, Messrs. W. A. Kenis and T. F. McMahon in the conduct of this study.

Assistance in computer analysis was provided by Dr. C-Y Chang and Mr. A. M. Abdullah. The laboratory testing was done under the supervision of Mr. J. H. Wilson, Supervisor of Woodward-Lundgren & Associates' laboratories.

During the course of this and previous work on materials characterization, the authors have benefited greatly from discussions with Professors Carl L. Monismith and Karl S. Pister of the University of California at Berkeley, Professor F. Moavenzadeh of MIT, and Mr. Fred N. Finn of our staff.

Ms. Lydia M. Buckley was responsible for preparing the report and the drafting department of Woodward-Lundgren & Associates under Mr. Carlos Escalante prepared the figures.

TABLE OF CONTENTS

Page

DEVELOPMENT OF PROCEDURES FOR CHARACTERIZATION OF UNTREATED GRANULAR BASE COURSE AND ASPHALT-TREATED BASE COURSE MATERIALS

SUMMARY

During the course of the last four years, Materials Research & Development has conducted research in materials characterization for the Federal Highway Administration. A previous study (FH-11-7319) attempted to determine the applicability of elasticity and viscoelasticity to characterize asphalt concrete and cement-treated base course materials. The study presented in this report deals with untreated and asphalt-treated base course materials. It was considered appropriate for this report to prepare a brief summary of the significant results obtained in both these studies. Some general concepts of material characterization are presented. The major significant response characteristics for each material are identified and both ideal and practical constitutive relationships and failure criteria are presented. Future research needs in materials characterization are discussed.

CONCEPTS IN MATERIAL CHARACTERIZATION

The rational pavement design and analysis techniques developed in recent years are based on the determination of primary response variables (stress, strain, and deflection) of pavements through the formulation and solution of boundary value problems. In formulating boundary value representations of pavements it is necessary to describe, in mathematical form, the behavior of various materials comprising the pavement system. This description is in

the form of constitutive equations which describe the stress-strain relationships of the materials. In the design or analysis process, solving a boundary value problem to determine the primary pavement response is not sufficient in itself. It is also necessary to conduct a damage analysis to evaluate the predicted primary responses in terms of possible pavement distress. To perform this evaluation, it is necessary to establish limiting (failure) criteria in terms of the primary responses for the appropriate loading and environmental conditions. The term materials characterization as used in this report is defined as the selection of constitutive equations and failure criteria (limiting response) for a material.

The ability to solve boundary value problems and conduct damage analyses imposes limitations on the generality of the models that can be used. No model of ideal material behavior can accurately represent all aspects of the response of a real paving material. The selection of models that retain the significant features of material response and are within the bounds of practicality is the art of mathematical modelling. This requires an understanding of the constitutive equations and failure theories and the nature of the physical phenomena that is being modelled. It is the blending of theory and physical reality that is the key to the development of the necessary material characterizations for utilization in improved methods for the structural design of pavements.

It is important to recognize that it will not be possible, on the basis of experimental results, to obtain exact functional relations for a real paving material. The

adequacy of a particular model depends on the problem under study and the overall system in which it will be used. Different components of the same problem may require the material to be characterized differently according to which aspect of material response is important in solving that particular component of the problem.

Materials characterizations is a dynamic (changing) process. As our ability to define input parameters improves and better models of the overall pavement system are developed, material characterizations which are now considered adequate will have to be re-evaluated.

CHARACTERIZATION OF ASPHALT CONCRETE AND ASPHALT-TREATED BASE COURSES

Constitutive Equations

The response of these materials under a variety of loading and environmental conditions representative of in-service pavement conditions has been found to be dependent on time (e.g., duration of load), temperature, and stress state. For asphalt-treated (liquid asphalts and emulsions) base courses, the response is also a function of curing time. The discussion to follow deals with the properties of ATB after the ultimate cure condition has been reached.

Based on the evidence, a viscoelastic characterization provides the means of accommodating most of the aspects of material response. From a practical standpoint, only linear viscoelastic characterization can be considered to be implementable. The majority of currently available computational techniques for determining the mechanical state in a pavement system and the corresponding failure

criteria utilize a linear elastic characterization. Therefore, the validity of a linear elastic and linear viscoelastic characterization is discussed.

Tests indicate that a significant degree of anisotropy exists in the laboratory specimens as a result of sample preparation procedures. Whether this condition exists in the field has not been verified. Furthermore, available solution techniques for boundary value problems for the viscoelastic case can only consider isotropic materials. Therefore, only the isotropic case has been considered.

Linear Elastic Characterization

An isotropic linear elastic material is completely defined by two material constants, the modulus of elasticity (E) and Poisson's Ratio (ν).

A linear elastic characterization is appropriate if (i) the response that controls the performance of a pavement is the elastic deformation occurring under a single load application of short duration, (ii) the elastic properties are determined over a range of temperatures and stress states representative of in-service conditions, and (iii) the values used in the analysis represent the designer's determination (usually an iterative process) of the design temperature, time of loading, and stress state likely to exist in the pavement.

It should be emphasized that an elastic characterization does not permit the direct determination of permanent deformation. In order to do this, it would be necessary to develop an empirical relationship between the elastic

deformation and the permanent deformation that occurs under repeated load applications.

The recommended procedure for determining the elastic parameters is a repeated load triaxial test. Considering the nature of the applied stresses in the field, a procedure which cycles both radial and axial stresses is recommended. It is recognized that the apparatus to perform such tests may not be available at most state agencies who have the responsibility for the structural design of pavements. In such cases, the conventional M_R (modulus of resilience) test in which the radial stress is held constant and the axial stress cycled may be used. At the present time, it is recommended that the ratio of the repeated axial stress to the resilient axial strain be used to define the elastic modulus. Poisson's ratio may be computed on the basis of the ratio of measured values of the resilient axial and radial strain.

Linear Viscoelastic Characterization

An isotropic linear viscoelastic material can be completely defined by two functions which are in general time dependent. *If it is assumed that permanent deformation and time-dependent effects are the significant factors in determining the response of a pavement, then linear viscoelasticity should be utilized to characterize asphalt concrete and asphalt-treated base courses. It is important to recognize that both the shear and bulk properties have been found to be time dependent. Temperature effects can be accounted for by treating the material as thermorheologically simple.*

Since nonlinear effects are present, the characterization should cover a range of stress states representative of in-service conditions and the viscoelastic functions utilized

would depend on the designer's choice of the design stress states. However, because of anisotropic effects due to sample preparation techniques, it was not possible to develop a consistent relationship to predict the influence of stress levels under multiaxial stress states. Hence, the master compliance curves had to be constructed from uniaxial data. Therefore, until the question of whether anisotropic effects actually exist in the field is resolved, the utilization of uniaxial data with strains maintained below maximum field levels should be utilized. It should be noted that under a linear isotropic viscoelastic assumption all the necessary information could be obtained from unconfined tests (e.g., creep or sinusoidal loading).

Failure Criteria

Two categories of pavement failure were considered: (i) fatigue failure and (ii) permanent deformation.

Fatigue criteria are expressed in terms of the number of cycles to failure of the repeated application of a level of strain. This strain is the recoverable strain under a single load application. The relationship is determined from tests on simply supported beams under repeated load applications. There is some question as to whether the laboratory mode of testing (i.e., a simply supported beam) is representative of field conditions. The current techniques use a linear accumulation of damage and assume elastic behavior. Time-dependent behavior, rest periods, healing, and the sequence of loading are some of the factors that are not satisfactorily accounted for at the present time.

The accumulated permanent deformation can be calculated in a pavement if the material is treated as linear viscoelastic. However, the linear viscoelastic models that have been used to date have not been able to predict realistic values of permanent deformation. Alternatively, an empirical relationship would have to be developed to determine permanent deformation.

CHARACTERIZATION OF CEMENT-TREATED GRANULAR BASE COURSE MATERIALS

A linear elastic isotropic characterization is adequate for cement-treated granular base course materials.

It is recommended that the ratio of axial stress to resilient axial strain determined from an unconfined repeated load test be utilized to determine the elastic modulus. Poisson's ratio can be determined using the ratio of resilient radial to axial strain measurements.

Failure criteria for cement-treated base course materials were not evaluated in this study.

CHARACTERIZATION OF UNTREATED GRANULAR BASE COURSE MATERIALS

Constitutive Equations

It has been shown that the response of untreated granular base course material is dependent on the stress state but independent of time. A nonlinear elastic representation is, therefore, appropriate. A theoretically rigorous nonlinear formulation requires testing procedures and boundary value problem solution techniques which are not currently

implementable. *Therefore, an 'ad hoc' nonlinear formulation where a 'modulus' is computed as a function of the sum of the principal stresses is recommended.* This has to be combined with an iteration procedure for solving linear elastic problems. Poisson's ratio can be treated as constant. It is recommended that a confined resilient modulus test be utilized to determine the material properties. The degree of saturation influences the modulus. The modulus decreases with an increase in the degree of saturation. The same 'ad hoc' nonlinear modulus relationship can be used if effective stresses are utilized to determine the modulus.

Failure Criteria

For pavements designed by procedures considered acceptable in agencies responsible for the design of flexible pavements it has been shown that fatigue failure will not occur in the granular base course material. However, permanent deformation can occur which can result in unsatisfactory pavement performance. To date no satisfactory analytical method for predicting permanent deformation has been found. Empirical correlations based on laboratory and field data should be developed.

FURTHER RESEARCH IN MATERIALS CHARACTERIZATION

Asphalt Concrete and Asphalt-Treated Base Course Materials

Neither elasticity nor linear viscoelasticity can accurately model all the response characteristics of asphalt concrete or ATB. However, materials characterization for paving materials has reached a level of sophistication where further improvements would require significant investments in time and funds. For example, utilizing a nonlinear as

opposed to a linear characterization would require developmental work in testing techniques and methods of stress analysis. Furthermore, the overall pavement structural design sybsystem has not developed to a point which can take full advantage of a linear viscoelastic characterization. For example, failure theories used in pavement design do not consider the viscoelastic nature of the material to include the influence of rest periods and the rate and duration of loading.

It is recommended that:

a) Additional analytical and experimental work be conducted to develop failure theories for use in the structural design of asphalt concrete pavements for predicting fracture and permanent deformation under repeated loads which consider the viscoelastic character of asphalt concrete and ATB.

b) The degree of anisotropy that is present in asphalt concrete and ATB in the field be determined. Based on this information, sample preparation techniques should be evaluated.

c) If anisotropy is present in the field and sensitivity studies indicate that the degree of anisotropy is significant, available data should be re-evaluated and, where necessary, suitable testing techniques to quantify these effects should be developed. Solution techniques for representative boundary value problems which include these material characteristics should also be developed.

d) Because of possible errors in measuring strain using bonded strain gages which result from local reinforcement due to the bonding agent, it is recommended that bonding agents be evaluated. Because of the time involved in strain gage instrumentation and the doubtful accuracy of bonded strain gages, it is also recommended that improved techniques for measuring material response be developed.

Untreated Granular Base Course Materials

Further work (analytical and experimental) should be done to develop methods of predicting permanent deformation in untreated granular materials and in evaluating the effects of saturation on the modulus to be used in the analysis of pavements.

Sensitivity Analyses

Sensitivity analyses should continue to be conducted utilizing various models for representing the pavement system to determine the accuracy required in the characterization of various materials comprising the pavement system.

INTRODUCTION

This is the second study that Materials Research & Development has undertaken under the sponsorship of the Federal Highway Administration on the subject of materials characterization. The previous study (Contract FH-11-7319) dealt with characterization of asphalt concrete and cement-treated granular base course material. The study reported herein deals with the characterization of untreated granular base course and asphalt-treated base course materials.

The philosophy and approach to materials characterization has been explained in detail in Nair and Chang (1973) NCHRP Report No. 140 and in MR&D (1972). In conducting the present study considerable effort was spent in reviewing available information as a basis for formulating an experimental program. Our previous experience had shown that conducting similar test programs to those already reported in the literature did not provide any substantive new data. The necessity of conducting sensitivity analyses to determine the value of more refined characterization procedures had been established also.

Materials characterization is an essential step in the analysis and design of pavements; it should be treated as an adaptive process in which the ability to define other components of the total pavement system and implementation procedures should be considered in determining the adequacy of the material characterizations. It is under this philosophy of considering the past experience, the practical needs of the design engineer, and the available tools for implementation that the materials characterization studies presented in this report have been conducted.

OBJECTIVES AND SCOPE

The primary objectives of this investigation were: (i) to evaluate the applicability of elastic and viscoelastic constitutive relationships for untreated and asphalt-treated granular base course material, and (ii) to define failure properties for untreated and asphalt-treated granular base course material.

These objectives were accomplished by conducting a critical review of the existing information and laboratory experimental program on both the untreated granular base course and the asphalt-treated granular base course materials.

In order to assist in developing the experimental program and evaluating future needs in materials characterization, a sensitivity analysis was conducted to determine the relative effect of a selected number of variables on predicted pavement performance. The results of the sensitivity anlaysis are presented in Appendix A.

CHARACTERIZATION OF UNTREATED GRANULAR BASE COURSE MATERIAL

Previous studies contributing to the development of a rational design procedure for flexible highway pavements have led to the formulation of both elastic and viscoelastic boundary value representations of pavements. Necessary inputs to these rational representations of highway pavements are material properties. Therefore, the emphasis of this literature survey was on both elastic and viscoelastic material characterizations of untreated granular base course materials.

The study was restricted to material characterizations developed from a continuum mechanics viewpoint. Particulate mechanics approaches which attempt to relate interparticle forces were not considered. Furthermore, only material characterizations developed from conditions representative of in-service untreated granular base course material in highway pavements were reviewed.

This study was not intended to delve into the effects of numerous types of aggregates, gradations, or compaction techniques on the material characterization. While these factors will affect materials characterization, the primary purpose of this study was to establish the time dependency, degree of linearity, and effect of partial saturation on the properties of typical untreated granular base course material.

SUMMARY OF PREVIOUS INFORMATION

CONSTITUTIVE RELATIONSHIPS

Both elastic and viscoelastic constitutive relationships have been considered for untreated granular base course material. One of the critical tests used to evaluate the applicability of each is the degree to which material behavior is dependent on the duration (time) of load application. An elastic material has no time-dependent behavior; that is, once a load has been applied, the resulting material deformations are instantaneous and remain constant for the duration of the load application. On the other hand, a viscoelastic material will have both instantaneous and time-dependent response. Therefore, material behavior which is dependent on the duration of load application suggests a viscoelastic representation.

Time Dependency

Hicks (1970) has studied the effect of load duration on saturated untreated granular base course material using repeated load triaxial tests. Repeated deviator stress durations of 0.1, 0.15, and 0.25 seconds applied at a frequency of 20 cycles per minute were investigated. The test results showed no significant difference in resilient (elastic) modulus, Poisson's ratio, or transient pore water pressures for the load durations investigated.

Creep test results on untreated granular base and subbase material used at the AASHO Road Test have been reported by Coffman, et. al. (1964). Both axial and radial stress step loads were simultaneously applied with magnitudes of approximately 37 and 12 psi, respectively; (both of these magnitudes are somewhat higher than those expected for

most highways). Unfortunately, the actual creep test results were not reported. The test results were transformed from the time domain to the frequency domain using linear viscoelastic theory. From the transformed results, it was concluded that the material response was essentially elastic (not time dependent) for frequencies about 10 radians per second (frequency in the transformed domain is analogous to load duration in the time domain). Similar results were reported by Coffman (1967) for a different subbase material.

It appears that for load durations and stress states representative of those experienced by typical in-service untreated granular base course material, time-dependent effects during each load application are not significant. Thus, a constitutive representation of untreated granular base course by elastic theory should adequately reflect the primary response behavior under each application of load.

Elastic Constitutive Relationships

Most elastic constitutive characterizations of untreated granular base course materials to date (1973) have assumed isotropic material behavior. Therefore, the elastic modulus and Poisson's ratio completely define the material.

The test that has found widest application for determination of the properties of untreated granular materials is the repeated load axial test. A conventional triaxial cell is usually used to apply a sustained all-around confining pressure; then repeated axial (deviator) compressive stress pulses are applied. Measurement of the resulting

axial and radial strains allows definition of the resilient modulus, M_r, and resilient Poisson's ratio, ν_r.

The resilient modulus, M_r, is defined by

$$M_r = \frac{\Delta\sigma_d}{\Delta\varepsilon_{zz}}$$

where

$\Delta\sigma_d$ = repeated deviator stress

$\Delta\varepsilon_{zz}$ = recoverable or resilient axial strain

and the resilient Poisson's ratio, ν_r, is given by

$$\nu_r = - \frac{\Delta\varepsilon_{rr}}{\Delta\varepsilon_{zz}}$$

where

$\Delta\varepsilon_{rr}$ = resilient radial strain.

The resilient modulus and resilient Poisson's ratio are equivalent to the modulus of elasticity and Poisson's ratio for an elastic material. For a given untreated granular base course material, the value of modulus and Poisson's ratio may depend on the stress level to which it is subjected and its degree of saturation.

Stress Level Effects

The effects of stress level on the modulus and Poisson's ratio determine the degree of linearity of material response. If the material properties are dependent on the level of stress, the material is said to be nonlinear. It

has been found that the response of granular materials is significantly nonlinear.

Dunlap (1963), Mitry (1964), Seed, et. al. (1967), Shifley (1967), Kallas and Riley (1967), Brown and Pell (1967), Kasianchuk (1968), Hicks and Finn (1970), Hicks (1970), and Barksdale (1972a) have all reported a significant increase in resilient modulus for untreated granular base course material with an increase in confining pressure. Thus, the nonlinear influence of confining pressure is well documented. Smaller increases in resilient modulus are associated with increases in applied deviator stress at a constant confining pressure. The increase in resilient modulus with increase in confining pressure and to a lesser degree with deviator stress has often been approximated by:

$$M_r = K_1 \theta^{K_2}$$

where

M_r = Resilient modulus

K_1 and K_2 = Regression constants

$\theta = \sigma_1 + \sigma_2 + \sigma_3$

The above equation represents a linear relationship between M_r and θ on a log-log plot. Care must be exercised that the experimental stress states utilized to develop the relationship are representative of field stress states.

Stress analyses of flexible pavement systems have shown that small tensile stresses can be present in the untreated granular base course material layer. However, it is not possible to test untreated granular material in a triaxial

cell under applied tensile stresses. It is generally agreed that the behavior of untreated granular materials in tension is much different from that in compression. This difference is another manifestation of the nonlinear character of untreated granular material which should be accounted for in a constitutive characterization.

Heukelom and Klomp (1962) have suggested one mechanism for the behavior of granular materials under the small tensile stresses which might develop in a highway pavement. They suggested that the action of such tensile stresses causes local decompaction of the granular base which results in a reduction of modulus. They also suggested that the presence of compressive vertical stress acting perpendicular to any horizontal tensile stress could allow granular material to sustain a small tensile stress without failing due to granular interlock and frictional resistance induced by the vertical compressive stress.

The above mechanism would result in a reduction of modulus in the zone of tensile stress. This nonlinearity has been approximately accounted for by assigning a low modulus to material when θ is less than zero in the previously prescribed equation expressing resilient modulus as a function of θ.

Although much effort has been made to define the resilient modulus of untreated granular materials, comparatively little has been spent on the definition of resilient Poisson's ratio. Perhaps this has resulted from the difficulty in radial strain measurement as compared to axial strain measurements.

Morgan (1966) was one of the few investigators to make direct measurements of both axial and radial deflections on granular materials. These measurements allowed definition of resilient Poisson's ratio of a uniform sand. His results revealed that resilient Poisson's ratio generally varied between 0.2 and 0.4 and found no apparent relationship between resilient Poisson's ratio and confining pressure or deviator stress.

The most extensive evaluation of resilient Poisson's ratio of untreated granular base course materials to date (1973) is that reported by Hicks (1970). He found that Poisson's ratio increased with increasing repeated axial stress and decreasing confining pressure. This nonlinearity of resilient Poisson's ratio was expressed as a third degree polynomial function of the principal stress ratio, σ_1/σ_3.

Nair and Chang (1970 have indicated how an incremental formulation of a nonlinear elastic constitutive law can be utilized to characterize granular materials. The incremental constitutive law requires determination of five incremental coefficients. However, only four of the coefficients can be evaluated using a triaxial cell with independent cyclic load capabilities for both axial and radial stresses. Triaxial cells with only cyclic axial stress capabilities allow evaluation of only two of the five incremental coefficients. Therefore, while direct formulation of the nonlinear characteristics of untreated granular material is appealing from a mechanics point of view, evaluation of the five incremental constants requires true three-dimensional testing equipment. Furthermore, the boundary value solution using the incremental nonlinear elastic constitutive law needs to be developed.

Therefore, for the present it appears that representation of the nonlinear characteristics of untreated granular base

course material by a simple approximation would provide the best method for immediately incorporating the observed nonlinear response in boundary value representation of pavements. The nonlinearity can be incorporated using an iterative solution technique with equivalent linear material properties selected by evaluation of simple expressions of the nonlinear characteristics (i.e., $M_r = K_1\theta^{K_2}$) for each iteration.

Degree of Saturation Effects

The degree of saturation or water content of most untreated granular base course material has generally been found to affect its elastic response characteristics in both the laboratory and the field. It should be noted that for typical gradations and densities of untreated granular base course materials a small change in water content corresponds to a large change in degree of saturation (i.e., $\Delta\omega/c = 1\%$, $\Delta S = 13\%$).

Haynes and Yoder (1963) performed repeated load triaxial tests on both gravel and crushed stone base course material. It was found that the resilient modulus of the gravel at a degree of saturation of 97% was about one-half of value at a degree of saturation of 70%. The decrease in modulus with increase in degree of saturation appeared to be approximately linear. However, both stresses utilized for all testing ($\sigma_3 = 15$ psi, $\Delta\sigma_d = 70$ psi) are higher than those expected in typical highway pavements.

Kallas and Riley (1967), Shifley (1967), and Hicks and Finn (1970) have reported a linear decrease in the regression constant K_1 of the expression

$$M_r = K_1 \theta^{K_2}$$

with increase in degree of saturation when test results are analyzed on a total stress basis. The regression constant K_2 remained approximately constant with changes in degree of saturation. Thus, the slope of the M_r vs θ relationship remained unchanged with change in degree of saturations; however, the resilient modulus at given value of θ decreased with increase in degree of saturation.

From laboratory testing Hicks (1970) concluded that resilient modulus of untreated granular material decreases with increase in degree of saturation if test results were analyzed on the basis of total stress but remains approximately unchanged if analyzed on the basis of effective stress. He also analyzed the effect of degree of saturation on the resilient Poisson's ratio. It was concluded that Poisson's ratio decreased with increase in degree of saturation based on both total and effective stress analysis of the test data.

Seed, et. al. (1967) subjected a prototype pavement to repeated loading using circular loading plates. Their results indicated that when the granular base course was saturated, the resilient deformation within the base course layer increased by approximately 50%. From laboratory testing, it was reported that the resilient modulus of granular base course remained unchanged with changes in degree of saturation if the results were analyzed on the basis of effective stress.

It should be noted that the resilient material properties applicable to analysis of pavements in existing boundary

value representations are those determined based on total stresses. Therefore, it would appear that both modulus and Poisson's ratio are reduced to some degree as the saturation of the untreated base course layer increases.

FAILURE CRITERIA

Failure criteria for untreated granular base course material can arise from failure of base course material itself or failure of the pavement structure due to the base course properties, but without failure in the base course material. Because of the complexity of a general all-encompassing failure criteria, specific failure criteria are normally developed for individual failure mechanisms.

Failure in Base Course

For the purposes of this discussion, failure in the base course material is considered in the classical sense of rupture or yield. Failure theories currently in use for estimating the potential of failure in granular material have been based almost exclusively on variations of the Mohr Coloumb theory which implies a shear failure. Field evidence indicates that this mode of failure does not normally occur in well-designed highway pavements because induced stresses are well below their failure levels. If failure of field pavements did occur in this mode, it could be thought of as a bearing capacity type of failure. McLeod (1953) presented a method by which the ultimate bearing capacity of a logarithmic spiral shear surface entirely within the base course and surface layer could be approximated. However, the magnitude of the safety factor existing for this mode of failure for highway pavements designed by standard techniques was not determined.

It should be recognized that very little information currently exists concerning the Mohr Coloumb strength parameters for stress levels typical of highway base course materials. Ponce and Bell (1971) have reported that for sand at confining pressures below 5 psi, the use of the Mohr Coloumb theory led to the determination of an apparent cohesion intercept ranging from 0.14 to 0.22 psi. The angle of shearing resistance was not influenced significantly by the normal pressure at these low ranges. These findings are somewhat at variance with those obtained under higher pressures, pointing out the necessity of considering realistic stress levels.

Failure of Pavement Due to Base Course

In addition to those characteristics which control failure in the untreated base course material, it is also necessary to consider the possibility of failure of the pavement system without failure of the base material. This mode of pavement failure is of major concern. Based on theoretical studies and observed pavement performance, there are two properties of untreated granular base course materials which significantly contribute to distress of a pavement system. These are: (i) the elastic constitutive properties, and (ii) the susceptibility to accumulate permanent deformation.

Elastic Constitutive Properties

The elastic constitutive parameters of untreated granular base course materials affect the stress and strain distribution throughout the entire pavement system. Thus, the elastic properties affect the maximum horizontal stress and strain at the base of the asphalt concrete layer, the vertical strain distribution within the asphalt concrete layer, and the vertical strain at the surface of the subgrade.

Since these primary response parameters have been related to pavement failure mechanisms, the constitutive properties of the untreated granular base course materials directly affect failure of the pavement system.

The relationship between the maximum horizontal stress or strain at the base of the asphalt concrete and fatigue failure of asphalt concrete is well established in the literature. Surface distortion of the pavement surface can also lead to pavement failure. Heukelom and Klomp (1967) suggested use of the vertical strain distribution in the asphalt concrete layer calculated from elastic layered theory to estimate the permanent vertical strain occurring within the asphalt concrete layer. Dorman and Metcalf (1965) have suggested a design criteria based on the elastic vertical strain at the surface of the subgrade to minimize excessive permanent deformation at the pavement surface.

Accumulation of Permanent Deformation

Accumulation of permanent deformation within the untreated granular base course layer itself can also contribute to permanent distortion at the pavement surface. While the deformations of base course materials under each application of load representative of in-service stress conditions are essentially recoverable, for large numbers of load applications permanent deformations are observed.

Haynes and Yoder (1963) tested two base course materials used in the AASHO Road Test in repeated loading triaxial tests with a confining pressure of 15 psi and a repeated deviator stress of 70 spi. Both of these stresses are

somewhat higher than those normally experienced by base course materials in highways. The load duration used was 0.28 seconds at a frequency of 40 cpm. For these tests, it was observed that as the number of repeated load cycles increased, the permanent axial deformation continued to increase. The test results were presented in terms of permanent axial deflection but the axial length of the specimens tested was not reported. However, if an 8-inch specimen length is assumed, axial strains as high as 6% were observed after 1000 cycles of load for gravel specimens with high degrees of saturation (i.e., greater than 95%). For a 10-inch gravel layer, this would indicate over 1/2 inch of permanent deformation which could cause failure by surface distortion of a flexible pavement.

It should be noted that the degree of saturation of the test specimen had a very significant influence on the amount of permanent axial deformation occurring after a given number of load cycles. For degrees of saturation above approximately 85%, there was a dramatic increase in the permanent axial deformation at a given number of load cycles. For example, after 1000 cycles of loading the permanent axial deformation of gravel specimens at degrees of saturation of 95% or above was approximately 5 times as large as that for specimens at a degree of saturation of 85%.

Thompson (1969) reported on repeated loading tests in both a 6-inch-diameter mold and a small box model (6" wide by 51" long by 18"deep). Load was applied to the specimens in the mold with a standard 1.96-inch diameter CBR piston and to the boxed specimens with a 4- by 6-inch plate. For both test conditions, it was observed that the permanent

deformation of the AASHO crushed limestone base course material increased when the degree of saturation increased. The results compared well with test results obtained on the test track at the University of Illinois where pavements performed satisfactorily with low degree of saturation base course conditions but rapidly deteriorated when the saturation of the base course layer was increased. These results tended to substantiate the hypothesis by Barber and Steffens (1958) that rapid deterioration of pavements occurs when the degree of saturation of the base course is greater than 80%.

Holubec (1969 studied the accumulation of permanent deformation of base course materials using drained cyclic triaxial tests. Crushed gravel and rock base course materials were subjected to cyclic deviator stresses of approximately 30 psi at a constant confining pressure of approximately 4 psi. The cyclic deviator stress was applied by compressing the specimens until the desired deviator stress level was attained and then the load was released. A complete loading and unloading cycle required approximately 2 seconds for its application. He found that as the water content (degree of saturation) of a given material increased, the permanent axial strain also increased. For the crushed rock base course at 1000 load cycles, approximately 3 times the permanent axial strain was measured when the water content was increased from 3.1% to 5.7%. Similarly, for the crushed gravel, approximately twice as much permanent axial strain was measured for a water content increase from 3.0% to 6.6%. It should also be noted that a similar trend of increasing resilient (recoverable) axial deformations with increase in water content was found. This indicated a relationship between the cyclic permanent deformation and cyclic elastic behavior of the specimens. He also reported

that for a given confining pressure and number of load cycles, as the deviator stress level increased the permanent axial strain increased.

Holubec measured both axial and radial deformations after 1000 load cycles. This allowed separation of the permanent axial deformations into consolidation and lateral deformation components. The consolidation component was taken as that which occurred due to only volume change of the specimen. It was found that as the water content increased, the amount of axial permanent deformation of the specimens due to consolidation decreased. At the highest water contents for crushed rock specimens the volume of the specimens actually increased indicating dilation and corresponding decrease of density. Thus, it appears that at high water contents where the magnitude of permanent axial deformation is the greatest, the mechanism is not one of densification (consolidation) but rather one of geometrical changes due to lateral deformation.

Barksdale (1972a and 1972b) reported on a comprehensive program of drained repeated load triaxial testing of untreated granular base course materials performed to establish their permanent deformation characteristics. All specimens tested were subjected to repeated triangular deviator stress pulses of 0.1 second duration at a frequency of 30 cpm. The specimens were tested for 100,000 load repetitions at constant confining pressures of 3, 4, and 10 psi using deviator stress magnitudes varying from approximately 1 to 6 times the confining pressure. The test results revealed that the permanent axial strain at a given number of load repetitions increased with increase in deviator stress and decreased with increase in confining

pressure. For untreated crushed granular base course material at degrees of saturation of 50%, permanent axial strains of approximately 1% were determined for the higher deviator to confining stress ratios. Furthermore, increasing the degree of saturation from the compacted condition by soaking increased the amount of permanent axial deformation.

Barksdale plotted the permanent axial strain at 100,000 load repetitions as a function of deviator stress for a series of confining pressures to define stress vs. permanent strain curves. He suggested use of a hyperbolic stress-strain curve, analogous to that used by Duncan and Chang (1970) to describe static triaxial tests, to fit the cycled stress vs. permanent strain data. A sufficiently accurate fit to one set of experimental data was demonstrated. If such a stress-permanent strain law could be further verified, the amount of testing required for a given material would be substantially reduced and would allow extrapolation of these results to a wide range of stress conditions.

In summary, it has been demonstrated that untreated granular base course materials can accumulate permanent axial deformations under the action of repetitive loading. The magnitude of this permanent deformation may contribute significantly to surface distortion modes of failure for flexible pavements. It appears that the mechanism for accumulation of permanent deformation cannot be explained by mere densification of the specimens, especially at high degrees of saturation. For a given material and number of load cycles, the amount of permanent deformation increases with increase in deviator stress, decrease in confining pressure, and increase in degree of saturation.

EXPERIMENTAL PROGRAM

The approach taken in this study was to establish the predominant characteristics of untreated granular base course material. A suitable testing procedure and necessary testing equipment were established to define these properties. Similar tests could then be performed on other untreated base course materials to establish their specific properties.

MATERIAL SELECTED FOR TESTING

Throughout the United States, many different untreated materials have been used for highway base course layers. The material properties can be expected to vary accordingly. Even for a given material type, the properties may vary with material gradation and density. However, this study was not intended to delve into the effects of these variations. Rather, a typical untreated granular base course material was selected for testing.

The material selected for testing was a well graded, partially crushed gravel from the Kaiser Quarry in Pleasanton, California. This aggregate is typical of many untreated base course materials used in California and has been studied by previous investigators: Mitry (1964), Seed, et. al. (1967), Shifley (1967), Hicks (1970). The material meets State of California specifications as a 3/4 inch maximum Class 2 aggregate base. The material gradation used was:

Sieve Size	Percent Passing
3/4"	100
1/2"	83
3/8"	68
# 4	45
# 8	36
# 16	28
# 30	19
# 50	11
#100	5
#200	2-3

The minimum and maximum densities for this material have been established using ASTM D2049-64T. This resulted in a minimum dry density of 112.8 pcf and a maximum dry density of 142.5 pcf. The material tested was compacted to a dry density of 139.3 pcf which represents a relative density of 91.2%.

IN-SERVICE STRESS CONDITIONS

Before beginning any characterization testing of the untreated granular base course material, it was necessary to establish stress conditions representative of field conditions. Use of representative stress conditions insures that the material characterization will be applicable to untreated granular base material as typically used in highways. To establish these stress conditions, boundary value representations of a pavement system were formulated and solved on the computer.

The pavement system was modelled as a nonlinear layered elastic system. The conditions selected for analysis

were such that maximum stress conditions within the untreated base course layer could be estimated. Representative stress conditions could then be selected as stress levels at or below the maximum values. The pavement systems analyzed were all flexible pavements surfaced with 4 inches of asphalt concrete.

The AASHO Interim Design Guides, using layer equivalencies established by the Illinois Division of Highways, were used to design seven different structural sections. Three subgrade qualities and two base course qualities were considered. Base course thickness from 6 inches to 26 inches resulted, depending on the quality of materials.

A dual wheel load with 80 psi tire pressure and a 4,500 pound load per wheel was used to analyze each section. The load was applied over two circular areas whose centers were spaced at a distance of four load radii.

The asphalt concrete layer was represented as linearly elastic with an elastic modulus dependent on temperature. Each structural section was analyzed for three asphalt concrete moduli ranging from 100 to 1,500 ksi, representative of temperature environments, ranging from 95°F to 55°F. The moduli values used were representative of load durations of approximately 0.1 second. A Poisson's ratio of 0.4 was used for all cases.

The three subgrade qualities were represented by linear elastic modulu of 1,500, 4,500, and 13,500 psi. Poisson's ratio was fixed at 0.5 for all cases.

The untreated granular base course layer was characterized as nonlinearly elastic. Previous work on untreated granular base course characterizations was examined to establish a realistic range of material properties. The modulus was represented as a function of the sum of principal stresses, θ in the firm:

$$M_r = K_1 \theta^{K_2}$$

All experimental data examined could be bounded by the two extremes: $K_1 = 2{,}000$, $K_2 = 0.6$; and $K_1 = 5{,}000$, $K_2 = 0.6$. Therefore, both modular representations were analyzed for all seven structural sections. Poisson's ratio was assumed to be 0.3.

All together 52 boundary value solutions were performed to establish representative stress conditions for the untreated granular base course layer. Both the maximum vertical and horizontal stress conditions at the top, middle, and bottom of the base course layer were examined. Analysis of these results revealed that the vertical stress seldom exceeded 15 psi compression. Vertical stresses greater than 15 psi occurred only at the top of the base course layer for the high temperature environment. For the majority of the cases analyzed, the base course layers felt less than 5 psi vertical compressive stress at the middle or bottom of the layer.

The horizontal stresses were always less than 5 psi compression. Compressive horizontal stresses of 2 psi or less were typical values at the top of the base course layer. In most of the cases analyzed, horizontal tensile

stresses less than 2 psi existed at the middle and bottom of the base course layer.

In summary, it appears that the horizontal stress in the base course layer seldom exceeds 5 psi compression. The maximum vertical stress can be taken as 20 psi for all practical purposes. These maximum stress conditions, representative of field pavements, were utilized in the formulation of characterization testing program.

EQUIPMENT AND PROCEDURES

A specially designed triaxial cell was used for all testing of untreated granular base course material. A detailed description of this equipment has been given in previous reports, Nair and Chang (1970) and MR&D (1972). Therefore, only the essential features applicable to base course testing are described here.

A triaxial cell can test cylindrical specimens 4 inches in diameter by 8 inches in height. An important feature of the triaxial cell used was that it allowed simultaneous repeated load applications in both the axial and radial directions. The magnitudes of the axial and radial stresses can be controlled independently. Both stresses are applied in approximate rectangular wave shapes. A load duration of 0.1 second applied at a frequency of 20 cpm was used for all testing.

Axial and circumferential deformations (strains) were measured using a specially designed arrangement of linear variable displacement transducers (LVDTs). The LVDT measurement system has been described in Nair and Chang (1970). The essential features are that both axial and

circumferential deformations are measured over approximately the middle third of the specimen through the use of a clamping device placed around the outside of the specimen. This measurement system minimizes errors due to poor contacts at the specimen ends, compression in the testing equipment itself, and the effects of end restraint. When measuring small deformations on relatively stiff materials, these possible sources of measurement error can have a significant effect on the test results. The axial stress was measured using a load cell and the radial stress using a pressure transducer.

The procedure for testing an untreated granular base course specimen was to first compact the specimen in place on the triaxial cell base platen using a split ring mold. A membrane was then placed around the specimen and the LVDT deformation measurement system put in place. The specimen was then subjected to 1000 repeated load cycles to condition the specimen prior to testing. The specimen conditioning was performed to minimize imperfections in the specimen, and to seat the loading caps. A deviator stress of 10 psi and a confining pressure of 5 psi was used for specimen conditioning.

Once the specimen had been conditioned, the desired stress states were applied to the specimen. Measurement of the resulting specimen deformations for each stress state tested were recorded between the 50th and 100th load cycle for repeated load tests. It should be noted that Hicks (1970) has shown that stress sequence and the number of stress cycles have no significant effect on the resilient behavior of granular materials as long as the stress

states tested are compatible with those experienced in typical pavements.

TEST PROGRAM AND RESULTS

The experimental test program was formulated to determine if the untreated granular base course material exhibited time dependent deformation in a creep test and to investigate possible differences in resilient behavior under two different types of repeated loading tests.

In one type of repeated loading test, a constant all-round confining pressure was first applied, and then the sample was subjected to an additional repeated axial deviator stress. This type of test is referred to as a single cyclic test, as only a repeated deviator stress was applied. The other type of repeated loading test simultaneously applied repeated loads in both the axial and radial direction. This type of test is referred to as a double cyclic test, as both stresses were simultaneously applied. The stress states existing for each type of test are shown in Figure 1.

In order to compare the results of all three types of tests, the density and degree of saturation were held constant. A relative density of 91.2% (dry density = 139.3 pcf) and a degree of saturation of 67% (water content = 5.2%) were used for all testing.

Creep Test

A creep test on the untreated granular base course material was performed to investigate the degree of time-dependent behavior under sustained loading. A creep test consists

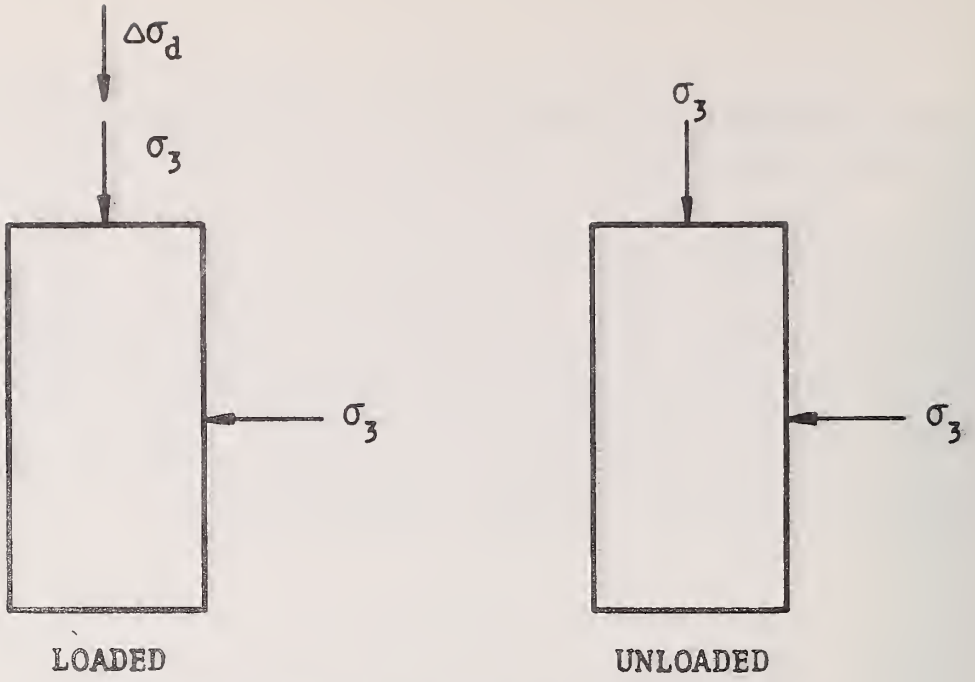

A) SINGLE CYCLIC TEST, $\theta = 3\sigma_3 + \Delta\sigma_d$

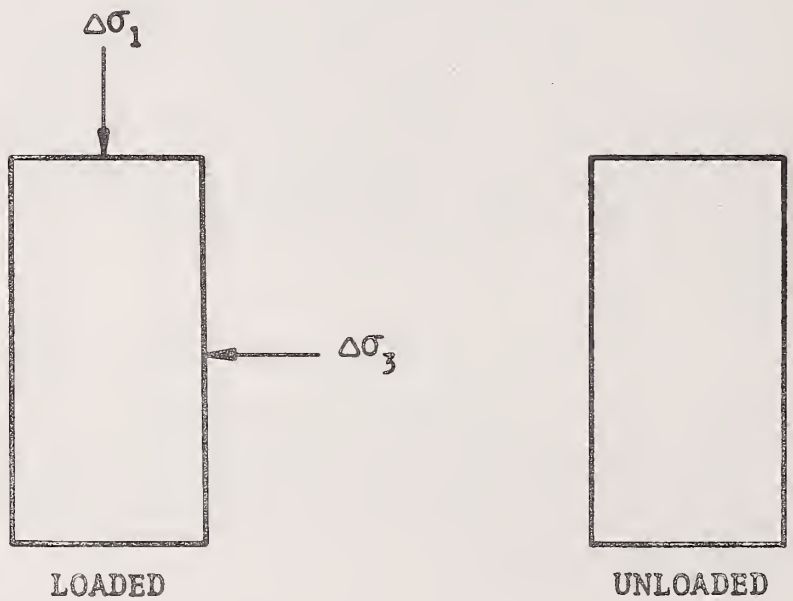

B) DOUBLE CYCLIC TEST, $\theta = 2\Delta\sigma_3 + \Delta\sigma_1$

FIGURE 1 - COMPARISON OF STRESS CONDITIONS EXISTING DURING A SINGLE AND DOUBLE CYCLIC REPEATED LOADING TRIAXIAL TEST

of applying a step load to the specimen and holding the load constant for the duration of the test. The resulting specimen deformations are measured as a function of time after loading to define time-dependent properties. The purpose of the creep test was to determine the applicability of a viscoelastic characterization of the material.

The stress levels used for the creep test were a radial stress of 3.0 psi and an axial stress of 13.0 psi. Both stress were applied to the specimen simultaneously in the form of step loads. The specimen deformed immediately after application of the load; however, no further change in deformation was observed over a period of 60 minutes after the load was applied. Therefore, there was no observable time-dependent behavior of the specimen under sustained load application.

The results of this test indicated that the response of the untreated granular base course material to a sustained load was purely elastic. Thus, further investigation of the applicability of a viscoelastic characterization was considered unnecessary.

Single Cyclic Tests

Previous investigations of the resilient (elastic) properties of untreated granular base course materials have used this type of repeated loading test. A single cyclic test can be performed in a standard triaxial cell which has repeated axial load capabilities.

The stress states utilized for the test program were selected based on the analysis of typical in-service stress

conditions previously described. Accordingly, sustained confining stresses of 1, 3, and 5 psi and repeated deviator stresses ranging from 2 to 21 psi were utilized in the test program. The specific combinations of stress states used yielded principal stress ratios (σ_1/σ_2) ranging from 2 to 7 and first stress invariants ($\theta = \sigma_1 + \sigma_2 + \sigma_3$) ranging from 5 to 35 psi.

Resilient Modulus

Figure 2 shows the resilient modulus data obtained from all single cyclic tests. It can be seen that the resilient modulus increases with increase in the sum of principal stresses ($\theta = 3\sigma_3 + \Delta\sigma_d$ for single cyclic tests). The relationship between M_r and θ can be approximated by a straight line on a log-log plot. The best fit regression line is shown on Figure 2 and results in the equation:

$$M_r = 2{,}940\ \theta^{0.59}\ \text{psi}$$

The statistical reliability of the linear log-log relationship can be measured by the statistical data associated with the regression analysis. The correlation coefficient is a measure of the degree to which the data fits a straight line. A correlation coefficient of 1.0 described a perfect linear fit. The correlation coefficient for the single cyclic data was 0.92, indicating a strong log-log linear dependence of M_r on θ.

The standard error of fit is a measure of the variation of the data about the best fit regression line. The standard error of fit is an estimate of the variance of M_r left unexplained by the regression of M_r on θ. If it is

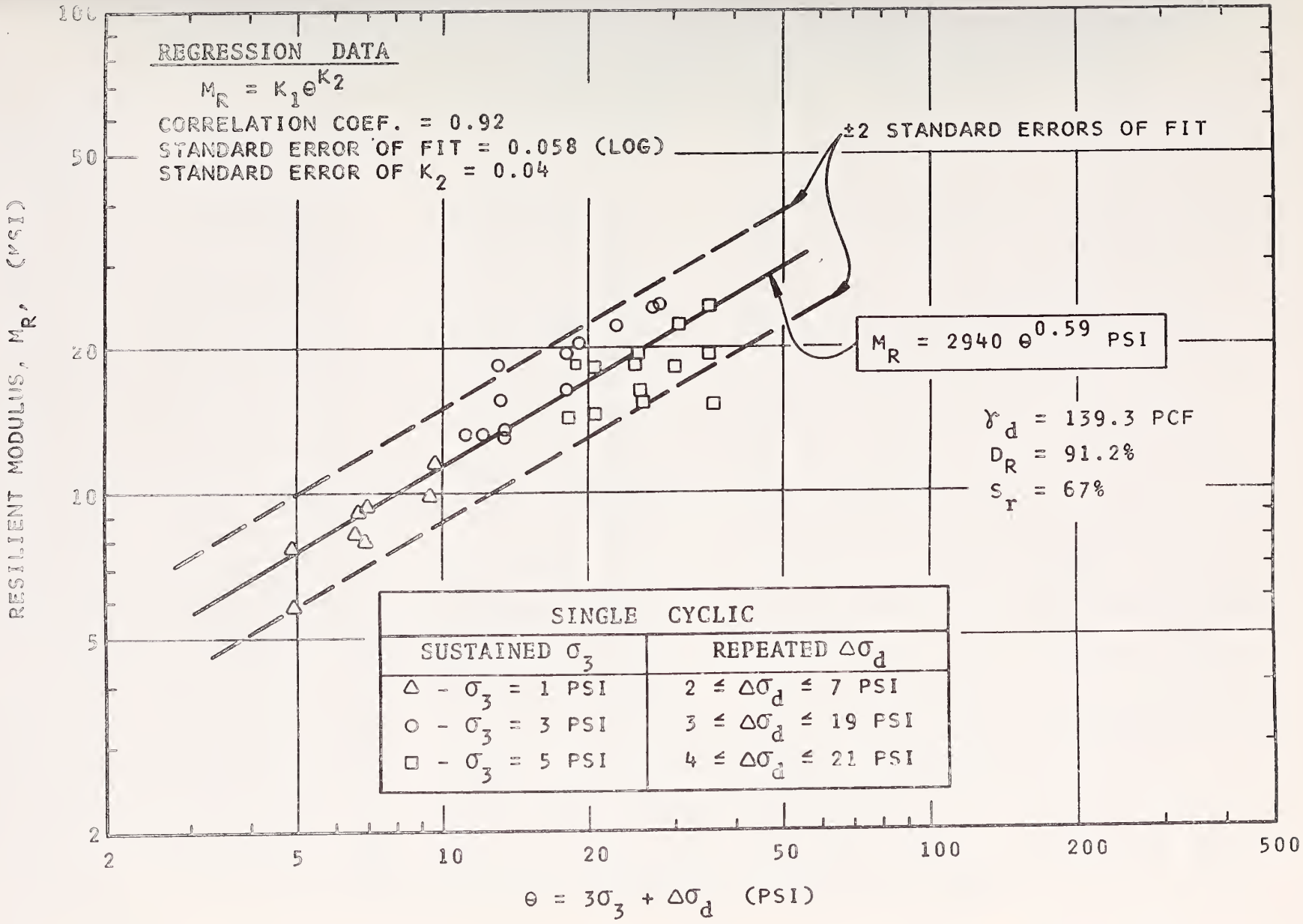

FIGURE 2 - RESILIENT MODULUS VS. SUM OF PRINCIPAL STRESSES FOR SINGLE CYCLIC TEST ON PARTIALLY SATURATED UNTREATED GRANULAR BASE COURSE

assumed that the distribution M_r for each value of θ is normally distributed with a constant standard deviation, then 68% and 95% of the data will fall within ±1 and ± 2 standard errors of fit, respectively. The standard error of ±2 for the single cyclic data was 0.058 (log). The ± 2 standard error of fit lines are shown on Figure 2.

The standard error of the regression constant K_2 is useful to assess the error associated with the regression fit of the power of θ (slope of the regression line). The standard error of K_2 for the single cyclic data was 0.04. If the regression coefficient K_2 is assumed normally distributed, the probability is 0.69 that K_2 would fall in the range of 0.55 to 0.63 for the single cyclic data.

Poisson's Ratio

The resilient Poisson's ratio ($-\varepsilon_{rr}/\varepsilon_{zz}$) data for single cyclic tests is shown in Figure 3. It can be seen that Poisson's ratio increased with increasing principal stress ratio. A similar dependence of Poisson's ratio on principal stress ratio for single cyclic tests has been reported by Hicks (1970).

Double Cyclic Tests

The resilient (elastic) properties of the untreated granular base course material were also defined using double cyclic repeated load tests. The magnitudes of simultaneously cycled axial and radial stress covered the same range investigated for single cyclic tests.

Resilient Modulus

The resilient modulus data for all double cyclic stress states tested is shown in Figure 4. As with the single

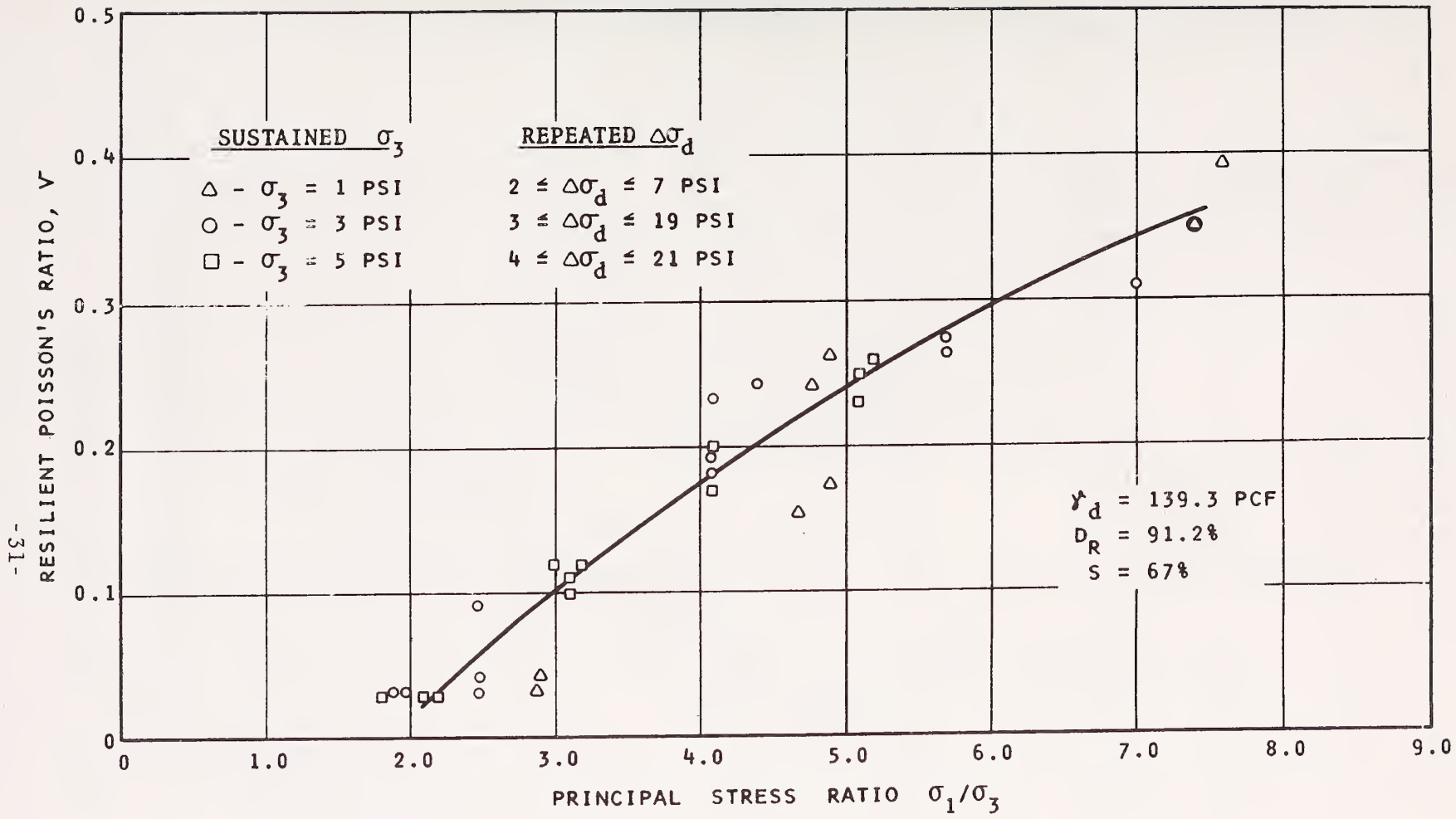

FIGURE 3 - RESILIENT POISSON'S RATIO VS. PRINCIPAL STRESS RATIO FOR SINGLE CYCLIC TEST ON PARTIALLY SATURATED UNTREATED GRANULAR BASE COURSE

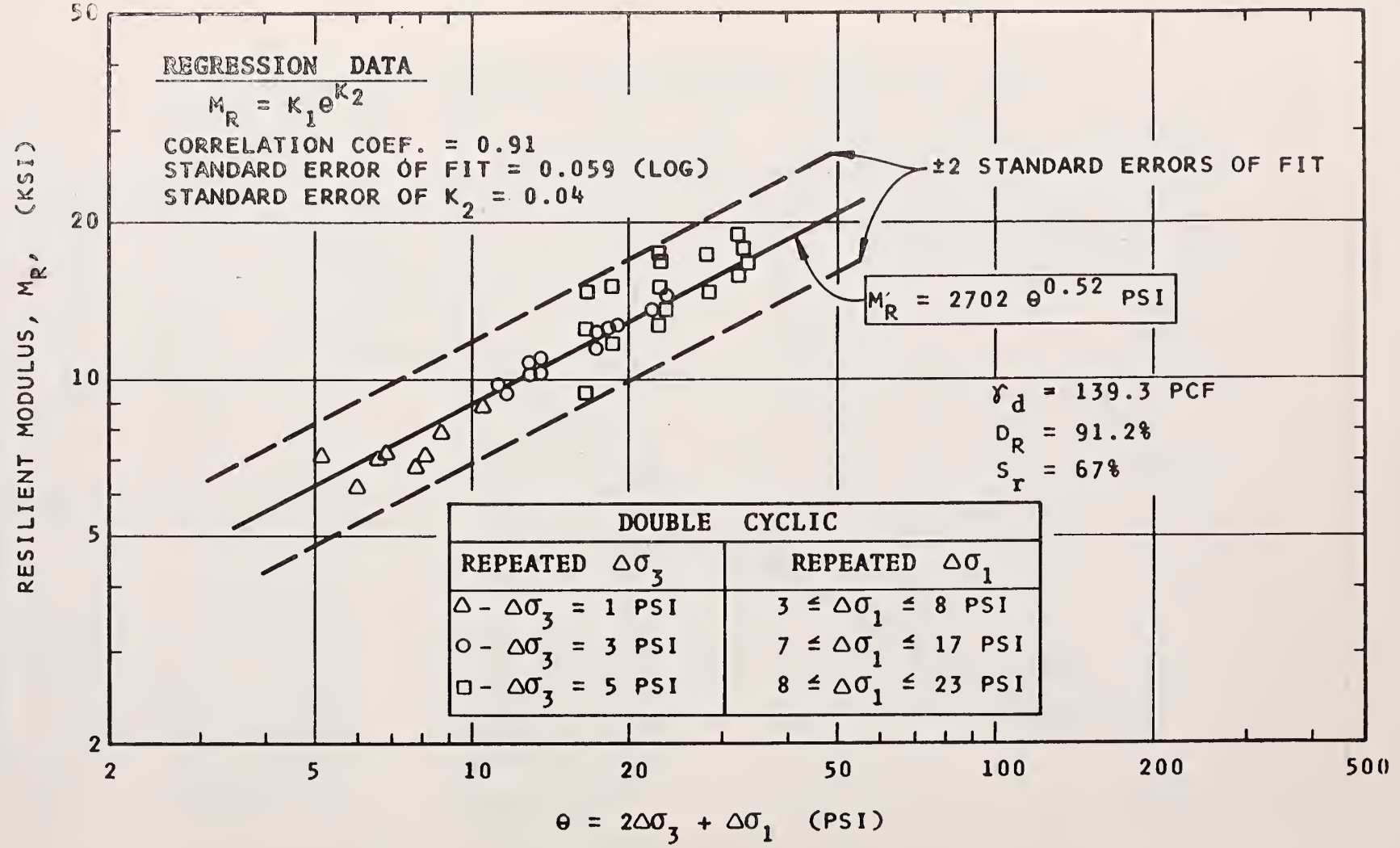

FIGURE 4 - RESILIENT MODULUS VS SUM OF PRINCIPAL STRESSES FOR DOUBLE CYCLIC TESTS ON PARTIALLY SATURATED UNTREATED GRANULAR BASE COURSE

cyclic tests, M_r was found to increase with increase in θ. The best fit linear log-log relationship was found to be:

$$M_r = 2{,}702\ \theta^{0.52}$$

The measures of statistical reliability of the regression fit were almost identical to those determined for the cyclic data.

Poisson's Ratio

Figure 5 shows the resilient Poisson's ratio data determined for all double cyclic stress states. Contrary to the single cyclic test data, no dependence of Poisson's ratio on principal stress ratio was found. The majority of the test data indicated Poisson's ratio to be between 0.3 and 0.4.

DISCUSSION OF TEST RESULTS

Constitutive Relationships

The creep test performed on the untreated granular base course material indicated that the material response under sustained loading was not time dependent. Therefore, an elastic constitutive relationship appears most applicable for characterizing the primary response characteristics. Barksdale (1972) and others have shown that untreated granular materials do accumulate permanent deformations under repeated load applications. While this behavior is not characteristic of a purely elastic material, these observed permanent deformations cannot be explained by viscoelastic characterization. An approach to permanent

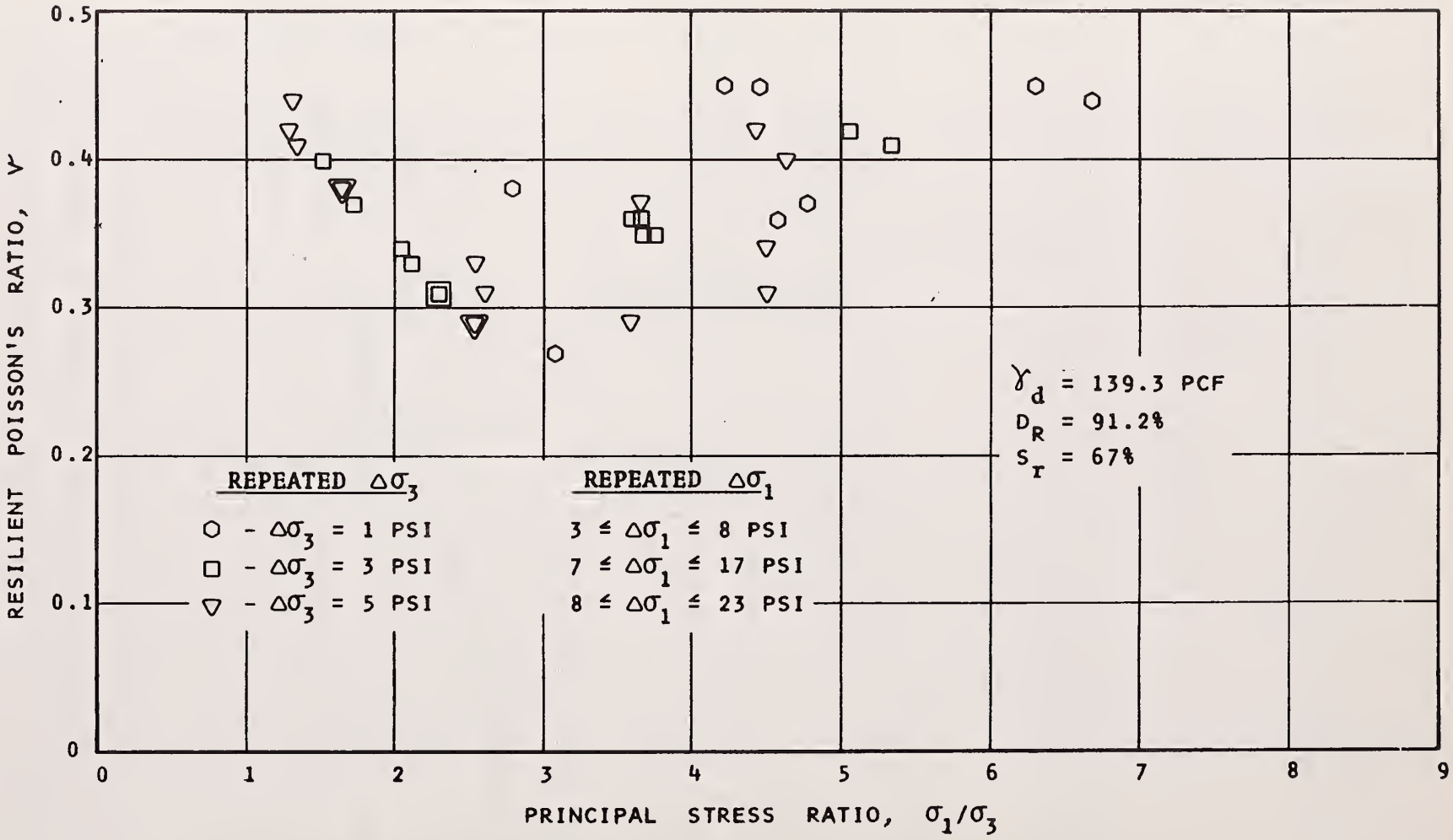

FIGURE 5 - RESILIENT POISSON'S RATIO VS PRINCIPAL STRESS RATIO FOR DOUBLE CYCLIC TEST ON PARTIALLY SATURATED UNTREATED GRANULAR BASE COURSE

deformation prediction in untreated granular base course material subjected to repeated loading is discussed in the following section.

The resilient (elastic) properties of the untreated granular base course material were determined using both single and double cyclic repeated load tests. Figure 6 is a summary plot of resilient moduli determined for both types of tests. While the data from both tests appear very similar, the best fit linear regression lines indicate that for a given value of θ, the resilient moduli for single cyclic tests is somewhat greater than that from double cyclic tests. The resilient Poisson's ratio calculated from single and double cyclic repeated load tests was also found to be dependent on the type of test. The single cyclic data indicated a dependence of Poisson's ratio on the principal stress ratio while the double cyclic data indicated an approximately constant value independent of the principal stress ratio.

In the field an untreated granular base course material is subjected to both cyclic axial and confining stresses as a vehicle passes. Therefore, the double cyclic test more closely represents the field stress pattern. Consequently, it is felt that the double cyclic test results are more representative of base course material behavior in the field. However, an important question to answer is whether or not the differences observed between double and single cyclic test results are significant. The significance of differences can be evaluated both from statistical measures of error and utilizing the sensitivity analysis results presented earlier.

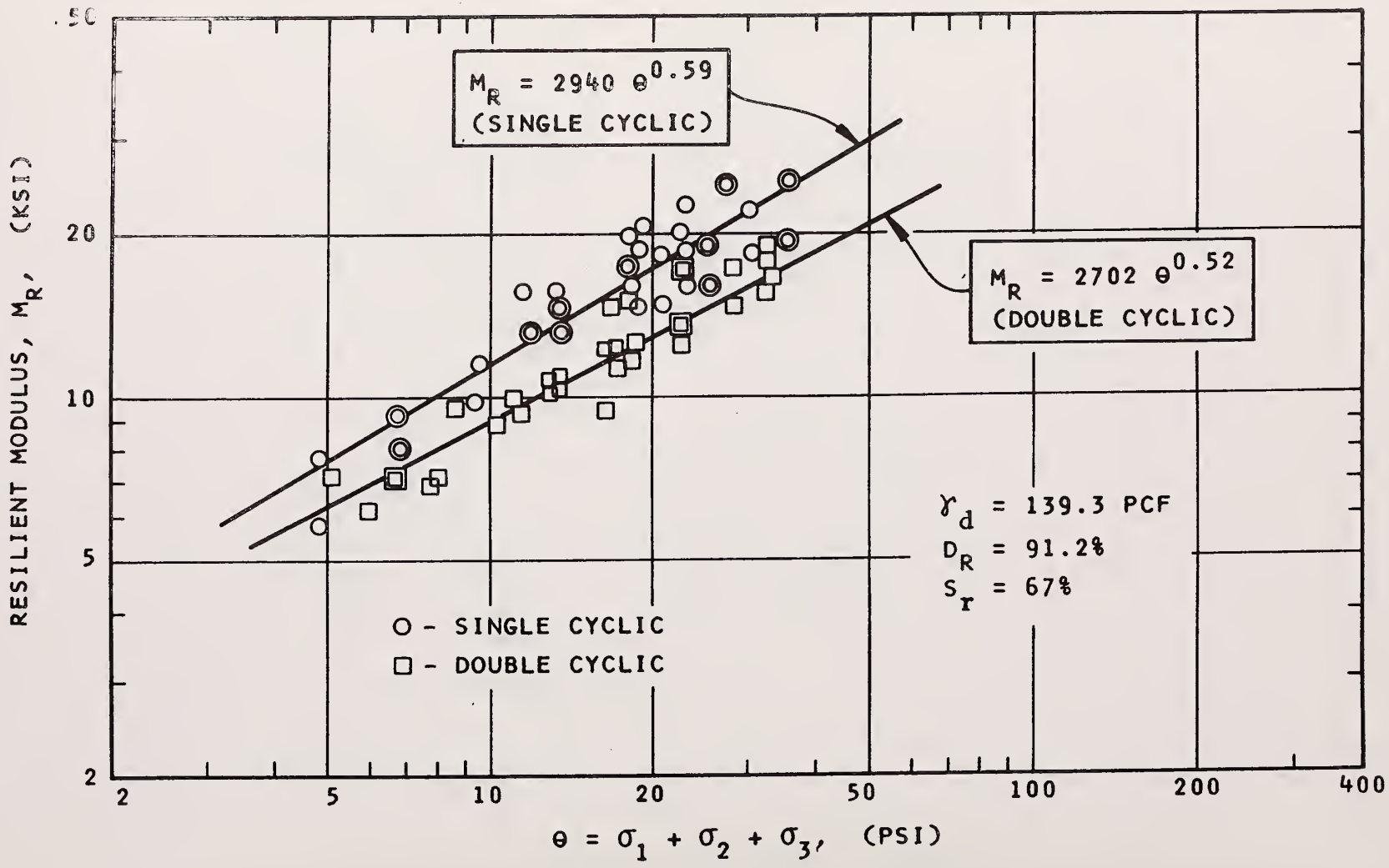

FIGURE 6 - COMPARISON OF RESILIENT MODULUS VS SUM OF PRINCIPAL STRESS FOR DOUBLE CYCLIC AND SINGLE CYCLIC TEST ON PARTIALLY SATURATED GRANULAR BASE COURSE

Analysis of the single cyclic and double cyclic data for resilient modulus shows that a variation of two standard errors of fit below the single cyclic best fit line approximately coincides with the double cyclic best fit line. Likewise, two standard errors of fit above the double cyclic best fit line approximately coincides with the sinble cyclic best fit line. If it is assumed that the distribution of M_r for each value of θ is normal with a constant standard deviation, statistical theory predicts that approximately 50% of the data developed from both types of tests would fall between the best fit regression line for each type of test. The validity of this prediction can be visually verified by inspection of Figure 6. Since approximately one-half of the data is somewhere between the two best fit regression lines, the statistical significance of the difference between the two regression lines is quite low.

The results of the nonlinear elastic boundary value solutions used to determine realistic stress levels for untreated granular base course characterization testing can be used to select a typical average value of θ. Boundary value solutions for structural Sections 2 and 3 of the sensitivity analysis indicated that a typical average value of θ was 8 psi. This corresponds to a resilient modulus of 10,000 psi as predicted by the best fit regression line for the single cyclic data. The corresponding resilient modulus for double cyclic data is 8,000 psi which represents a 20% reduction in modulus. Thus, the relative sensitivity results for a 25% reduction in base course modulus can be utilized to estimate the significance of this modular reduction on the prediction of the fatigue performance of flexible pavements.

The results of the relative sensitivity analysis indicate that a 25% reduction of base course modulus is normally of relatively minor significance when compared with the significance of other variables. As the average temperature environment of the pavement increases or the thickness of asphalt concrete surfacing decreases, the significance of a 25% reduction in base course modulus increases but was always of less significance than the limits of field control of air voids in the asphalt concrete or the determination of the fatigue failure criteria of the asphalt concrete.

The relative sensitivity analysis results indicated an almost negligible effect of 0.1 variation in Poisson's ratio of the base course layer. Furthermore, Hicks (1970) incorporated the dependence of Poisson's ratio on principal stress ratio found from single cyclic tests in a finite element program. From boundary value solutions of typical pavements he concluded that if a reasonable estimate of a constant Poisson's ratio was used, the inclusion of a stress dependent Poisson's ratio would not significantly alter the response of the pavement system. Therefore, the difference between Poisson's ratio values determined from single or double cyclic tests could be expected to be of only minor significance.

Both single and double cyclic repeated load test results show that the modulus of untreated granular material is highly dependent on the sum of principal stresses, θ. For example, an increase in θ from 10 psi to 20 psi results in approximately a 50% increase in modulus. This magnitude of modulus change will significantly affect the performance prediction of pavements.

In summary, it appears that differences in modular values predicted from single or double cyclic tests on partially saturated untreated granular base course is of minor significance in view of the statistical measures of regression fit errors and the relative sensitivity analysis results. The significance of differences in Poisson's ratio is also minor. Therefore, it appears that the resilient (elastic) parameters for partially saturated untreated granular base course material can be determined with sufficient accuracy using either single or double cyclic repeated load tests. No matter which test is used, the most essential consideration is that the dependence of modulus on the sum of principal stresses (confining pressure) be recognized.

It is not possible to subject untreated granular base course material to tensile normal stresses in either single or double cyclic laboratory testing. However, stress analysis of layered pavement systems indicates that small tensile stresses may develop in the base course material. Since the modulus of the material is controlled by the stress state under which it exists, it is expected that the modulus would be quite low under tensile stress. For small tensile stresses, failure is not expected because of dead load stresses and granular interlock. Although the modulus value for small tensile stress conditions cannot be determined experimentally, it is considered necessary to provide for a reduced modulus under these conditions. It is suggested that when the sum of principal stresses is less than zero, a modulus close to zero be assigned.

Degree of Saturation Effects

Previous studies have shown that the degree of saturation of untreated granular base course materials can affect the

resilient response characteristics. It is generally agreed that the resilient response of dry and most partially saturated granular materials are very similar. However, as complete saturation is approached, the resilient behavior may be significantly affected. In general, previous laboratory investigations have indicated that some reduction in modulus occurs as complete saturation is approached if the results were analyzed based on total stresses. Based on effective stress analysis of laboratory results, the modulus appears to be independent of degree of saturation. Thus, changes in modulus appear to be caused by pore water pressure effects.

Analysis of highway pavements are generally based on a total stress approach; that is, no direct account of pore water pressure is considered in the analysis. Any degree of saturation effects are normally accounted for by selecting the modulus of the material in accordance with expected field levels of saturation and laboratory tests under those conditions. Thus, the modulus determined from laboratory tests can be based on a total stress analysis of the data. As with any soil mechanics analysis based on total stresses, accurate representation of field conditions is essential to insure that the laboratory results are applicable to the field.

While available laboratory results based on total stresses indicate a reduction in modulus at high degrees of saturation, the magnitude of the reduction does not appear to be compatible with field behavior of flexible pavements. For example, Hicks (1970) has reported that for undrained single cyclic repeated load tests on saturated specimens the magnitude of transient pore water pressure developed

under each load cycle was instantaneous and generally of the order of 5 to 10 percent of the repeated deviator stress. Since the modulus of untreated granular base course material has been found to be independent of degree of saturation based on effective stress analysis of the data, the reduction in modulus based on total stresses can be computed. A repeated deviator stress of 15 psi would induce a pore water pressure of approximately 1.0 psi in a saturated specimen. Based on effective stresses, this would result in a decrease in sum of principal stresses of 3.0 psi. For a sustained confining pressure of 5.0 psi, the effective sum of principal stresses would be reduced from 30 psi to 27 psi due to the pore water pressure increase. This reduction in the sum of principal stresses would correspond to approximately a 10% reduction in modulus for saturated specimens based on total stresses and the test results found in this study. Analysis of other possible strain states indicates a similar percent reduction in the modulus due to complete saturation.

A 10 percent reduction in base course modulus when the material becomes saturated would not induce large changes in the primary responses of flexible pavements. Therefore, only small increases in distress manifestations of flexible pavements could be expected to occur should the base course complete saturation. However, this is contrary to observed field performance where high degrees of saturation of base course materials correspond to dramatic increases in pavement failures. Therefore, it appears that modulus reductions of greater magnitudes would be necessary to explain observed field performance.

As previously noted, total stress analysis of pavement behavior requires accurate duplication of field conditions in laboratory testing if reliable material properties are to be obtained. In single cyclic repeated load tests only the deviator stress is repeatedly applied. In the field, however, both vertical and horizontal stresses are simultaneously applied in a cyclic fashion with the passage of each vehicle. Therefore, double cyclic repeated load tests more closely duplicate field stress conditions. Consider the difference in behavior that could be expected for saturated specimens tested in the laboratory under single cyclic load conditions as opposed to double cyclic conditions more representative of the actual field conditions.

The difference in modular properties in single cyclic tests with change in degree of saturation has been found to result from the increase in pore water pressure (decrease in effective sum of principal stresses) occurring with each deviator stress application. Thus, any change in modulus for double cyclic tests would also be expected to arise from pore water pressure effects. In double cyclic tests both the repeated axial and radial stresses would contribute to increases in pore water pressures in contrast to single cyclic tests where only the deviator stress induces pore water pressures. The pore water pressure parameters commonly used in other soil mechanics applications can be used to estimate the difference in induced pore water pressures for the two tests.

The change in pore water pressure for undrained tests due to increases in both all-round confining pressure (hydrostatic pressure) and deviator stress can be expressed as:

$$\Delta u = B\Delta\sigma_3 + D\Delta\sigma_d$$

where:

Δu = Change in pore water pressure

$\Delta\sigma_3$ = Change in all-round confining pressure

$\Delta\sigma_d$ = Change in deviator stress ($\Delta\sigma_1 - \Delta\sigma_3$)

B = Pore water pressure parameter expressing change in pore water pressure due to hydrostatic ($\Delta\sigma_3$) increase in total stress

D = Pore water pressure parameter expressing change in pore water pressure due to deviatoric ($\Delta\sigma_d$) increase in total stress

For saturated soils, B = 1.0. Thus, repeated load cycles of all-round confining pressure would induce pore water pressures equal to the applied change in hydrostatic stress. Therefore, application of a cyclic hydrostatic pressure to completely saturated undrained specimens would result in no increase in effective confining pressure beyond that which existed prior to application of the cyclic confining pressure. The experimental data of Hicks (1970) indicate that D = 0.05 to 0.10. Therefore, application of both cyclic hydrostatic and deviatoric stresses to undrained saturated specimens would result in a small decrease in effective confining pressure. Since the modulus of untreated granular materials has been shown to be controlled by effective stresses, the modulus of saturated specimens would be substantially lower than that of dry specimens for the same applied (total) stress conditions.

Although the drainage conditions of saturated base course materials in the field may not be perfectly undrained as simulated in laboratory testing, an undrained condition is probably the best representation. Hicks (1970) has presented an analysis of typical base course conditions considering permeability and thickness of base course layer, length of drainage path, slope of drainage path, and magnitude of excess pore water pressure. The results indicated that saturated material should be tested undrained in the laboratory to best represent field conditions during periods of saturation. Consideration of the short duration of each load application also indicates that undrained conditions are more appropriate.

For base course materials that are not completely saturated, the pore water pressure parameter B will be less than 1.0. Thus, increases in hydrostatic stress would not be completely transmitted to the pore water and the effective confining pressure would increase somewhat upon load application. However, B values of 0.7 or greater associated with high degrees of saturation would only allow a maximum of 30% of the applied hydrostatic stress increment to be transmitted as effective stress.

While deviations from completely saturated undrained behavior of base course materials in the field can exist, it appears that cyclic increases in pore water pressure induced by simultaneous increases in both vertical and horizontal stresses for base course materials with high degrees of saturation can substantially alter the modulus applicable to field conditions. The modulus applicable for analysis is controlled by the value of θ based on effective stresses. For dry or low degrees of saturation,

no cyclic pore water pressures develop and the value of θ is the same based on both effective and total stresses. However, as the degree of saturation increases, pore water pressures become significant. For completely saturated materials, the value of θ based on effective stresses is substantially lower than that based on total stresses.

To establish the modulus of base course material, the value of θ based on effective stresses is needed. The effective stresses can be found if both the total applied stresses and pore water pressure are known. The pore water pressure parameters can be used to calculate pore water pressures for a given total stress condition. Therefore, the effective value of θ needed to establish the modulus of base course material can be found.

For example, consider an untreated granular base course material with high degree of saturation subjected to simultaneous increases in axial and radial stress of 15 and 5 psi, respectively. Assume that the stress conditions prior to load application were: no pore water pressure and an axial and radial stress of 1 and 0.5 psi, respectively (representing dead load stresses). Typical values of the pore water pressure parameters for this material might be $B = 0.9$ and $D = 0.05$. The induced pore water pressure upon load application would be 5 psi. The sum of principal stresses based on total and effective stresses would be 27 psi and 12 psi, respectively. Since the effective stress value controls the modulus, the modulus established from double cyclic tests performed in this study would be approximately 10 ksi. This is the modulus applicable to field conditions which should be used in stress analysis of the pavement system. The

modulus based on the total stress value of θ would be 15 ksi. Thus, dry untreated granular base course material would have a modulus 50% greater than that of highly saturated material for the conditions considered in this example. The reduction in modulus for saturated base course conditions would, therefore, correspond with the observed field performance of pavements which show that when the base course becomes saturated, the pavement condition will deteriorate rapidly.

Consideration of the difference in pore water pressures induced by single cyclic and double cyclic tests for the same value of θ also provides an explanation of the difference in modulus found for the two types of tests at a degree of saturation of 67% shown in Figure 6. The values of θ shown on Figure 6 tests are based on total stresses for both types of tests. Since the double cyclic tests would induce greater pore water pressures than single cyclic tests, the effective value of θ would be lower for double cyclic tests. Thus, the resilient modulus at a given total stress value of θ would be lower for double cyclic tests. The magnitude of difference would be expected to be small for this degree of saturation as indicated by the test results.

It should be noted that while double cyclic tests are more representative of field stress patterns, single cyclic tests are sufficient as long as the difference in pore water pressure behavior is considered. The pore water pressure parameters B and D can be determined using a standard triaxial cell. The pore water pressure parameters should be determined and used to calculate pore water pressures that would be induced for double cyclic

test conditions. Single cyclic test results at high degrees of saturation should then be adjusted for the pore water pressures that would develop had a double cyclic test been used. The adjusted single cyclic data would then be respresentative of field stress conditions.

Failure Criteria

The modes of flexible pavement failures which are most commonly associated with the properties of untreated granular base course material are fatigue cracking and surface distortion. Little evidence of failure of base course material in the classical sense of rupture or shear failure is found for pavements designed using standard techniques.

Fatigue Cracking

Fatigue failure of a pavement is often assumed to be controlled by the value of the maximum horizontal tensile strain in the asphalt concrete. Since the constitutive properties of untreated granular base course material affect the stress and strain distribution throughout the entire pavement system, the fatigue life is influenced to some degree. For example, as part of the sensitivity analysis presented in this report (Appendix A), the fatigue life expected for different values of the parameters for the constitutive relationship representing the base course was established for several typical pavements.

It should be noted that the results of this study indicate that if a dry base course layer became saturated, the modulus would be substantially reduced. Therefore, the degree

of saturation of the untreated base course layer would be an important determinant of pavement fatigue life.

Surface Distortion

Surface distortion of the pavement is caused by permanent deformations occurring in the pavement system. Since the value of constitutive parameters for the base material affect stresses and strains in the entire pavement system, it would be expected that the amount of permanent deformation occurring in each material layer of the pavement would likewise be affected.

For untreated granular base course material, the test results revealed that no time-dependent deformation occurred under a sustained load. However, under repeated load applications permanent deformations do accumulate. Therefore, neither an elastic nor viscoelastic constitutive characterization can explain both these aspects of observed material behavior. The mechanism of permanent deformation appears to be associated with particle rearrangement causing geometrical changes in shape and densification. There are several possible compromises that can be made to compensate for observed deviations from each of the two theoretical constitutive behaviors.

One approach would be to ignore the fact that no time-dependent response occurred under a sustained load application and characterize the base course as viscoelastic. The viscoelastic properties would be selected such that the permanent deformations observed under repeated loading conditions were correctly predicted. Thus, pseudo-creep functions which describe the permanent deformation characteristics rather than creep functions that characterize

the stress-strain-time behavior would be used. Although this approach may yield reasonable permanent deformation predictions, the stresses and strains throughout the pavement system would not be realistic. Furthermore, viscoelastic analysis of layered systems is normally restricted to linear materials due to the complexities and expense of nonlinear viscoelastic solution. Thus, the highly nonlinear response of untreated granular base course materials could not be considered. The shortcomings of this approach appear to outweigh the benefits.

A second approach is to consider the untreated granular base course material as elastic and represent the accumulation of permanent deformation as a failure mechanism. The nonlinear characteristics of the material can be approximated by considering the modulus to be dependent on the sum of principal stresses. Thus, the stresses and strains throughout the pavement for each load application could be realistically determined. The computed elastic strains or stresses occurring in the base course material could then be related to the accumulation of permanent strain in much the same manner as other failure criteria for pavements are considered. The base course layer can be subdivided into a number of sublayers and permanent deformations occurring in each sublayer summed over the total thickness of the layer to determine the total permanent deformation. This approach to permanent deformation prediction has been previously suggested by Romain (1969) and Barksdale (1972) and appears to be worthy of continued consideration.

In order to utilize the second approach, the manner in which permanent strain is accumulated in an untreated

granular base course material must be established under repeated load applications in the laboratory. Test results that can be utilized for this purpose have been reported by Haynes and Yoder (1963), Holubec (1969), and Barksdale (1972 a and b) and were discussed in the literature survey. The most comprehensive data is that reported by Barksdale (1972b) who tested ten different base materials. Barksdale showed that the permanent strains could be related to applied stresses through a hyperbolic stress-strain law. The permanent deformation for a given material has been found to increase with increase in number of load cycles, increase in deviator stress, decrease in confining pressure, and increase in degree of saturation. Available data indicate that the mechanism of permanent deformation changes with degree of saturation. As the saturation increases, the mechanism becomes primarily one of geometrical changes rather than densification.

Failure criteria for surface distortion (permanent deformation) can be established by the pavement designer by setting a maximum acceptable value of permanent deformation in the wheel path at the pavement surface. The portion of permanent deformation contributed by the untreated granular base course layer can be established from triaxial repeated load testing of the material at the density, water content (degree of saturation), number of load repetitions, and stress states expected for the particular pavement.

CONCLUSIONS

The results of characterization testing of untreated granular base course material have indicated the following conclusions:

1) The primary response behavior can be best represented by a nonlinear elastic constitutive relationship. A modulus expressed as a function of the sum of principal stress, θ , in the form:

$$M_r = K_1 \theta^{K_2}$$

describes the experimental results for stress states typical of flexible pavements with sufficient accuracy.

2) The differences in modulus for a given total stress value of θ found for single and double cyclic tests can be explained by consideration of pore water pressure effects in each test.

3) Single cyclic tests can be used to define the modulus relationship for all degrees of saturation provided that the pore water pressure parameters B and D are determined and used to adjust the single cyclic data to the effective stress conditions that would be induced by double cyclic conditions representative of field conditions.

4) The modulus value applicable to analysis of pavements decreases with increase in degree of saturation.

5) Poisson's ratio can be considered to be a constant value independent of stress state. A value of 0.35 is a reasonable average value for partially saturated material.

6) The influence of untreated granular base course material properties on the fatigue cracking mode of flexible pavement failure can be adequately determined by utilizing the characterization expressed in (1).

7. Further work needs to be done to verify currently used and suggested techniques to determine the permanent deformation that accumulates in an untreated granular base course under repeated load.

CHARACTERIZATION OF ASPHALT-TREATED GRANULAR BASE COURSE MATERIAL

There are three principal types of granular aggregate bases where asphalt acts as a cementing agent: (i) asphalt macadam base, spray application; (ii) asphalt concrete base, hot mixed; and (iii) asphalt-treated base, cold mixed. This study is concerned with the characterization of (iii), i.e., cold mixed asphalt-treated granular base (ATB), which utilizes emulsified asphalt or liquid (cutback) asphalt as the cementing agent.

This study was not intended to examine the effects of numerous different types of asphalt treatment, aggregate characteristics,aggregate gradation, curing conditions, aging and compaction procedures on the material response. The purpose of this investigation was to establish constitutive relationships and failure characteristics of typical ATB material.

SUMMARY OF PREVIOUS INFORMATION

CONSTITUTIVE RELATIONSHIPS

There has been only a small amount of published information regarding the constitutive properties of ATB material. Available information has been primarily concerned with the definition of resilient or elastic properties. Finn, et. al. (1968) reported resilient modulus values for thirty-five field cores of emulsion treated base course material. Triaxial repeated load tests were performed using uniaxial (unconfined) stress conditions. The cores had a wide variety of gradations, densities, percent emulsions, and ages. The resilient modulus values at a temperature of 77°F ranged

from 50 to 961 ksi with an average value of 318 ksi. A linear regression equation for ultimate aged resilient modulus as a function of penetration of recovered asphalt, density, and sand fraction was presented but the correlation coefficient was 0.66 indicating only a fair fit. A pavement design procedure was developed and indicated that allowing for a reduced resilient modulus for a two-year curing period of the emulsion treated base course material required less than 0.35 inches of additional base material to compensate for the time required to cure.

Terrel (1967) and Terrel and Monismith (1968) presented results of resilient modulus testing of SM-K (CMS-2S) asphalt emulsion treated and MC-800 liquid asphalt-treated granular base course materials. Laboratory prepared specimens 4 inches in diameter and 8 inches high were tested in repeated load triaxial tests. Repeated load tests were conducted with an approximate square wave shaped load of 0.1 second duration and frequency of 20 cpm. Tests were conducted at 68°F for sustained confining pressures from 5 to 40 psi and repeated deviator stresses from 5 to 30 psi. The testing focused on the stress dependence and effect of curing on the resilient modulus of the asphalt-treated materials.

It was found that amount of curing and stress conditions both affected the resilient modulus. The resilient modulus of both the SM-K and MC-800 asphalt-treated material increased rapidly during the first few days of curing at a temperature of 68°F and 50 percent relative humidity. The resilient modulus continued to increase with age but at a slower rate for longer cure times. After 90 days of curing

the resilient modulus of the SM-K materials was approximately 300 ksi and MC-800 approximately 150 ksi.

The modulus of both the SM-K and MC-800 treated material at a given age increased with increase in confining pressure and decrease in deviator stress. This indicates that the behavior was nonlinear with respect to stress. However, the stress dependence of modulus on the confining pressure for the SM-K treated material decreased with increase in curing time and at the ultimate cure condition was only slightly dependent on confining pressure. These results suggest that during the early stages of curing the behavior of the asphalt-treated material is similar to that of an untreated granular material with a modulus primarily dependent on the confining pressure. As curing progresses the modulus increases in magnitude and the asphalt-treated material behavioral characteristics became more similar to those of asphalt concrete. Consequently, the selection of constitutive equations to represent asphalt-treated materials will be influenced by the curing time that has elapsed.

Although not part of this study, it should be mentioned that several studies of asphalt emulsion treated granular materials to which a small amount of portland cement or lime was added have shown that the curing process can be significantly altered. Terrel and Wang (1971) have shown that addition of as little as 1.0% cement to asphalt emulsion treated material leads to a rapid gain in resilient modulus for short cure times even under adverse cure conditions (40°F and 95% relative humidity). Schmidt, et. al. (1973) have also shown rapid development of resilient modulus for asphalt emulsion treated material modified with 1.3% cement. Furthermore, partially cured cement modified

asphalt emulsion materials were more resistant to decrease in modulus upon increase in degree of saturation than pure asphalt emulsion materials. Therefore, cement modified asphalt emulsion materials do exhibit desirable constitutive properties during curing.

FAILURE CRITERIA

Failure criteria for asphalt-treated granular base course material arise from possible failure modes of pavements. Pavement failure modes related to ATB material can be subdivided into two categories: (i) failure in the ATB and (ii) failure of pavement due to ATB properties.

Failure in ATB

Possible failure modes for ATB materials include cumulative damage (cracking) under repeated loads (fatigue) and failure (rupture) due to excessive loads (shear or tensile). A very limited amount of research has been performed to define failure criteria for ATB for these failure mechanisms.

Fatigue Failure

Should ATB develop cracks due to fatigue failure, the structural integrity of the ATB layer would be lost inducing high stresses in both the underlying and surface layers. The increased stresses and strains could then induce failure of the pavement section.

A great deal of work has been done in the area of fatigue failure of asphalt concrete and many of the concepts developed may be applicable to cured ATB material. For ATB material the residual asphalt content is usually less

than that of asphalt concrete and may have an important influence on the fatigue failure properties.

Schmidt, et. al. (1973) have reported fatigue test results on asphalt concrete and asphalt emulsion treated material. A sand aggregate was used for both materials and the mixes were designed such that the residual asphalt content of the SS-1h emulsion treated mix was the same as the asphalt concrete (5.5%). Fatigue tests were performed on beams in the fatigue equipment developed at the University of California, Berkeley. The results indicated that fatigue failure relationship for the ATB was of a similar form as that of the asphalt concrete. That is, the fatigue life of the ATB specimens was controlled by the maximum bending strain and material stiffness. For the two materials tested the asphalt concrete had a somewhat longer fatigue life than the ATB at the same values of strain and stiffness.

These results indicate that for ATB material with rather high residual asphalt contents fatigue criteria can be developed using similar techniques as have been used for asphalt concrete. No fatigue tests on ATB material at lower residual asphalt contents were found in the literature.

Shear or Tensile Failure

Field evidence indicates that this mode of ATB failure does not normally occur in well designed highway pavements because induced stresses are well below their failure levels. However, failure criteria to estimated failure through rupture of yield due to excessive shear or tensile stresses are available. The Mohr Coloumb failure theory is normally

used to estimate the shear strength and tensile failure can be considered using the maximum stress theory first proposed by Rankine. Only a small amount of testing of ATB materials have been performed to establish values of the strength parameters for these failure theories.

Davies and Stewart (1969) have reported triaxial shear strength test results on SS-1 emulsion treated sand base course material. Specimens were tested by constant rate of strain tests at a rate of 0.016 inches per minute. The results indicated an approximate average value of angle of friction, ϕ, of 33° and a cohesion value of 7 psi. These strength parameters can be utilized with the Mohr Coloumb theory to estimate ultimate shear strength.

Failure of Pavement Due to ATB

Failure of the pavement system can be induced by the properties of the ATB material without 'failure' of the ATB material itself. The significant properties of ATB material which can cause distress in a pavement section are: (i) the values of the constitutive parameters and (ii) the susceptibility to accumulate permanent deformation under repeated loading. The pavement distress induced by these ATB properties are normally reflected in the surface layer through applicable surface failure modes such as fatigue cracking or distortion (rutting). Both ATB properties can be taken into account in the selection of constitutive relationships. However, as previously discussed, constitutive relationships for ATB to date (1973) have employed elastic theory to represent the stress-strain characteristics. By definition, all deformations of an elastic material are completely recoverable and, therefore, only

the stress and strain conditions in the pavement as influenced by the value of the ATB constitutive parameters could be considered.

The behavior of cured ATB material has been found to be similar to that of asphalt concrete. It has been found that the constitutive properties of asphalt concrete can be described by viscoelastic theory, MR&D (1972). A viscoelastic constitutive relationship allows prediction of permanent deformations in addition to the stress and strain conditions throughout the pavement. Therefore, it would appear desirable to evaluate the applicability of a viscoelastic constitutive characterization of ATB material.

EXPERIMENTAL PROGRAM

MATERIAL SELECTED FOR TESTING

An attempt was made to select an asphalt-treated base course for testing which is widely used throughout the United States. Based on existing pavements using asphalt-treated base course material and anticipated future usage, it was decided that a granular aggregate treated with asphalt emulsion would be representative of many asphalt-treated base courses used in pavement construction.

The characterization test program on asphalt-treated base course material (ATB) was performed using a sandy soil treated with CMS-2S (SM-K) asphalt emulsion. CMS-2S is a medium setting cationic emulsified asphalt. The properties of CMS-2S emulsion used for this study are shown in Table 1.

TABLE 1

PROPERTIES OF ASPHALT EMULSION

CMS-2S (SM-K)

Viscosity @ 122°F., SSF.	350
Storage Stability, 1-day, %	0.2
Aggregate Coating - Water Resistance	
Dry Aggregate, % Coated, minimum	95
Wet Aggregate, % Coated, minimum	80
Sieve, % Retained on #20 Mesh	0.02
Particle Charge Test	Positive
pH	4
Adhesion, S-4 Test, % Coated	100
Residue by Distillation, %	62
Tests on Residue from Distillation	
Penetration @ 77°F	120
Ductility @ 77°F, cm	100+
Solubility in Trichlor, %	99.5

The aggregate used for specimen preparation is from a natural deposit found along Highway 1 near Watsonville, California. The gradation of the material was:

Sieve Size	Percent Passing
# 16	100
# 30	91
# 50	56
#100	9
#200	3

The mix design was made based on the coating characteristics of the material, the moisture susceptibility of the mix, and stability considerations. Based on the above considerations, an emulsion content of 6 percent (by weight) was used. Thus, the residual asphalt content of fully cured specimens was approximately 3.6%.

Six percent CMS-2S emulsion was added to dry aggregate and mixed in a mechanical mixer for three minutes. This time was selected to achieve a uniform mix. The specimens were compacted immediately thereafter. All mixing and compaction were performed at room temperature which was approximately 65°F.

Both cylindrical (4 in. dia. x 8 in. ht.) and beam (4 in. ht. x 4 in. width x 15 in. length) specimens were prepared. Considerable experimentation with compaction procedures were necessary to achieve uniform densities throughout each type specimen and similar densities for both cylindrical and beam specimens.

A low-cost kneading compactor was used to compact both specimen types. The cylindrical specimens were compacted using a gage pressure of 7 psi (foot pressure = 90 psi) in 5 layers using 15, 18, 21, 25, and 28 blows/layer. Beam specimens were compacted using a gage pressure of 9 psi (foot pressure = 50 psi) in 3 layers using 25, 30, and 35 blows/layer. A static pressure of 400 psi was applied to both specimens immediately after kneading compaction and held for 1 minute. The resulting specimens had an average dry density of 109.8 pcf.

The compacted specimens were removed from the compaction mold, placed in a 50 percent relative humidity and 70°F environmentally controlled room and cured under these conditions until subsequent characterization testing was performed. Each beam specimen was cut into four beams of dimension 1.5 in. x 1.5 in. x 15 in. prior to use for fatigue testing.

IN-SERVICE STRESS CONDITIONS

Past research on asphalt-treated base course material has shown that during the early stages of curing the response of ATB material is similar to that of untreated material. Therefore, the boundary value solutions used to determine typical in-service conditions for untreated granular base course material are also applicable to ATB during the early stages of curing. These results indicated that an approximate unconfined condition with axial stress less than 15 psi would be suitably representative for ATB testing during the early stages of curing.

As curing progresses, the ATB behavior changes from that similar to an untreated material to that similar to asphalt concrete. Boundary value solutions for Sections 2 and 3 of the sensitivity analysis for base course moduli values of 100 and 1,000 ksi were used to estimate in-service stress conditions in ATB material after long periods of curing. The stress conditions existing in the base course layer vary through the depth of the section.

Near the top of the ATB layer both axial and radial stress were compressive and generally of magnitude less than 60 and 30 psi, respectively. Near the middle of the ATB layer axial stress less than 20 psi and radial stress near zero were most representative. At the base of the ATB layer axial stress was small and tensile radial stress was generally less than -20 psi.

Thus, layered elastic stress analysis suggests that ATB material should be characterized under three basic stress conditions to be representative of in-service stress conditions through the depth of the ATB at the latter stages of curing. Confined compressive tests would be representative of the top of the layer, unconfined compressive tests of the middle of the layer, and unconfined tensile tests of the bottom of the layer (assuming an isotropic material). Tests conducted under these stress conditions with magnitudes less than the approximate maximum values described above are representative of typical in-service ATB stress conditions.

EQUIPMENT AND PROCEDURES

All cylindrical specimens were tested in the triaxial cell which allows simultaneous load application in both the

axial and radial directions. The cell also allows temperature control ranging from 40°F to 140°F. A more detailed description of the triaxial cell can be found in Nair and Chang (1970) and MR&D (1972).

Beam specimens were tested in the fatigue testing equipment developed under the direction of Prof. Monismith at the University of California, Berkeley. This equipment subjects a simply supported beam to repeated flexural bending at a controlled load level. A more detailed description of the equipment can be found in Deacon (1965). One significant modification to the equipment described by Deacon (1965) was made for this study. Screw clamps which were used to hold the beam specimen in place were replaced with hydraulic clamps that maintained a constant clamping force throughout the duration of a fatigue test. The constant clamping force has been found to reduce the scatter of fatigue test results.

Both elastic and viscoelastic characterization tests were performed on cylindrical specimens at controlled temperatures. For both types of tests axial and circumferential strains were measured using bonded strain gages. Micro-Measurements strain gages of 2-inch active length were used and bonded with EPY-150 epoxy. Appendix B describes a limited test program conducted to evaluate the accuracy of such measurements. Strain gages were placed near the mid-height of the specimens to minimize end restraint effects. A temperature compensating strain gage bridge was used to eliminate fictitious strain readings caused by small temperature drifts. Axial stress was measured using a load cell and radial stress using a pressure transducer.

For all elastic characterization tests repeated stress pulses of a rectangular wave shape with a duration of 0.1 second applied at a frequency of 20 cpm were used. These load characteristics are in agreement with in-service conditions expected for ATB material. The elastic properties for each stress state tested were measured between the 50th and 100th load repetition.

For creep tests the stresses were applied in step functions and held constant for the duration of loading. Rise time for load application was less than 0.05 seconds and creep function determinations were begun 0.5 seconds after load application to eliminate any transient effects due to the finite rise times. For each creep test the duration of load application was 20 minutes (1200 seconds).

Previous creep testing of asphalt bound material (MR&D, 1972) had indicated that prior to taking data one cycle of load should be applied to condition the specimens. It was found that creep properties measured for the second and subsequent load cycles were repeatable. This procedure was followed for each stress state tested and the data reported are for the second cycle of load application. It was found that approximately 1.5 hours of unloading between load cycles was sufficient to allow the specimens to return to an equilibrium state. For many of the creep tests a longer period of unloading was allowed prior to application of the second load cycle.

Fatigue tests of ATB beams were performed at preselected load levels. The load was applied in a rectangular wave shape with a duration of 0.1 seconds applied at a frequency of 20 cpm. The maximum deflection at the midspan of the

beam was measured using an LVDT. Simple beam theory, measured deflection, and measured specimen geometry were used to calculate the maximum tensile strain at the extreme fiber of the beam. The strain occurring between the 100th and 200th load cycle is termed the initial strain. Repeated loading of constant magnitude was applied until the beam fractured into two segments. The number of load cycles required to fracture the specimen was recorded as the fatigue life of the specimen.

TEST PROGRAM AND RESULTS

The test program for the asphalt-treated base course material (ATB) can be considered to consist of four components. All testing, except fatigue, was performed on cylindrical 4 x 8-inch specimens. Repeated load triaxial testing was performed at 70°F to determine the change in modulus with age after compaction. These tests also defined the time to achieve an ultimate cure condition. The ultimate cure condition was defined to be that when the modulus remains approximately constant with time. Once the ultimate cure condition was achieved three additional types of tests were performed.

The ultimate cure elastic constitutive properties were defined by triaxial repeated load tests at temperatures of 40, 70, and 100°F. Creep tests were also performed at temperatures of 40, 70, and 100°F to define the linear viscoelastic properties at ultimate cure and evaluate time-temperature equivalency. Finally, fatigue testing of beams was performed at 70°F to define the fatigue failure properties at ultimate cure.

Determination of Elastic Properties

Repeated load triaxial tests were used to define the elastic properties of ATB both during curing and at an ultimate cure condition.

Properties While Curing

All tests performed on specimens during curing were at a temperature of 70°F. Unconfined tests with repeated compressive axial stress levels of 2.5, 5, 7.5, 10, and 15 psi were performed on three different specimens. Each specimen was tested at ages of 20, 27, 48, and 120 days after compaction.

The modulus of the specimens was found to increase with age but remained approximately constant over the range of axial stress tested at each age. Poisson's ratio remained constant with age and axial stress level with an average value of 0.33. Since axial stress level had no significant effect on the material properties, the ATB can be considered to behave linearly under these uniaxial stress conditions.

The increase in modulus for the ATB specimens over a total of 120 days is shown in Figure 7. Although it would have been possible to test specimens shortly after compaction, equipment failure prevented such testing. It can be seen that an ultimate cure condition was achieved by 120 days of curing. The modulus increased from 70% of its ultimate value during the period of 20 days to 120 days of curing.

Ultimate Cure Properties

The properties of specimens tested at the ultimate cure condition are representative of the long-term equilibrium

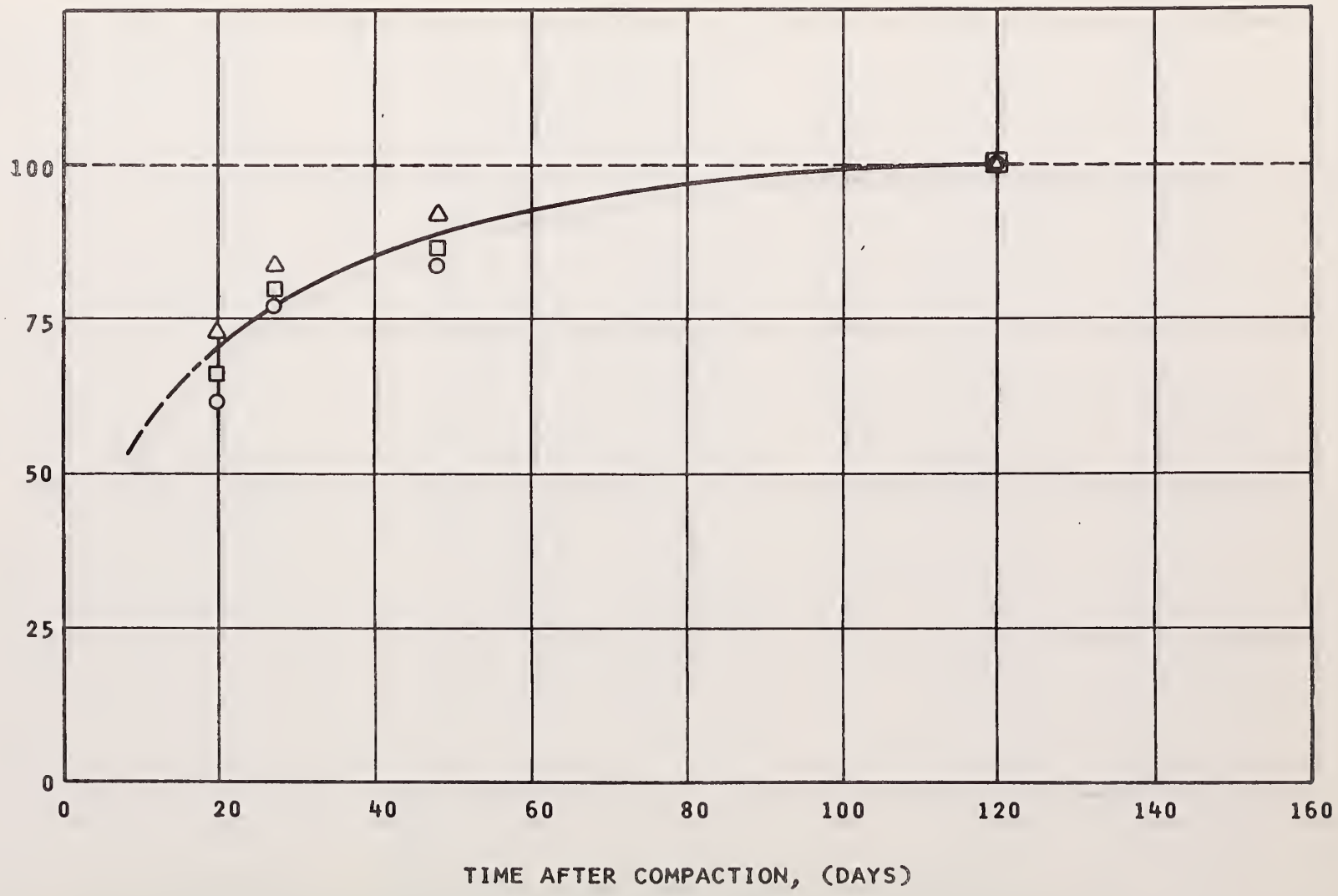

FIGURE 7 - INCREASE IN MODULUS OF ATB WITH AGE

properties of field materials. The test program performed on specimens at the ultimate cure condition is shown in Table 2. The range stresses utilized at each temperature were selected based on expected in-service stress conditions. For each temperature tested the degree of isotropy of the specimens was evaluated by applying repeated axial and radial stresses of equal magnitude.

For triaxial tests with equal axial and radial applied stresses the induced axial and circumferential strains are equal if the material is perfectly isotropic. The test results for isotropic applied stress conditions are shown in Figure 8. It is evident that the ATB specimens were not isotropic. The induced circumferential strains were approximately 3.5 times greater than the axial strains for all temperatures tested. This indicates that the specimens were stiffer in the axial direction than in the radial direction.

Similar results have been found for asphalt concrete specimens prepared with the same compaction equipment, MR&D (1972). It is felt that the specimen anisotropy is induced by the compaction equipment and procedure used to prepare the specimens. The degree of isotropy exhibited by ATB material compacted in the field is not known.

Undoubtedly, the ATB specimens prepared for this study could be more accurately characterized by cross-anisotropy rather than isotropy. However, an anisotropic characterization of the material was considered to be beyond the scope of this study. Furthermore, in view of the limited availability of anisotropic layered system boundary value solutions and the unknown degree of isotropy of ATB in field,

TABLE 2

ELASTIC CHARACTERIZATION TESTS ON ATB SPECIMENS AT ULTIMATE CURE

T = 40°F

REPEATED AXIAL STRESS $\Delta\sigma_{ZZ}$ (PSI) \ REPEATED RADIAL STRESS $\Delta\sigma_{RR}$ (PSI)	0	10	20	30	40	60
-15	X					
-10	X					
-5	X					
0		X	X			
10		X				
20		X	X			
30		X		X		
40			X	X	X	
60			X	X	X	X

T = 70°F

REPEATED AXIAL STRESS $\Delta\sigma_{ZZ}$ (PSI) \ REPEATED RADIAL STRESS $\Delta\sigma_{RR}$ (PSI)	0	10	20	30
-20	X			
-10	X			
-5	X			
0		X	X	
5	X			
10	X	X		
15	X			
20	X	X	X	
30		X		X
40			X	
50			X	

T = 100°F

REPEATED AXIAL STRESS $\Delta\sigma_{ZZ}$ (PSI) \ REPEATED RADIAL STRESS $\Delta\sigma_{RR}$ (PSI)	0	5	10
-5	X		
-2.5	X		
0		X	X
2.5	X		
5	X	X	
10		X	X
15		X	X

Note 1 - Minus sign denotes tension.

Note 2 - X indicates test performed.

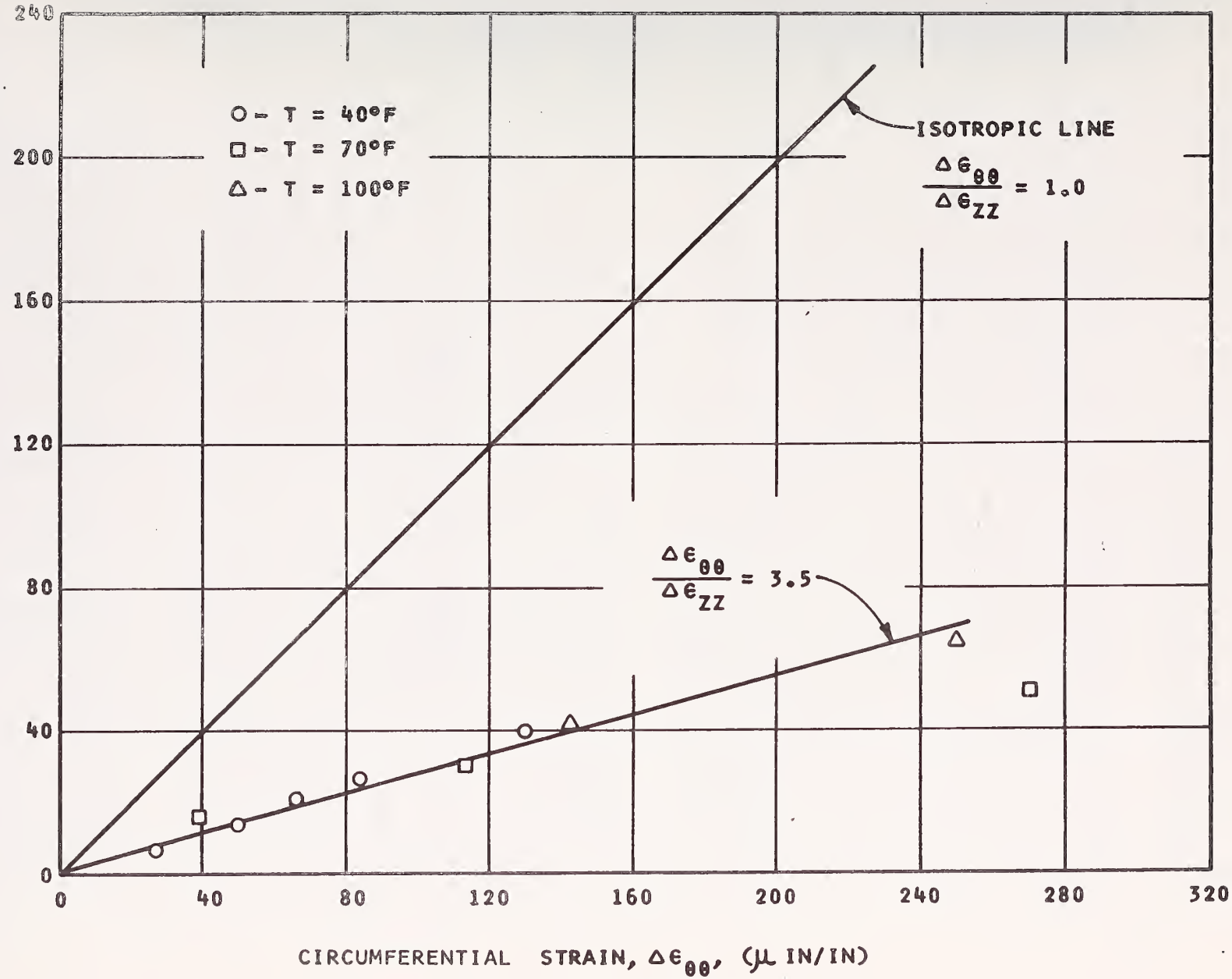

FIGURE 8 - EVALUATION OF SPECIMEN ISOTROPY USING ISOTROPIC APPLIED STRESS ($\Delta\sigma_{ZZ} = \Delta\sigma_{RR}$)

an anisotropic characterization was considered to be unwarranted at the present time.

The results of this study have been analyzed assuming the ATB to be isotropic. Thus, the effect of observed anisotropic behavior on the assumed isotropic properties can be evaluated. It should be noted that only material properties calculated for tests in which both axial and radial stresses were applied are affected by the isotropy assumption. Therefore, the same material properties would be calculated for uniaxial tests ($\sigma_{RR} = 0$) based on isotropic or cross-anisotropic behavior. However, an anisotropic characterization would recognize that the calculated material properties were only applicable for the specific specimen orientation.

The modulus of ATB specimens tested at 40, 70, and 100°F for uniaxial stress states is shown in Figure 9. The vertical bar at each test temperature indicates the total range of values determined for all tensile and compressive stress states tested. For small range of values at each temperature represents approximately a ±10% variation from the best fit line. This indicates that the ATB response is approximately linear with respect to uniaxial stress magnitude and that compressive and tensile properties can be considered equal. It can be seen that temperature has a major influence on modulus values. The modulus decreases from 500 ksi at 40°F to 62 ksi at 100°F.

Poisson's ratio values of the ATB for all stress levels of uniaxial testing were approximately constant at each test temperature. Furthermore, the values increased only slightly with increase in temperature. The average values

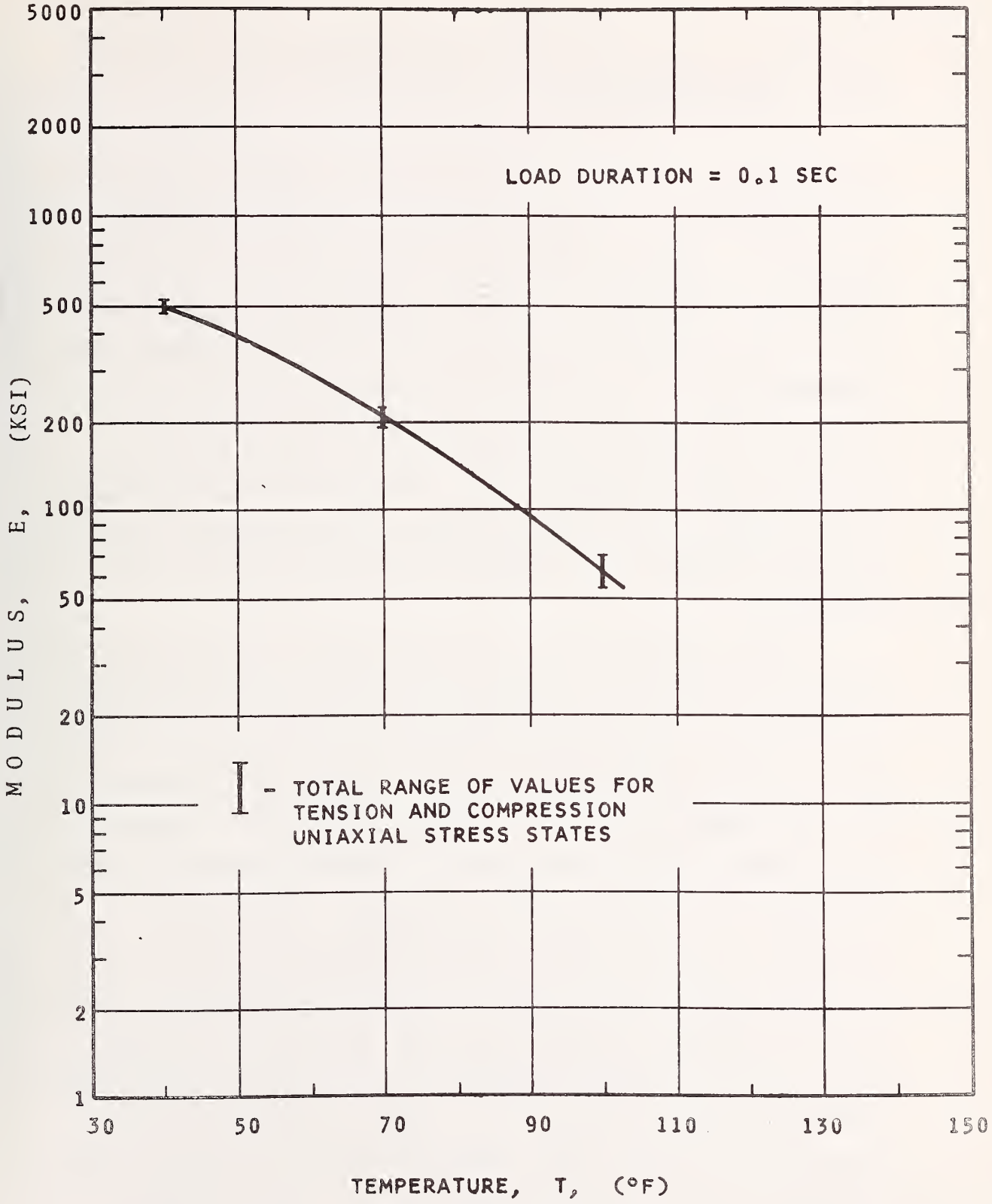

FIGURE 9 - TEMPERATURE INFLUENCE ON ATB MODULUS AT ULTIMATE CURE CONDITION

were 0.23, 0.24, and 0.31 at temperatures of 40, 70, and 100°F, respectively.

In addition to uniaxial tests, several repeated load tests were performed at each temperature where only radial stress was applied. Under these conditions, for assumed isotropic behavior, a modulus and Poisson's ratio can be calculated. While the isotropy assumption indicates that these values apply for all directions, the modulus value is primarily associated with the horizontal direction. These results indicated that both the assumed isotropic modulus and Poisson's ratio were approximately one-half the values determined from uniaxial tests. This reflects the anisotropic nature of the ATB specimens shown in Figure 8 where the ATB specimens were found to be stiffer in the axial direction.

Repeated load tests for which axial and radial stresses were simultaneously applied were also performed at each temperature. A specimen modulus and Poisson's ratio can be calculated for assumed specimen isotropy. However, the calculated isotropic material properties for these test conditions were very erratic and sometimes physically meaningless. This indicates that anisotropic behavior strongly influenced these test results. Each of the measured axial and circumferential strains consists of two components associated with modular and Poisson response in each direction. If the modulus and Poisson's ratio values are significantly different in each direction, the assumed isotropic behavior can lead to very inaccurate separation of each strain component and, therefore, inconsistent isotropic material properties. These results indicated that the degree of anisotropy exhibited by ATB

specimens preclude determination of assumed isotropic material properties when both axial and radial stresses are applied.

Determination of Viscoelastic Properties

Creep tests were performed on ATB specimens at 40, 70, and 100°F. These tests were performed to define the time-dependent behavior of ATB. The complete testing program conducted is shown in Table 3. Uniaxial and confined creep tests were performed at each temperature. Uniaxial tensile creep tests were attempted at each temperature; however, results were only obtained at 40°F. Repeated attempts for the higher temperatures were unsuccessful due to separation at the epoxy bond between the specimen and end platens.

For creep tests the applied stress state remained applied to the specimens for twenty minutes. Since this duration of load is much longer than that normally occurring in the field for moving traffic, a trade-off between applied stress and induced strains must be made to keep both stresses and strains typical of in-service values. For the higher values of stress typical of in-service conditions, strains greater than in-service values would be induced. Therefore, a compromise was made and the lower range of stress states typical of in-service conditions were tested at each temperature. The resulting maximum strain values (μ in/in) after twenty minutes of load application for each test temperature were:

$$T = 40°F,\ -175 < \varepsilon_{zz} < 420,\ -45 < \varepsilon_{\theta\theta} < 100;$$

$$T = 70°F,\ \varepsilon_{zz} < 840,\ -260 < \varepsilon_{\theta\theta} < 365;$$

TABLE 3

CREEP TESTS ON ATB SPECIMENS

AT ULTIMATE CURE

$T = 40^{\circ}F$

AXIAL STRESS σ_{zz} (PSI)	RADIAL STRESS σ_{RR} (PSI)	
	0	15
-15	X	
10	X	
20	X	
30		X

$T = 70^{\circ}F$

AXIAL STRESS σ_{zz} (PSI)	RADIAL STRESS σ_{RR} (PSI)	
	0	5
2.5	X	
5	X	
10	X	X

$T = 100^{\circ}F$

AXIAL STRESS σ_{zz} (PSI)	RADIAL STRESS σ_{RR} (PSI)	
	0	2.5
2.5	X	
5	X	X

$$T = 100°F,\ \varepsilon_{zz} < 800,\ -330 < \varepsilon_{\theta\theta} < 155.$$

These maximum values of strains are reasonably consistent with the maximum strain values expected for in-service materials for moving wheel loads. Thus, both applied stresses and induced strains for the creep testing program were compatible with expected in-service values for ATB material.

The results of the creep testing program were analyzed as if the ATB material behaved isotropically for the same reasons discussed in the elastic characterization section. The data obtained for each creep test can be presented in several forms. For linear isotropic viscoelastic materials, two creep compliance functions are needed to completely describe specimen behavior. This is analogous to linear isotropic elasticity where any two elastic constants completely characterize the material (Young's modulus, Poisson's ratio, shear modulus, or bulk modulus.) The layered isotropic linear viscoelastic boundary value representation of a pavement system under development by FHWA (VESYS II) requires a modular creep compliance for material property input. Therefore, the results of creep tests are presented in the form of modular creep compliance and time-dependent Poisson's ratio. For triaxial stress conditions these two linear viscoelastic creep compliance functions are defined by the equations:

$$\Psi_{EZ}(t) = \text{Modular Creep Compliance}$$

$$\Psi_{EZ}(t) = \frac{\varepsilon_{zz}(t)}{\sigma_{zz} - 2\upsilon(t)\sigma_{rr}} \qquad (1)$$

ν (t) = Poisson's ratio

$$\nu(t) = \frac{\varepsilon_{\theta\theta}(t)\,\sigma_{zz} - \varepsilon_{zz}(t)\,\sigma_{rr}}{2\,\varepsilon_{\theta\theta}(t)\,\sigma_{rr} - \varepsilon_{zz}(t)\,(\sigma_{zz} + \sigma_{rr})} \qquad (2)$$

Modular Creep Compliance

The modular creep compliance data for a temperature of 40°F are shown in Figure 10. Results for uniaxial compressive tests at two levels of axial stress and a uniaxial tensile test can be considered to define one modular creep compliance function. This indicates that at 40°F the material behavior during loading is linear with respect to uniaxial stress states. The results for the confined compressive creep test fall below and are approximately parallel to the uniaxial curve.

Figure 11 shows the modular creep compliance results at a temperature of 70°F. The compressive uniaxial test results at three levels of stress approximately superpose indicating linear behavior with respect to compressive stress level in uniaxial tests. The results for confined compressive tests fall below the uniaxial results.

The modular creep compliance results at a temperature of 100°F are shown in Figure 12. As for 40 and 70°F test results, the compressive uniaxial results indicate linear behavior with respect to stress level. The confined compressive test results are only slightly below the uniaxial curve at 100°F.

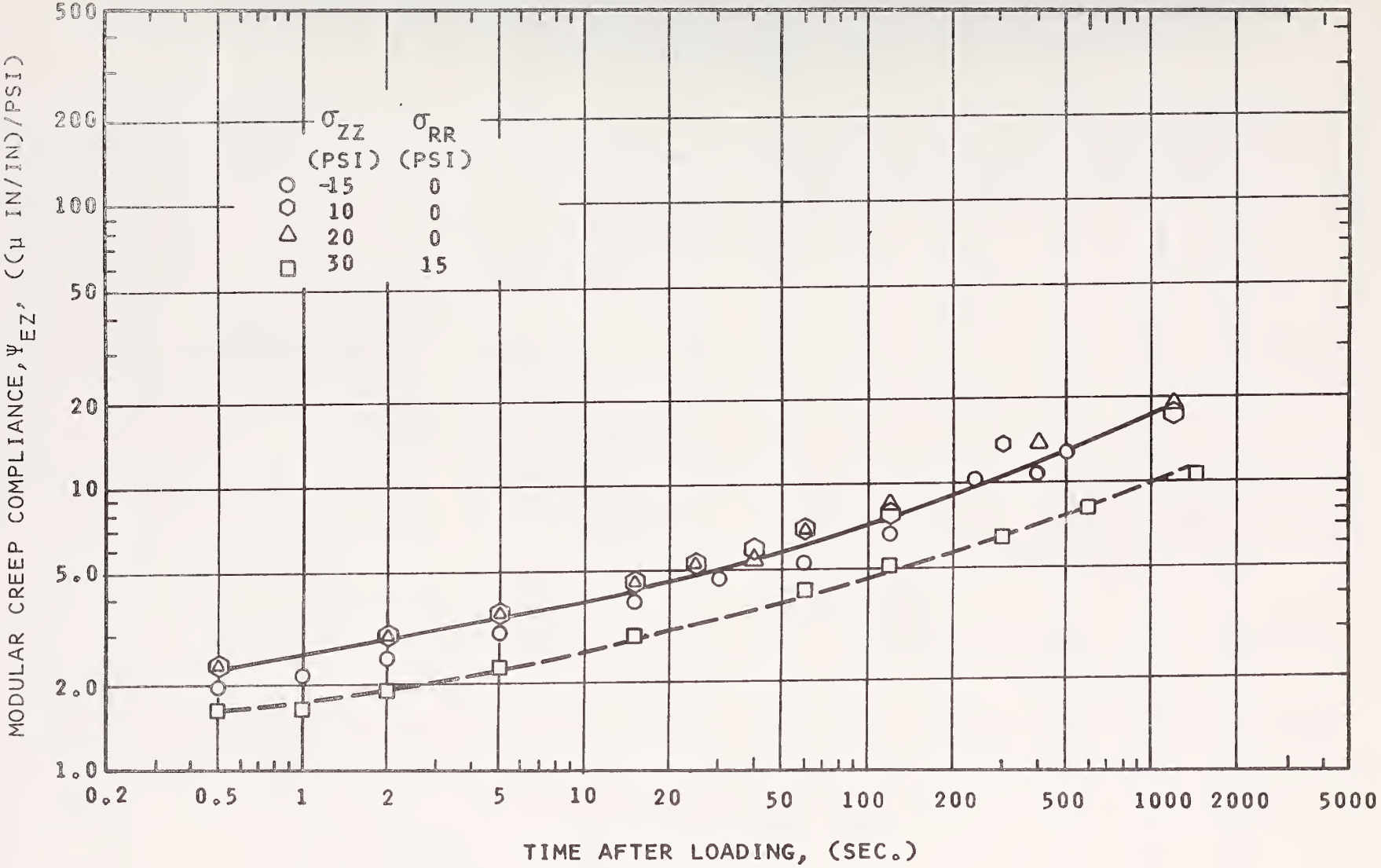

FIGURE 10 - MODULAR CREEP COMPLIANCE FOR ATB AT ULTIMATE CURE AT T = 40°F

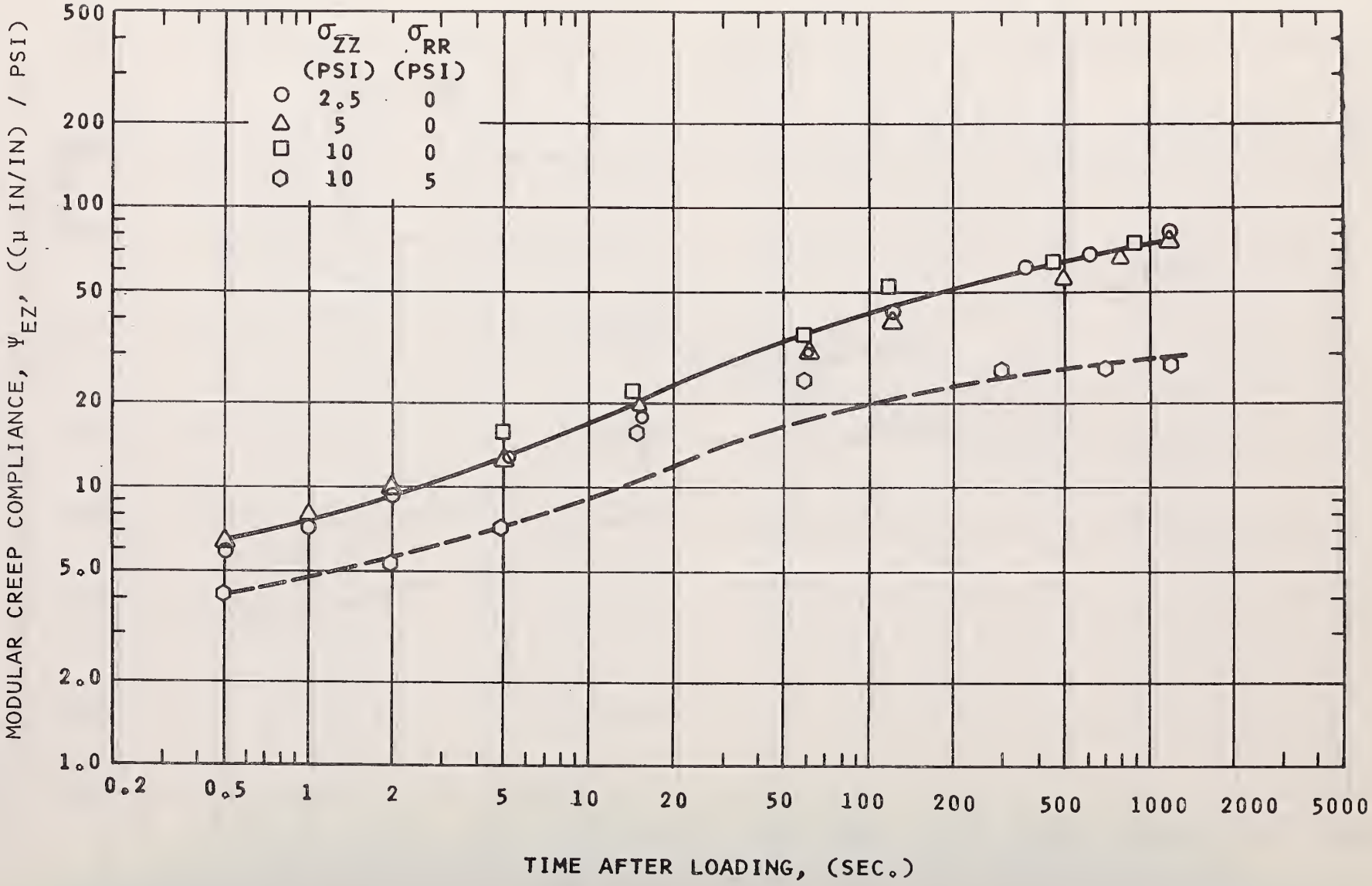

FIGURE 11 - MODULAR CREEP COMPLIANCE FOR ATB AT ULTIMATE CURE AT T = 70°F

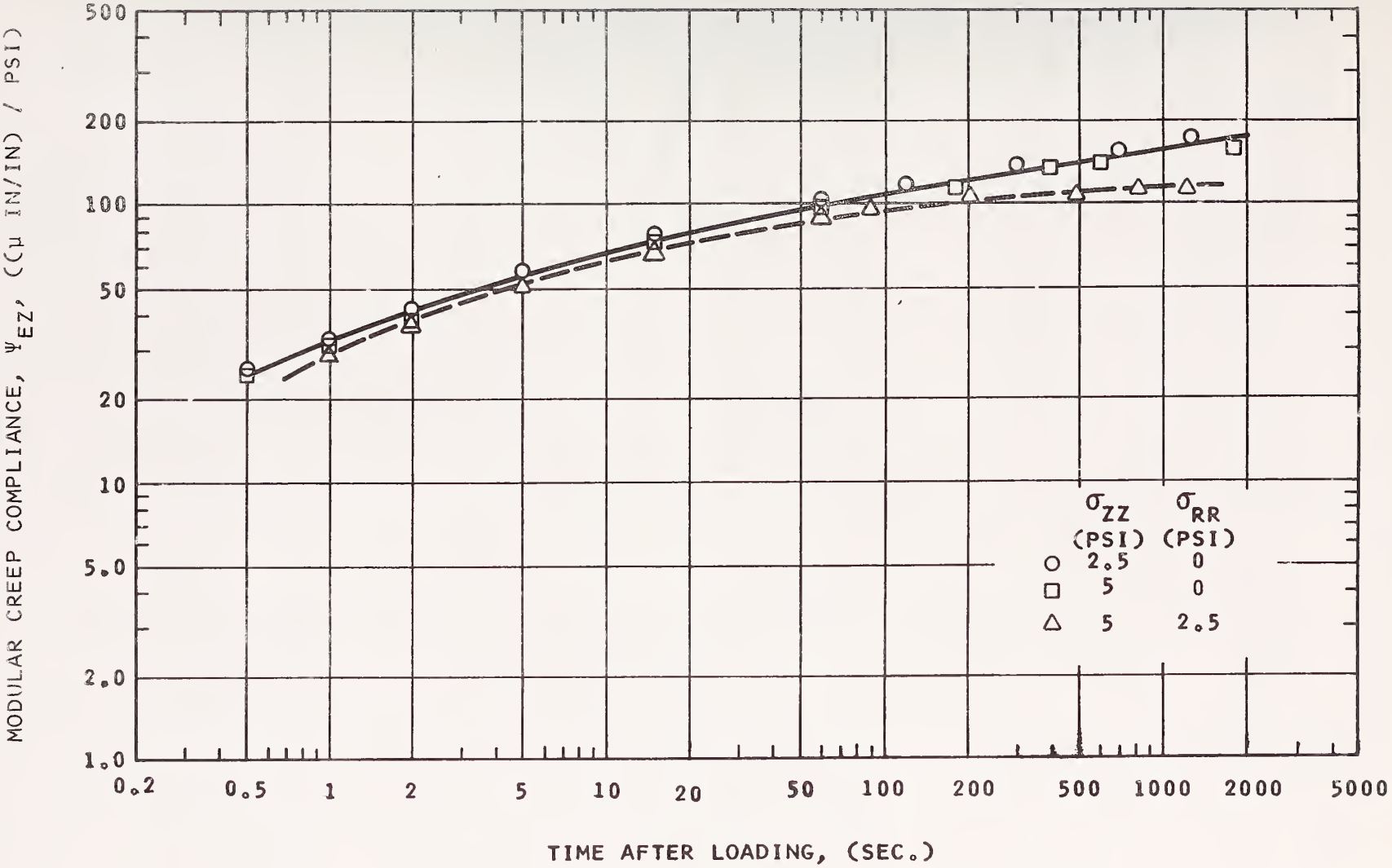

FIGURE 12 - MODULAR CREEP COMPLIANCE FOR ATB AT ULTIMATE CURE AT T = 100°F

Poisson's Ratio

On the basis of creep data obtained from confined and unconfined tests, Poisson's ratio was determined as a function of time. These results are presented in Figures 13, 14, and 15 for temperatures of 40, 70, and 100°F, respectively. Although the results for unconfined uniaxial tests are somewhat scattered, they generally lie within a reasonably narrow band. The Poisson ratio values determined for confined tests are considerably different from those of uniaxial tests.

At temperatures of 40 and 70°F the uniaxial results indicate that Poisson's ratio decreases slightly with increased time of loading. However, considering the scatter of the results and magnitude of change with time, Poisson's ratio could be approximated to be a constant value independent of time. For uniaxial results an average constant value of 0.25 at 40°F and 0.30 at 70°F would represent the majority of the data within a range variation of ± 0.05 from the average value. Generally, a change of ± 0.05 in Poisson's ratio will not significantly affect calculated pavement responses. The Poisson's ratio values for confined tests at 40°F and 70°F were somewhat erratic and considerably less than those of uniaxial tests.

The Poisson ratio values at 100°F are similar for both uniaxial and confined tests for times after loading less than approximately 20 seconds with a value of 0.28. For longer load durations the uniaxial results indicate an increasing value and confined results, a decreasing value.

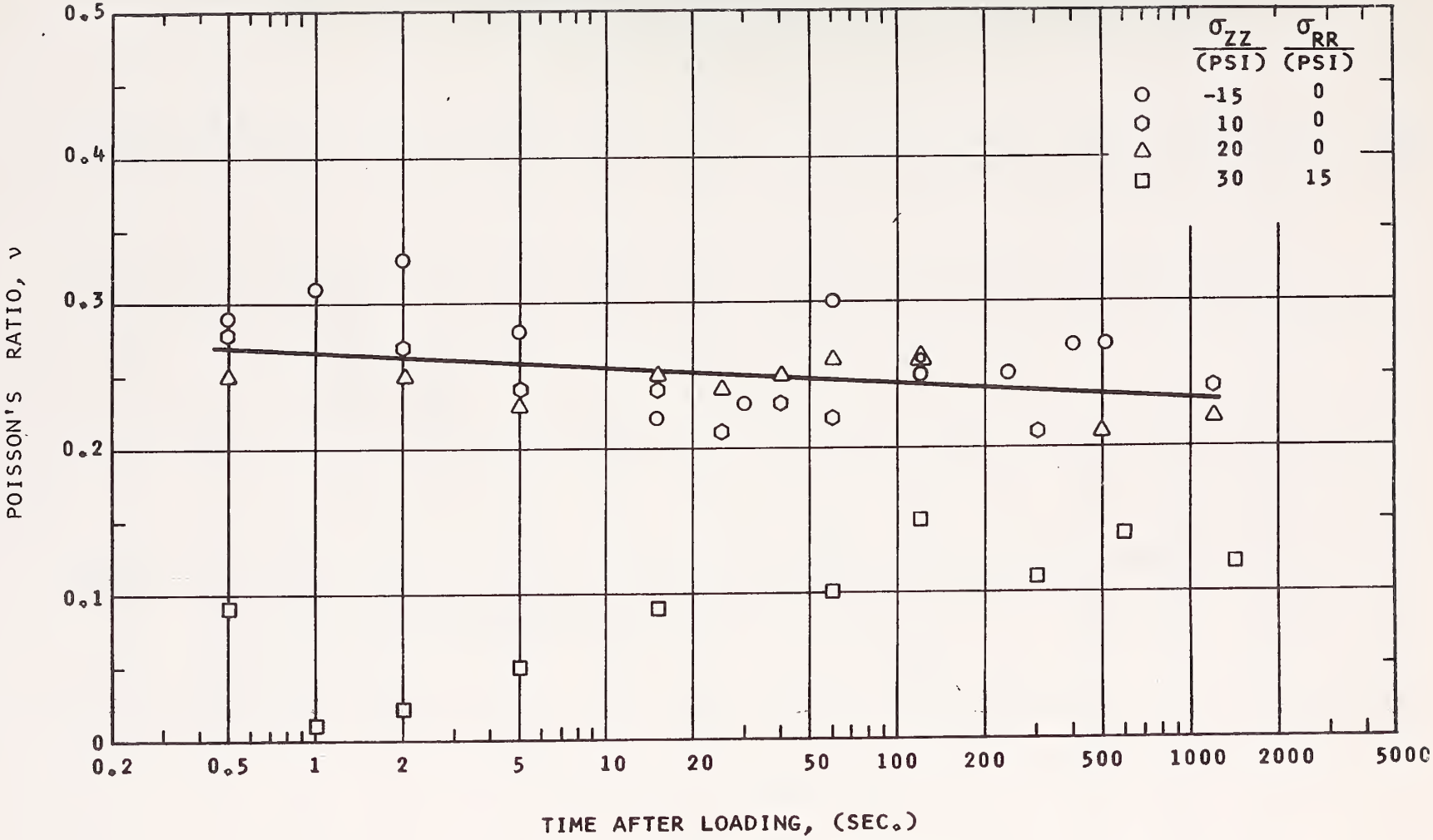

FIGURE 13 - POISSON'S RATIO FOR ATB AT ULTIMATE CURE AT T = 40°F

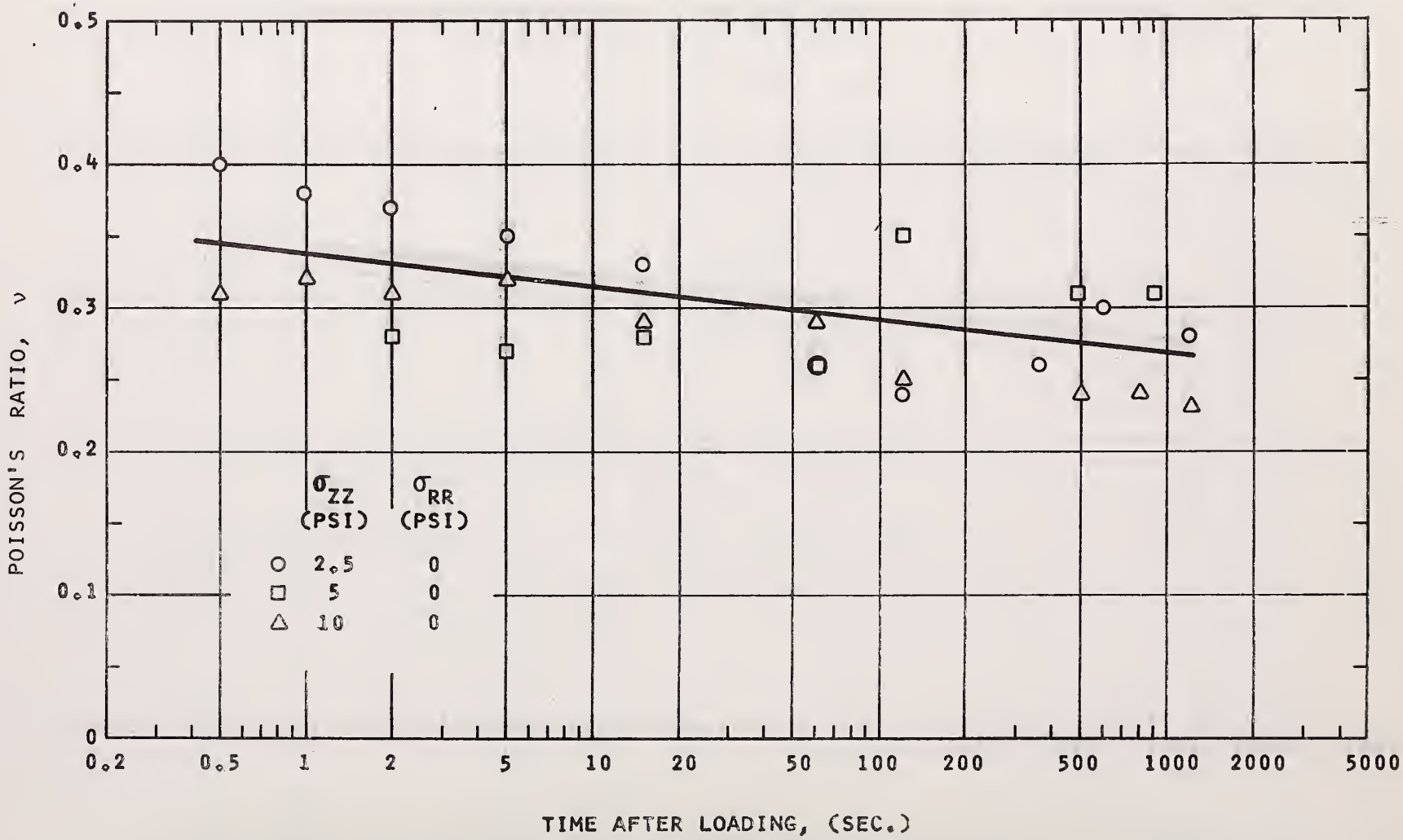

FIGURE 14 - POISSON'S RATIO FOR ATB AT ULTIMATE CURE AT T = 70°F

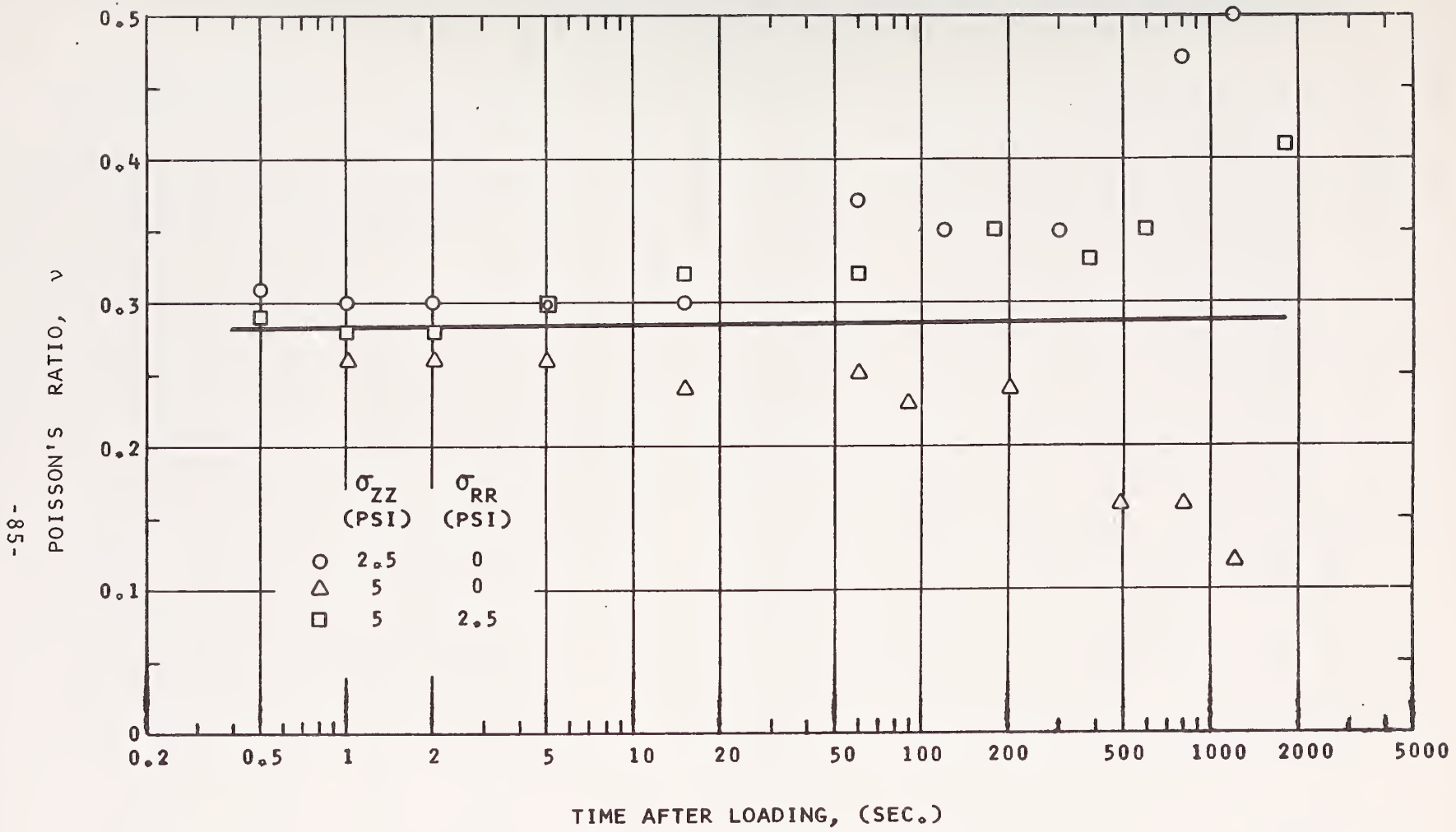

FIGURE 15 - POISSON'S RATIO FOR ATB AT ULTIMATE CURE AT T = 100°F

Time-Temperature Equivalency

The time-temperature equivalency of modular creep compliance determined for uniaxial stress conditions was evaluated for results obtained at temperatures of 40, 70, and 100°F. All results were shifted horizontally along the time scale to a reference temperature of 70°F. The resulting master modular creep compliance curve obtained is shown in Figure 16. It can be seen that results from different temperatures can be shifted to obtain one smooth curve. Thus, a well-defined equivalency between time and temperature exists for ATB material.

The amount of horizontal time scale shift required to obtain the master curve is indacated in Figure 17. The shift factor, a_T, is defined by:

$$a_T = \frac{t_T}{t_{T_o}}$$

where: t_T = time to obtain value of material property at temperature T.

t_{T_o} = time to obtain same value of material property at reference temperature T_o.

By definition, no shift of the material properties is required at the reference temperature. For temperatures other than the reference temperature the time scale of the master curve must be multiplied by the shift factor applicable to that temperature. Figure 17 defines the

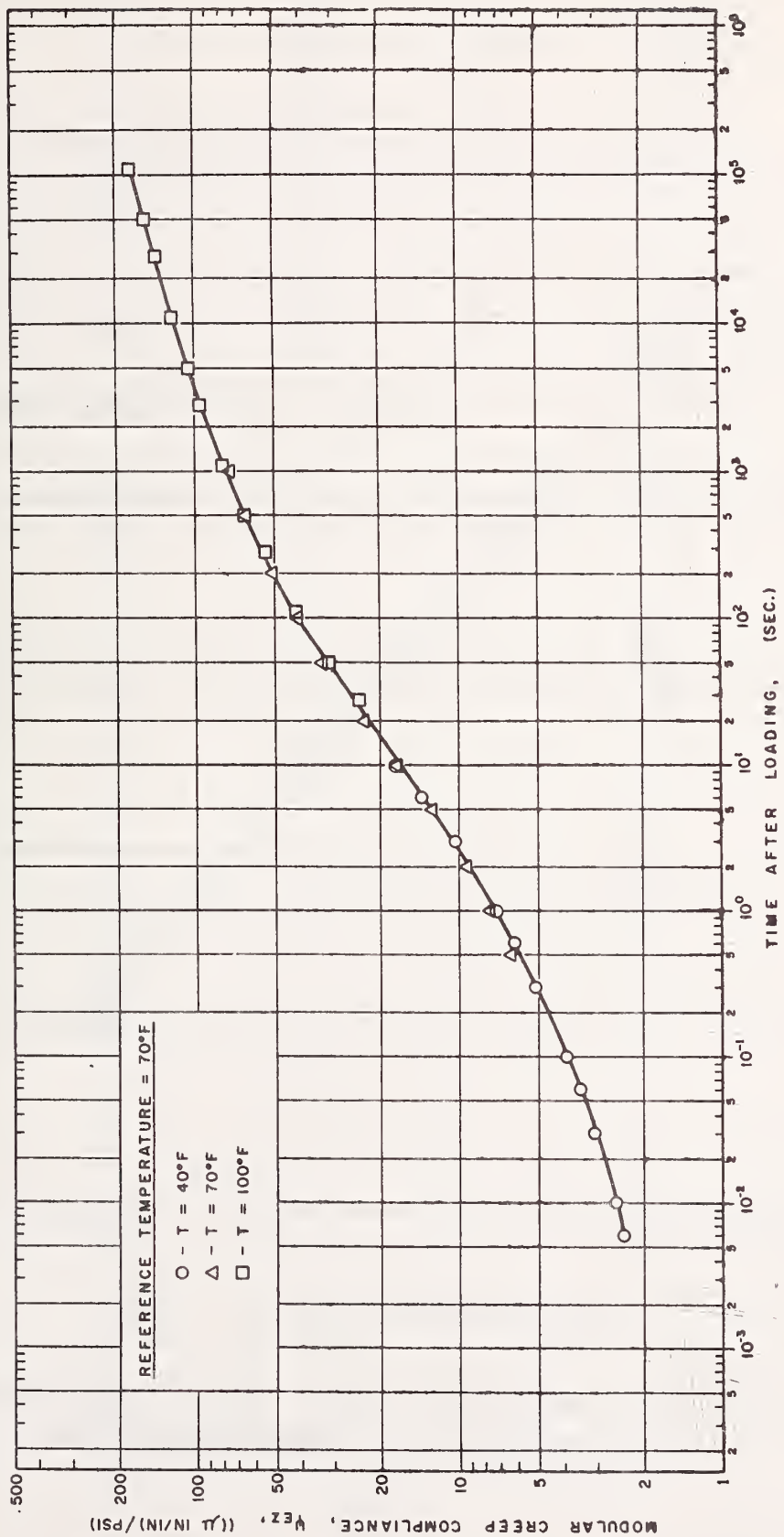

FIGURE 16 - MASTER MODULAR CREEP COMPLIANCE FOR ASPHALT TREATED BASE COURSE AT ULTIMATE CURE AND UNCONFINED STRESS STATES.

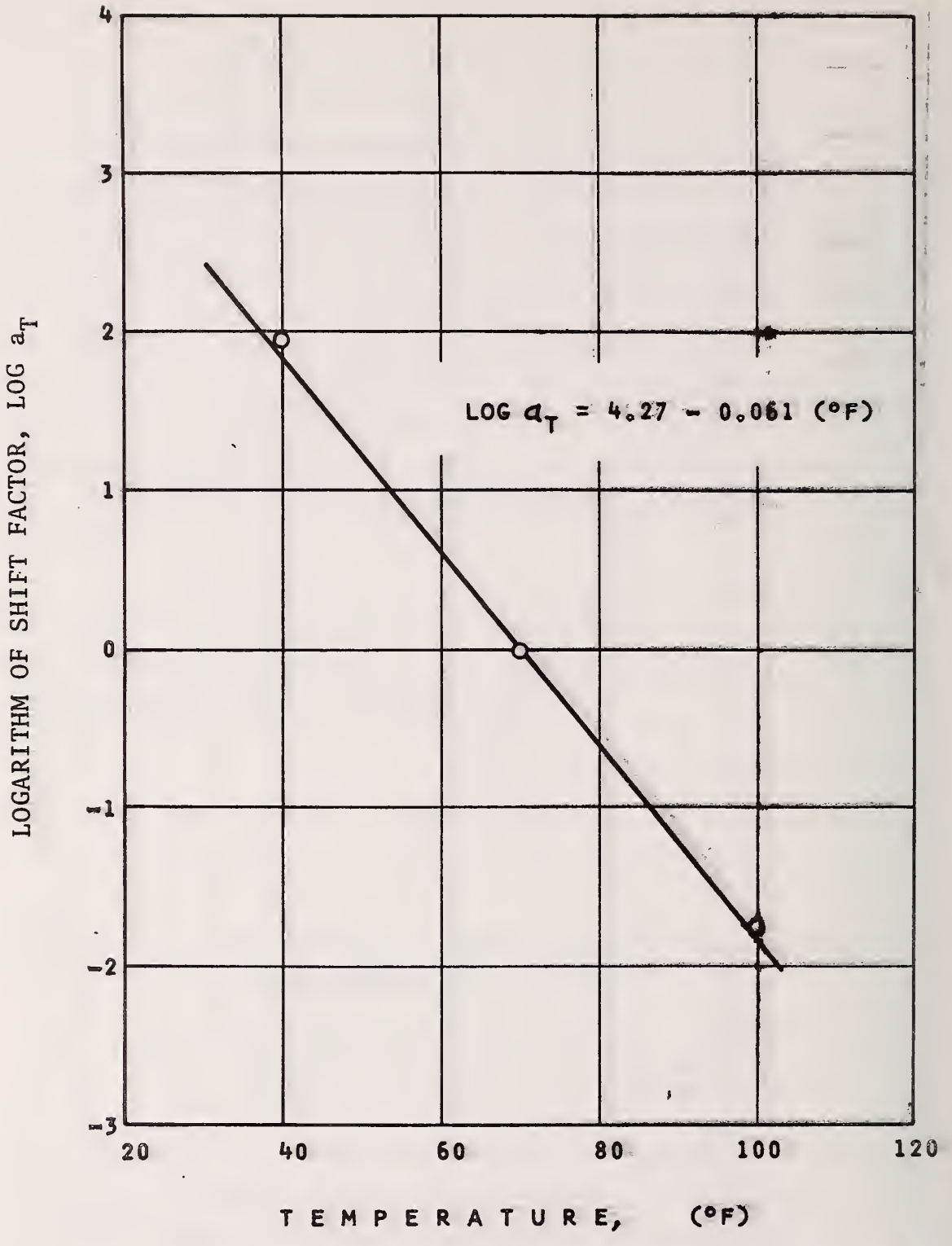

FIGURE 17 - TIME-TEMPERATURE SHIFT FACTOR, a_{T_u}, FOR ATB AT ULTIMATE CURE (REFERENCE TEMPERATURE = 70°F)

the value of the shift factor as a function of temperature for a reference temperature of 70°F.

Fatigue Failure Criteria

The results of the fatigue testing program on ATB at ultimate curve are shown in Figure 18. It can be seen that the fatigue life (number of repetitions to failure) decreases with increase in the magnitude of the repetitively imposed tensile strain. The fatigue failure relationship can be represented by a straight line on a log-log plot of tensile strain vs. number of repetitions to failure. This form of fatigue failure criteria has also been applied to asphalt concrete.

The best fit linear regression line of data is shown on Figure 18. The equation of the best fit line was:

$$N_f = 4.36 \times 10^{-8} \, (1/\varepsilon)^{3.47}$$

A correlation coefficient of 0.93 indicates a good fit by the log-log straight line relationship. The standard measures of regression error are also indicated on Figure 18 and are measures of the statistical reliability of the fatigue failure line.

DISCUSSION OF TEST RESULTS

The discussion of the test results is subdivided into the two basic components of material characterization: (i) Constitutive Properties and (ii) Failure Criteria. The implications of all test results have been coalesced and are discussed where relevant.

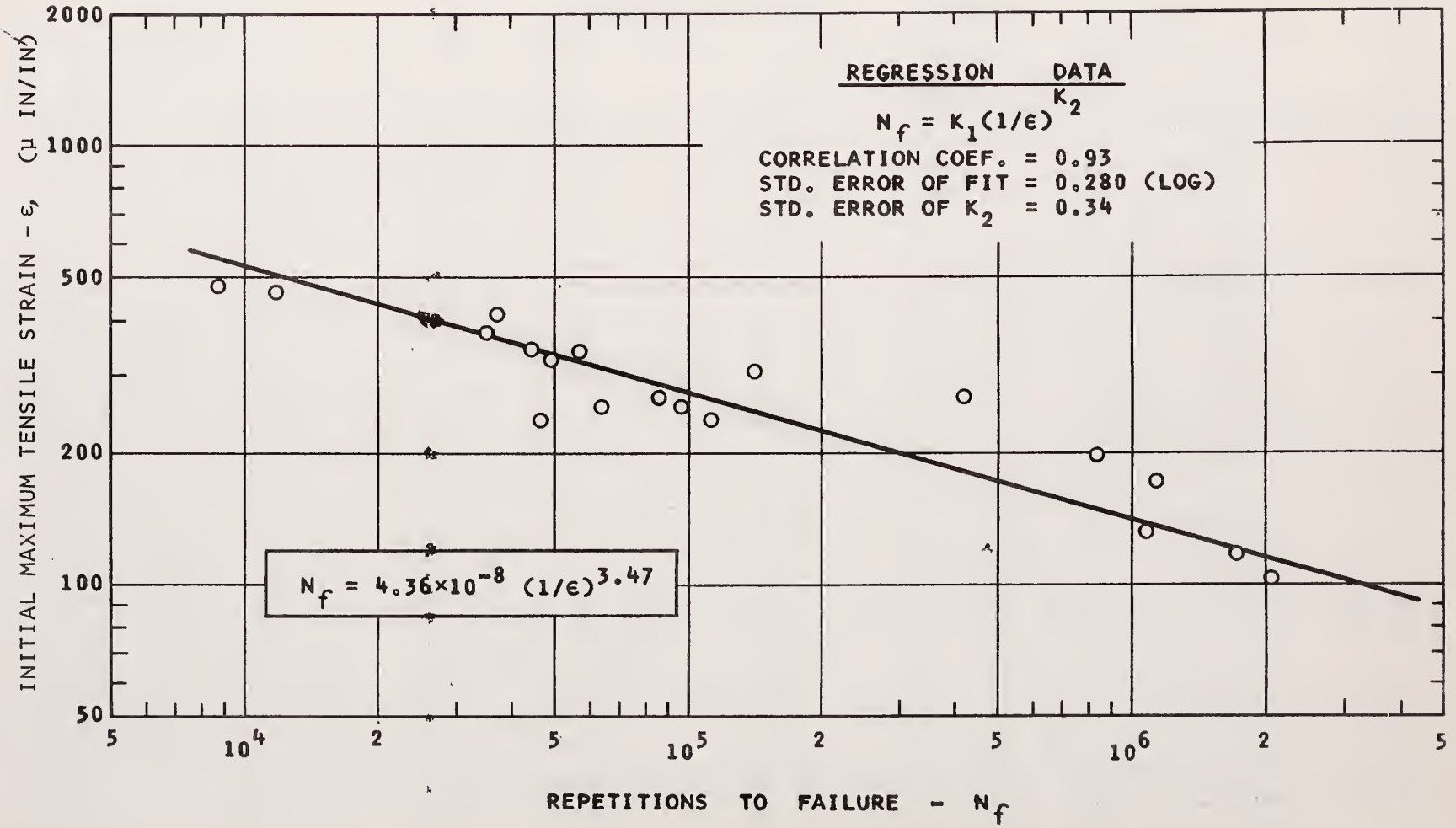

FIGURE 18 - FATIGUE FAILURE CRITERIA FOR ASPHALT-TREATED BASE COURSE MATERIAL, T = 70°F

Constitutive Properties

The constitutive properties of ATB have been found to be influenced by a number of factors. The effects of: (i) Curing, (ii) Temperature, (iii) Load Duration, (iv) Degree of Isotropy, (v) Stress State, and (vi) Stress Level on the constitutive properties are individually discussed.

Curing

The properties of ATB are influenced by the degree to which curing has progressed. Time is required for volatiles present in the CMS-2S asphalt emulsion to evaporate. When all volatiles have evaporated, an ultimate cure condition is achieved at which time curing effects no longer influence the material properties. The time to achieve an ultimate cure condition for ATB is dependent on many factors including: (1) temperature and moisture environment, (ii) density of the mix, and (iii) distance of points in the ATB from a point at which evaporating volatiles can escape.

In this study curing was investigated under one controlled moisture and temperature environment (70°F and 50% relative humidity). The effect of curing was reflected by the change in modulus of the ATB with age (time after compaction) of the specimens. The modulus of the ATB specimens increased with age until an ultimate cure condition was achieved at approximately 120 days.

The modulus at 70°F increased from approximately 140 ksi after 20 days of curing to 200 ksi at the ultimate cure condition. Poisson's ratio remained approximately constant

with age at a value of 0.3. As noted above, the time to achieve an ultimate cure condition could substantially increase or decrease for curing conditions different from those used in this study. Therefore, the factors controlling the rate of curing must be carefully evaluated for each situation in which ATB is used to establish the time required to achieve ultimate cure.

The emphasis of ATB characterization testing in this study was on the properties at an ultimate cure condition. Although the ATB properties at ages less than 20 days were not determined in this study, previous work by Terrel (1967) with material treated with the same asphalt emulsion indicated that immediately after compaction the ATB behavior was similar to that of an untreated granular material. Therefore, the modulus of the ATB material would be substantially less than the values found in this investigation. For the analysis of pavements during its early life, ATB material properties representative of short curing times should be utilized. Immediately after compaction ATB material properties similar to those of untreated granular base course material presented earlier in this report should be used. As time progresses and curing takes place, increasingly higher modulus values intermediate between those of untreated material and an ultimate cure condition can be utilized. When curing is complete the ultimate cure properties discussed in the remainder of this section are applicable.

Temperature

Temperature has been found to exert a major influence on the ultimate cure constitutive properties of ATB. The

effect of temperature on the elastic modulus of ATB for 0.1 second load duration is shown in Figure 9. The modulus decreases dramatically with increase in temperature with average values of 490, 210, and 62 ksi at temperatures of 40, 70, and 100°F, respectively. Poisson's ratio increased only slightly with increase in temperature with average values of 0.23, 0.24, and 0.31 at temperatures of 40, 70, and 100°F, respectively.

A comparison of the temperature dependence of ATB and asphalt concrete moduli is shown in Figure 19. The asphalt concrete moduli values shown are those reported by Nair & Chang (1970). The modulus for ATB is less than that of asphalt concrete but the difference decreases with increase in temperature. At 100°F the two modulus values are approximately equal.

The results from creep tests at the three test temperatures also reflect the major influence of temperature on the modular creep compliance, Ψ_{EZ}. Figures 10, 11, and 12 show the modular creep compliance curves at 40, 70, and 100°F, respectively. At a given time after loading for each temperature, the modular creep compliance value increases with increase in temperature. For example, at a load duration of 1 second the modular creep compliance values were 2.6, 7.6, and 32 (μ in/in)/psi for temperatures of 40, 70, and 100°F, respectively.

The creep test results revealed that Poisson's ratio could be approximated as independent of time at each test temperature. Furthermore, the Poisson ratio value was not significantly influenced by temperature. An average constant

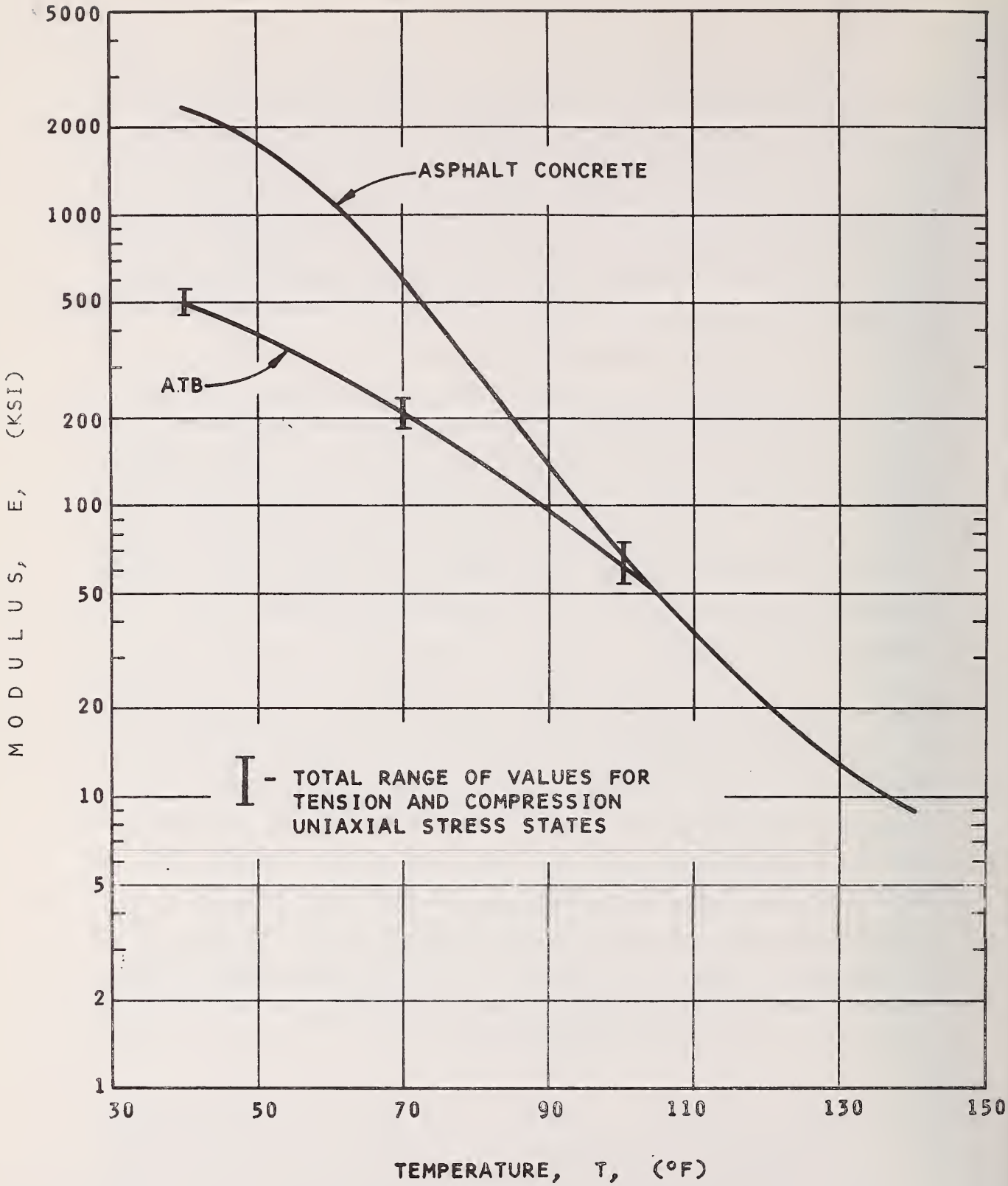

FIGURE 19 - COMPARISON OF ASPHALT CONCRETE AND ATB ULTIMATE CURE MODULI

value of approximately 0.3 would be an adequate description of the test results at all three temperatures.

Load Duration

The effect of load duration on the ATB constitutive properties can be determined from the creep test results. At a given temperature, the modular creep compliance increases with increases in load duration. The increase in Ψ_{EZ} over the total twenty-minute load duration at each test temperature is dramatic. However, for the range of load durations representative of moving loads on pavements at a given temperature the effects are much smaller.

A comparison of the master modular creep compliance curves for ATB and asphalt concrete (MR&D, 1972) is shown in Figure 20. The master curve for ATB is above that of the asphalt concrete. This indicates that for a given time of loading and applied stress the ATB will have more induced strain than asphalt concrete. The difference between the two master curves decreases with increasing time of loading (increasing temperature). These results are in agreement with those for elastic modulus shown in Figure 19 where the difference in modulus values for ATB and asphalt concrete decreased with increase in temperature with approximately equal moduli values at 100°F.

The effects of load duration and temperature on the modular creep compliance were found to be interrelated and an equivalency between both was established. The equivalency between time and temperature allowed construction of the master modular creep compliance curve shown in Figure 16. The amount of horizontal shift along the time

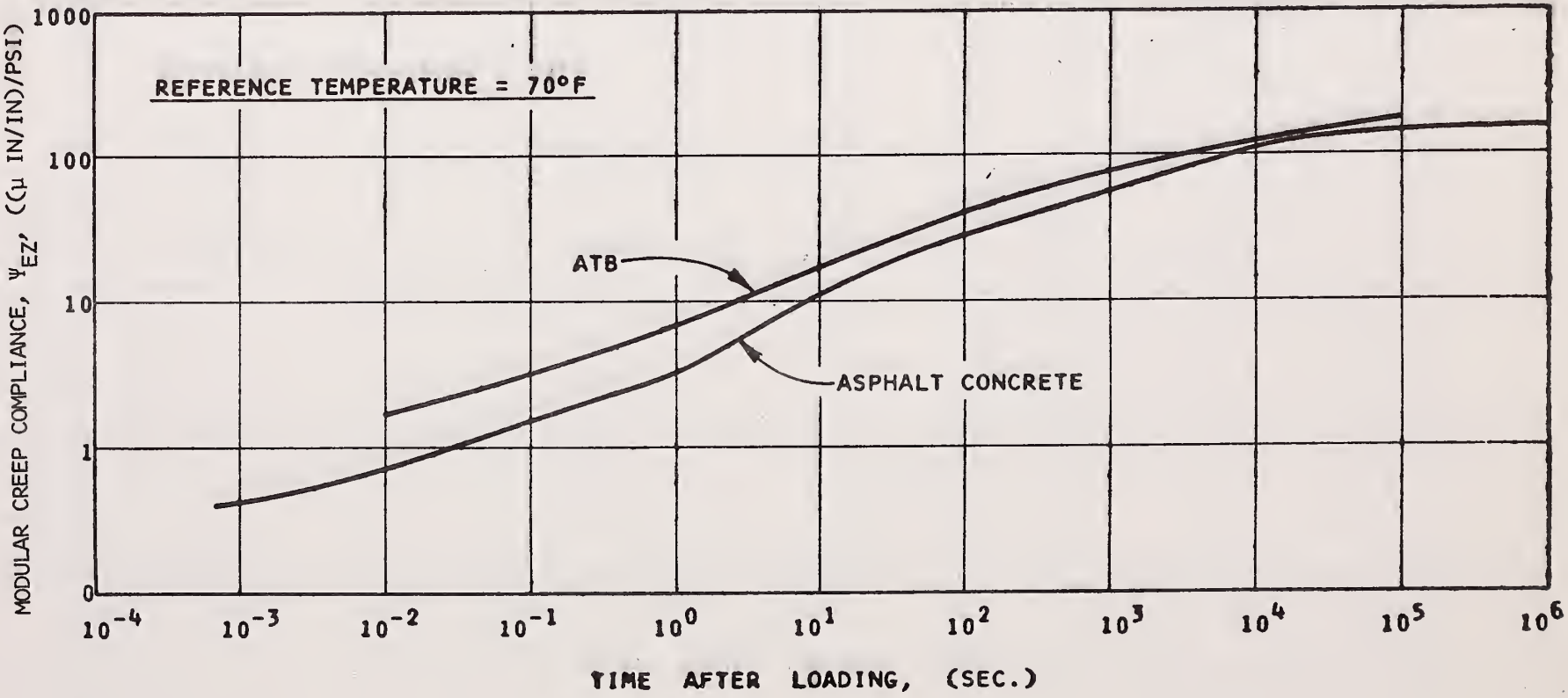

FIGURE 20 - COMPARISON OF ASPHALT CONCRETE AND ATB ULTIMATE CURE MASTER MODULAR CREEP COMPLIANCES

scale required to attain the master curve from the results at each temperature is depicted in Figure 17. For a reference temperature of 70°F the shift factor, A_T, for 40°F was 90 (log 90 = 1.95) and for 100°F was 0.018 (log 0.018 = -1.75). This indicates that the same value of modular creep compliance would occur at a given load duration, t, at 70°F as would occur at load durations of 90t at 40°F and 0.018t 100°F. Thus, a given modular creep compliance would occur at a much shorter load duration at 100°F than at 70 or 40°F.

A common assumption in linear viscoelastic analysis is that of thermorheologically simple material behavior. If all linear viscoelastic material properties can be shifted along the time scale by the same amount for each temperature change, the material is called thermorheologically simple. The shift function found for the modular creep compliance is described above. Since it was found that Poisson's ratio was approximately independent of time and temperature, Poisson's ratio for ATB can be approximated as a constant value. Since Poisson's ratio is a constant value, the time-temperature shift function has no effect on its value. Therefore, the shift function found for the modular creep compliance can also be applied to Poisson's ratio and the ATB behavior can be considered thermorheologically simple.

The master modular creep compliance curve and shift factors can be used to estimate the effect of load duration on the ATB 'modulus' at given temperature. Using a similar engineering approximation to that suggested by Van Der Poel (1954), the 'modulus' can be estimated from the creep compliance curve as $E \simeq 1/\Psi_{EZ}$ for a given

temperature and load duration. For example, at 70°F the modulus for a load duration of 0.1 second would be estimated to be:

$$E \simeq 1/\Psi_{EZ} = 1/3.9 \times 10^{-6} = 256 \text{ ksi}$$

The value measured in the repeated load tests at the same load duration was 210 ksi. Similarly, using the master creep curve and shift factor for 100°F, the modulus at a load duration of 0.1 second would be estimated at 76 ksi as compared to the repeated load test value of 62 psi. The degree of agreement between the estimated and measured values is sufficient to utilize for examination of the effect on modulus of small changes of load duration at each test temperature.

At a temperature of 70°F the estimated modulus values for load durations of 0.01, 0.05, and 0.1 seconds are 392, 303, and 256 ksi, respectively. At 100°F similar modulus estimates are 163, 95, and 76 ksi for the same load durations. The range of load durations is representative of those that might be expected for in-service ATB material under moving traffic loads, Barksdale (1971). The magnitude of the $1/\Psi_{EZ}$ changes indicate that the duration of load can have a significant influence on the ATB response characteristics.

Degree of Isotropy

The degree of isotropy exhibited by ATB specimens is an important consideration when selecting a constitutive relationship. The isotropy of ATB specimens was experimentally evaluated using repeated load tests of 0.1 second

load duration for all temperatures tested. The results of these tests are shown in Figure 8 and indicate that the ATB material was substantially stiffer in the axial direction than in the radial direction. This indicates that the ATB specimens tested would be best represented by an anisotropic constitutive theory such as cross-anisotropy. However, an anisotropic characterization was beyond the scope of this investigation.

The ATB specimen anisotropy is influenced by the compaction technique. While the laboratory compacted specimens were anisotropic, field compacted ATB may not be. The degree of isotropy exhibited by field compacted ATB material is not known. Until such information is available, an anisotropic characterization of laboratory compacted specimens would appear unwarranted. The experimental results obtained in this study were analyzed using isotropic theory. Thus, the effect of observed anisotropic behavior on assumed isotropic properties can be evaluated.

Stress State

The stress states under which ATB specimens were tested can be subdivided into four categories: (i) uniaxial compression (σ_{ZZ} = comp., σ_{RR} = 0), (ii) uniaxial tension (σ_{ZZ} = tension, σ_{RR} = 0), (iii) uniradial compression (σ_{ZZ} = 0, σ_{RR} = comp.), and (iv) confined compression (σ_{ZZ} = comp., σ_{RR} = comp.). The numerous stress states tested allows evaluation of their effect on the constitutive properties.

Repeated load tests at 40, 70, and 100°F indicated that the ATB constitutive properties for uniaxial compression and tension stress states were very similar. The small

range in modular values at each test temperature is indicated in Figure 19. Creep test results at 40°F were also the same for uniaxial tension and compression as shown in Figures 10 and 13. Although uniaxial tensile creep tests at higher temperatures could not be performed, it is felt that these tests might have indicated some difference in material properties from those of uniaxial compressive tests as such behavior was found for asphalt concrete in a previous study, MR&D (1972).

Repeated load tests in which only the radial stress is cycled indicated that both the calculated values of modulus and Poisson's ratio were approximately one-half those found in uniaxial stress states. This reflects the anisotropic character of the ATB specimens shown in Figure 8 where the ATB specimens were found to be stiffer in the axial direction than in the radial direction.

The ATB constitutive properties determined from confined stress states were substantially different from those determined in uniaxial stress states. For repeated load tests in which axial and radial stresses were simultaneously applied the calculated values of modulus and Poisson's ratio at each temperature were very erratic and sometimes physically meaningless. These results indicated that the degree of anisotropy exhibited by the ATB specimens precludes meaningful determination of assumed isotropic material properties for short load durations and the confined stress states tested.

Confined creep tests were also performed at each test temperature. The modular creep compliance values of confined tests are compared with those from uniaxial tests

in Figures 10, 11, and 12. In all cases, the confined test results fall below those for uniaxial tests. However, at a temperature of 100°F the two modular creep compliance curves were nearly the same. Similar comments apply to the values of Poisson's ratio determined from the two stress states. It is felt that the anisotropic nature of the ATB specimens induced the difference between uniaxial and confined creep test results.

Stress Level

The influence of stress level indicates the degree of linearity of material response. For uniaxial stress states calculated material properties are not influenced by the degree of isotropy of the ATB specimens. For repeated load tests under uniaxial stress states the elastic properties were approximately equal for all stress levels tested. The results of uniaxial creep tests at different stress levels can be considered to define a single compliance curve at each test temperature. Thus, both repeated load and creep test results indicate that uniaxial stress level has no significant influence on the material properties and the ATB behavior can be considered linear under these conditions.

Failure Criteria

Pavement failure can occur both in the ATB material itself and in other pavement components due to the constitutive properties of the ATB material. The constitutive properties of the ATB have been discussed in the previous section and influence the state of stress and strain throughout the pavement system. Thus, failure in other pavement components influenced by stress or strain level can be estimated using applicable failure criteria.

Two modes of failure which can occur in the ATB material are fatigue cracking and accumulation of permanent deformation. The results of this study allow prediction of both modes of ATB failure.

Fatigue Cracking

Fatigue tests on ATB beams allowed definition of a fatigue failure criteria. It was found that the fatigue life, N_f (number of repetitions to failure), at 70°F could be represented by the equation:

$$N_f = 4.36 \times 10^{-8} \, (1/\varepsilon)^{3.47}$$

This form of fatigue failure relationship has been previously applied to asphalt concrete material. Furthermore, the numerical coefficients in the equation are very similar to those found for asphalt concrete material at the same stiffness (temperature), Monismith, et. al. (1970).

Permanent Deformation

The accumulation of permanent deformation in ATB material under repeated loading can be calculated using linear viscoelastic theory. The experimentally determined linear viscoelastic material properties must be fit with an equation before the results can be input to a computerized boundary value solution of the pavement system. The form and numerical coefficients in the equation as well as the degree of fit have an important influence on the magnitude of permanent deformation that will be calculated.

Normally, an equation in the form of an exponential series is used to curve fit the experimental results. The curve

fitting techniques which restrict the values of some equation coefficients may lead to inaccurate permanent deformation predictions. In addition, the number of terms in the series should be varied to determine the best fit equation.

CONCLUSIONS

The results of this study allow an evaluation of the applicability of an elastic or viscoelastic constitutive model of asphalt-treated granular base course material (ATB). It has been found that the constitutive properties of ATB are dependent on temperature and time (duration of load). An equivalency between time and temperature was established which is in agreement with thermorheologically simple behavior of viscoelastic materials. Thus, the effects of both time and temperature can be theoretically accounted for using a viscoelastic constitutive model for ATB.

Although the effects of time and temperature on material properties cannot be theoretically considered using an elastic constitutive model for ATB, temperature and time effects can be accounted for through the selection of appropriate constitutive values. The resilient (elastic) material properties must be defined over the range of temperatures and load durations of interest. The elastic ATB constitutive parameter values can then be selected for applicable temperatures and load durations.

The values of stresses and strains calculated for pavements under each repetition of a moving wheel load using a viscoelastic constitutive model of ATB or an elastic model with properties selected for applicable temperature and load durations would be approximately equivalent. However, a

viscoelastic constitutive relationship directly models the observed ATB properties more closely. Furthermore, if an appropriate viscoelastic model is chosen, permanent strains induced by repeated load applications can be directly calculated. Therefore, it is felt that a viscoelastic constitutive model of ATB should be utilized.

It was found that the laboratory prepared ATB specimens were anisotropic. The degree of anisotropy was such that material properties calculated assuming isotropic behavior were significantly affected. This was especially evident when calculated material properties for uniaxial and confined stress states were compared.

The ATB constitutive behavior was found to be linear with respect to uniaxial stress levels typical of in-service material. Evaluation of linearity for other stress states was complicated by the anisotropic behavior of the ATB.

Criteria which may be used to predict failure of pavements utilizing asphalt-treated granular base course material were defined. Permanent deformation accumulated under repeated traffic loading can be calculated using linear viscoelastic constitutive properties. The effects of load duration and rest period on the amount of permanent deformation can be directly considered using viscoelastic theory. Fatigue failure criteria for the ATB were defined and found to be similar to that commonly used for asphaltic concrete material.

A P P E N D I X A

SENSITIVITY ANALYSIS OF MATERIALS CHARACTERIZATION ON THE PREDICTION OF PAVEMENT FATIGUE PERFORMANCE

INTRODUCTION

In general terms, materials characterization is the art of selecting and quantifying a mathematical model that can represent material behavior for the conditions under which it will serve. Typically, the mathematical model of a material is used as input to a larger model which is used to predict the performance of some system. In the context of pavements, the material characteristics are inputs into a model of the pavement system so that the performance of the system may be predicted. Such systems approach to pavement design and evaluation was first proposed by MR&D (1968).

During the last decade, theoretically based methods (models) have been developed for designing pavement systems and predicting their performance. The mathematical representation of the materials comprising the pavement system is an essential component of these design and performance models. In order to utilize these models, a great deal of time, effort, and money have been spent in characterizing paving materials. Under a recent FHWA contract, Materials Research & Development (1972) has reported on the characterization of asphalt concrete and cement-treated granular base course material. It was shown that stress conditions, type of test, test procedures, sample preparation techniques, and

measurement techniques all influence the characterization of asphalt concrete.

Furthermore, it is impossible to eliminate all experimental error. The scope of the experimental program conducted in the above-mentioned contract permitted the examination, for the first time, of all these factors as they influence the selection and quantification of a constitutive equation for representing asphalt concrete. An attempt was made to evaluate the significance of factors influencing the asphalt concrete characterization. However, it was found that there was no published information which identified the degree of accuracy necessary in characterizing materials in their application to the design and analysis of pavement systems.

It is generally accepted that the level of characterization had reached a degree of sophistication that further refinement would require considerable investments in terms of time and money. Before making such commitments, it is pertinent to ask whether, in the present context of the state of development of the pavement design and performance prediction models, further refinements are necessary.

In more general terms, the objective of such a question is to determine the degree of accuracy (confidence) necessary in defining the inputs, considering the state of development of the analytical model and the degree of confidence required in the prediction of performance. To attain this objective, it is necessary to conduct a sensitivity analysis.

GENERAL CONCEPT OF SENSITIVITY ANALYSIS

Consider a system with the three essential components: inputs, a law of transformation, and outputs. Outputs are generally considered in the sense of performance of the system being modelled. Since the system is evaluated by its ability to perform its prescribed function, the definition of performance criteria is essential to the definition of the total system. The basic concept in a sensitivity analysis is to relate variations in input parameters to variations in the output. In general, a reduction in the uncertainty of the input parameters will result in a reduced variation in the output. However, since all system models represent idealizations of a real physical system, and since the effect on the output of each output parameter is not the same, it is not necessarily logical that each input parameter be defined to the same degree of accuracy (level of uncertainty). For example, a variation of 50% in one input parameter may have the same effect on the output as a 1% variation in some other input parameter.

It should be recognized that the system model within whose framework the sensitivity analysis is conducted is, in itself, an approximation. The accuracy of the overall model, in terms of the factors that are included or omitted, also has a bearing on the desired accuracy of the various components of the model. This line of reasoning leads to the conclusion that it is necessary to develop a complete system model prior to conducting any sensitivity analysis. However, since a complete model of a pavement system is not available at the present time, it is necessary to consider the specific subsystems that are available. Since materials characterization is primarily an input to the

structural subsystem, it is within the context of the structural subsystem that a sensitivity analysis with respect to materials characterization should be conducted.

PROCEDURE FOR CONDUCTING SENSITIVITY ANALYSIS

To explain the procedure for conducting a sensitivity analysis within the general framework of a structural subsystem, it is convenient to consider the block diagram representation of the structural subsystem shown in Figure 21. To perform a sensitivity analysis using this subsystem, it was necessary to identify the parameters affecting the inputs, select a structural analysis model, and select a failure model.

Based on the block diagram shown in Figure 21, the following factors were considered in the sensitivity analysis: (1) traffic, (2) material constitutive equations, (3) material failure characteristics, (4) environment, (5) structural section, and (6) construction effects.

In this sensitivity study, only initial design was considered; hence, maintenance effects were not included in the subsystem. Traffic was not directly considered in this sensitivity analysis, and the performance of the pavement system was measured in terms of the number of repetitions to cause failure. The life or performance of the pavement, in terms of time, is dependent on the level of traffic. No particular level of traffic was assumed in the analysis.

For the purpose of a general description of the sensitivity analysis, it is convenient to restructure the structural

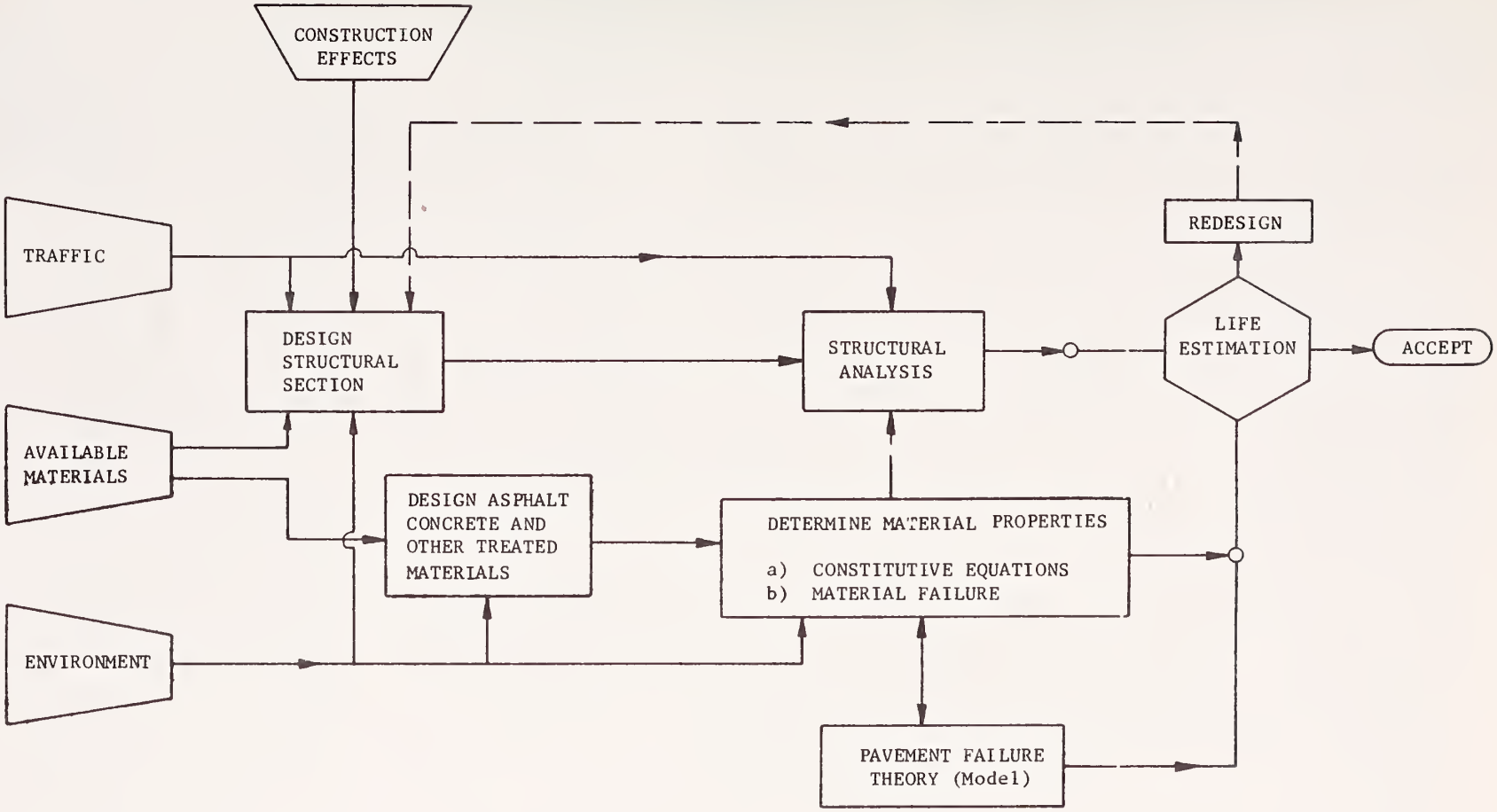

FIGURE 21 - STRUCTURAL SUBSYSTEM FOR PAVEMENTS

subsystem model as shown in Figure 22. The major difference between Figures 21 and 22 is that in the latter the restrictions mentioned above are included and examples of the structural analysis model, the failure model, and the appropriate material properties are given.

Upon examination of Figure 22, it becomes obvious that within the context of the model the influence of various factors such as environment, construction, etc., on the prediction of failure can only be analyzed through their effect on material properties and the structural section geometry. Therefore, in a computer-based experiment which utilizes this system, it is sufficient to examine for various structural sections, the effect of material properties on the prediction of failure. It is also necessary to establish the relationship between material properties and the various factors which are known to affect pavement life prediction.

With the above relationships between material properties and input variables and failure criteria, it was possible to examine the influence of each input variable on the prediction of pavement failure. This information could then be used to examine the relative importance of each variable on the prediction of pavement failure.

It should be recognized that, in reality, all inputs to the model have some statistical distribution and are not deterministic. In a detailed and comprehensive sensitivity analysis, it would be necessary to establish the probability distributions of each of the variables in the subsystem. A probabilistic sensitivity analysis could then be conducted to evaluate the influence of the

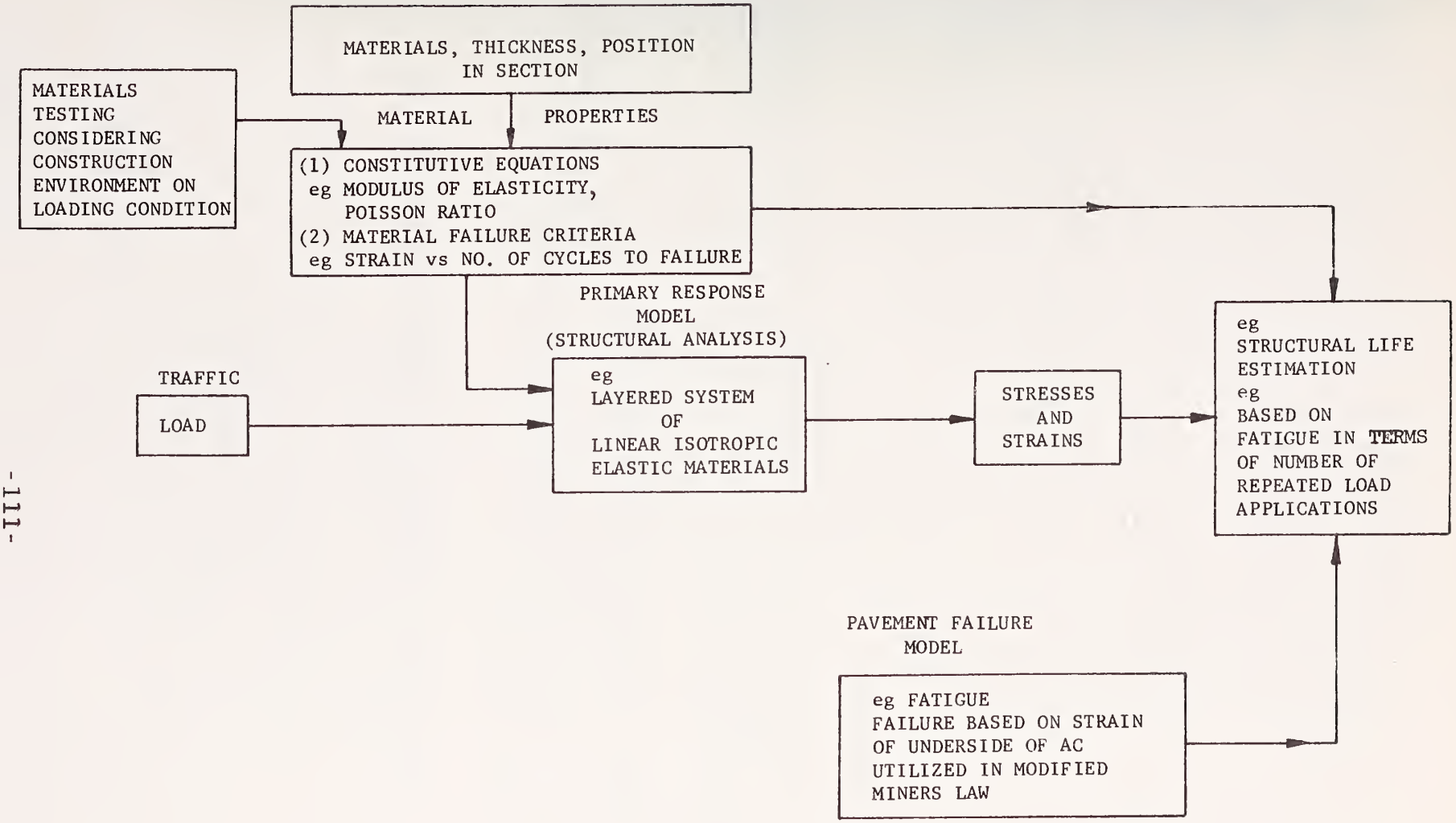

FIGURE 22 - SIMPLIFIED STRUCTURAL SUBSYSTEM WITH EXAMPLES OF VARIOUS COMPONENTS

distributions of each variable on the distribution of predicted performance. At the time this sensitivity analysis was performed, a probabilistic model of the subsystem shown in Figure 22 was not available. Furthermore, little information concerning the statistical distribution of input variables was available. Therefore, a deterministic approach was used in which ranges in the values of the various parameters were analyzed to determine the effects of input uncertainties on the predicted performance. By the establishment of ranges of values and an average value for each input parameter, a factorial experiment (computer based) was designed to examine the sensitivity of fatigue life prediction to variations of uncertainties in the input variables.

The procedure utilized to conduct the sensitivity analysis can be summarized in the following steps and is illustrated schematically in Figure 23.

I. Select Performance Prediction Model

Select failure prediction model; i.e., select the system. The performance of the sensitivity analysis is based on the system selected.

II. Select Input Parameters for Sensitivity Analysis

1. Select typical sections.
2. Select types of materials to be investigated and their average properties.
3. Select failure characteristics.
4. Select the loading condition.

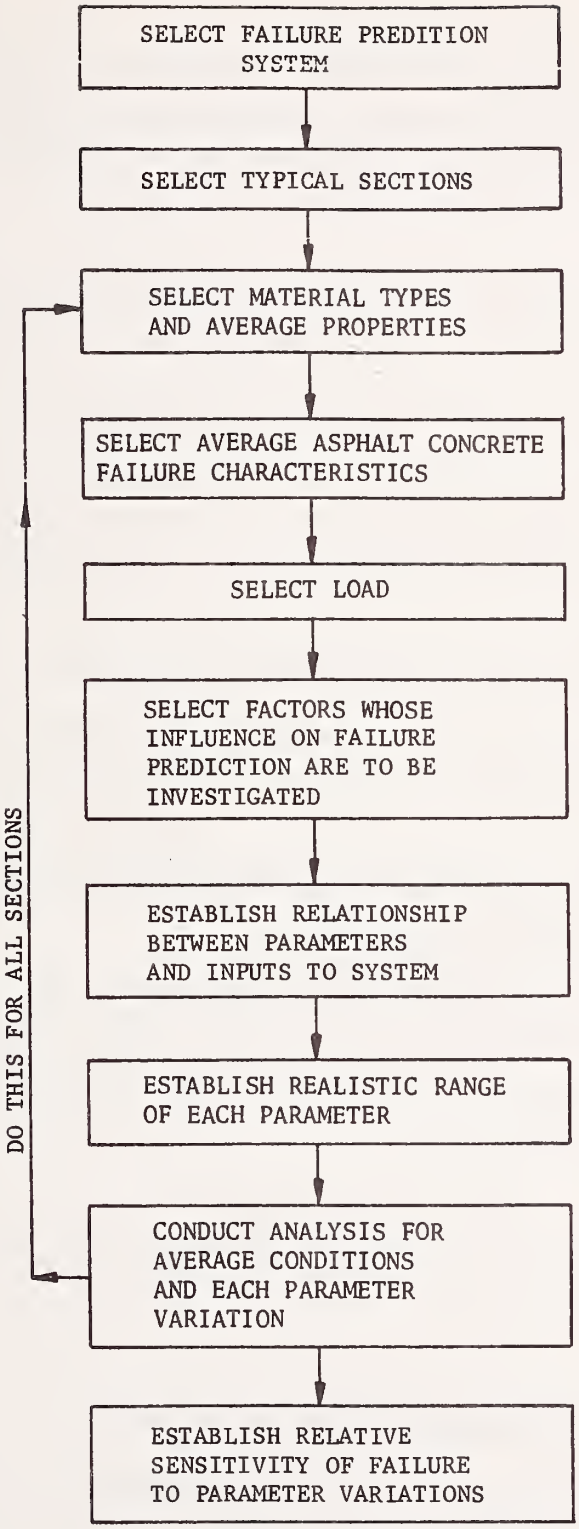

FIGURE 23 - PROCEDURE FOR CONDUCT OF SENSITIVITY ANALYSIS

5. Select those parameters; e.g., material properties, air voids whose influence on failure prediction is to be investigated. Some of these parameters may be direct inputs to the system.

6. Establish relationships between the parameters selected in (5) and inputs to the system.

7. Select ranges in material properties about the average properties selected in (2) based on the likely variations of parameters selected in (5) and the relationships established in (6).

III. Conduct Analysis and Present Results

Conduct the analysis; i.e., predict failure for each section for the range of material properties investigated.

IV. Establish Relative Influence of Input Parameters on Performance Prediction

On the basis of the information developed in III, and the relationships established in II (6), the relative influence of the parameters selected in II (5) on the prediction of failure can be examined.

The remainder of this chapter describes the sensitivity analysis conducted in accordance with the steps outlined above.

SELECTION OF PERFORMANCE PREDICTION MODEL

As for the total pavement system, the structural subsystem must also satisfy certain user-based performance criteria. Consequently, any performance criteria are subjective and

must be related to the output of a pavement model which is expressed in terms of measurable physical quantities. Such a relationship evolved from the AASHO Road Test. The Present Serviceability Index, PSI, was developed which related user-based performance to rutting, cracking, and slope variance. Since the AASHO Road Test, various subsystems of the pavement structural subsystem model have been developed to predict the individual components of a PSI pavement rating.

Although local conditions may cause variations in pavement behavior, it is generally agreed that traffic associated cracking is the dominant manifestation of pavement distress, Finn (1970). Pavement cracking can be of many types (longitudinal, alligator, transverse, etc.) and can be caused by many factors. However, cracking caused by repeated load applications (fatigue) is a major contributor to pavement distress. Thus, it has not been coincidental that in the past ten years more effort has been made to define the fatigue failure criteria of asphalt concrete than any other failure mechanism. These efforts have led to the development of a subsystem to predict the fatigue failure of asphalt concrete pavements. Since fatigue cracking is of major significance in the failure of pavement systems, and a fatigue subsystem is the most highly developed subsystem of the total pavement system model, it is logical that this initial sensitivity analysis of materials characterization be conducted utilizing the fatigue components of the structural subsystem. Within the context of the fatigue subsystem selected, it was necessary to select the method of structural analysis and the fatigue failure characteristics.

The structural analysis of the pavement system was performed using a layered, isotropic, linear elastic boundary value representation of the pavement system. While other boundary value representations that are possibly more representative of a pavement system are available; e.g., non-linear elastic layered systems and linear visco-elastic layered systems, the linear elastic representation was selected for several reasons. The primary reason for the selection of a layered linear elastic cystem was that it was felt that it could adequately reflect the behavior of a pavement system if proper consideration was given to the effect of temperature, time of loading, and stress levels. In addition, information concerning material properties and failure characteristics are most commonly analyzed and reported assuming linear elastic behavior. Furthermore, this representation is the most commonly used and widely understood.

The fatigue failure characteristics of asphalt concrete have been extensively studied in the past ten years. Although similar fatigue failure criteria have been proposed by many investigators, perhaps the most completely developed criteria are available through the research work at the University of California, Berkeley. For this reason, the UCB fatigue failure criteria were utilized for this sensitivity analysis.

The fatigue subsystem involves the determination of the maximum tensile strain in the asphalt concrete. The strain is then used to determine the number of repetitions of this strain that would cause cracking based on experimentally established fatigue failure curves. The fatigue failure curve corresponding to the stiffness (temperature)

of the asphalt concrete is used in conjunction with the tensile strain values to predict the number of repetitions necessary to cause fatigue failure.

The computer program CHEV5L, representing an isotropic linear elastic layered system, was used to conduct the structural analysis to determine the maximum tensile strain in the asphalt concrete.

SELECTION OF INPUT PARAMETERS FOR SENSITIVITY ANALYSIS

Typical Structural Sections

Three pavement section geometries were considered in the sensitivity analysis. The three geometries were selected to be representative of possible design alternatives for a major highway. The pavement sections range from full depth asphalt concrete to a thin surface layer of asphalt concrete over an untreated base course material. These sections are representative of a highway built on a relatively weak subgrade (CBR $\cong$ 3, E $\cong$ 5000 psi, R $\cong$ 15) with a relatively high traffic volume (DTN $\cong$ 550, TI $\cong$ 10.5). DTN is the abbreviation for the Design Traffic Number used by The Asphalt Institute, and TI is the abbreviation for the Traffic Index used by the State of California. The geometry of the actual sections analyzed is shown in Figure 24.

Material Types and Average Properties

The three types of materials most commonly used in flexible pavement construction were analyzed in the sensitivity analysis. They were an asphalt concrete surfacing, an untreated granular base course, and the subgrade.

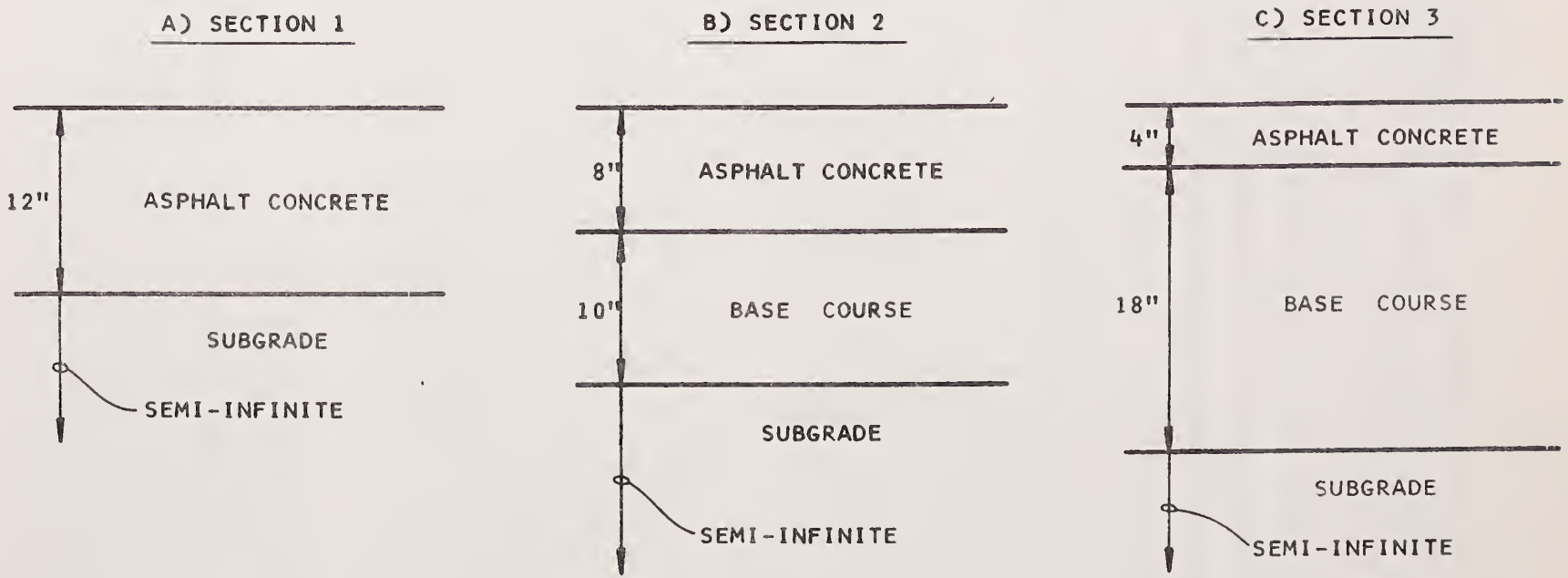

FIGURE 24 - GEOMETRIES OF STRUCTURAL SECTIONS CONSIDERED IN THE SENSITIVITY ANALYSIS

Asphalt Concrete

The average asphalt concrete properties used were those reported by MR&D (1970) and are shown in Figure 25. These results were for a typical California type mix containing 6% 85-100 asphalt with an average air void content of approximately 4% and a load duration of 0.1 seconds. The vertical bars for each test temperature represent the total range of values for the total stress range tested. The asphalt concrete specimens were subjected to the wide range of simultaneously cycled axial and radial stress pulses given below:

	$\Delta\sigma_{zz}$(psi)	$\Delta\sigma_{RR}$(psi)
T = 40°F	-70 → +70	0 → +70
T = 55°F	-40 → +70	0 → +70
T = 70°F	-40 → +70	0 → +70
T = 100°F	-40 → +70	0 → +70
T = 140°F	0 → 30	0 → +70

The average elastic modulus of the asphalt concrete was taken from the dotted line in Figure 25 for each temperature analyzed. An average value of 0.4 was assumed for Poisson's ratio for all temperatures analyzed. The influence of this assumption on the sensitivity results is discussed later in the chapter.

Untreated Base Course

It was recognized that both the modulus and Poisson's ratio of untreated base course material are strongly affected by stress level (non-linearity elastic). However, the material was taken to be linearly elastic in accordance with

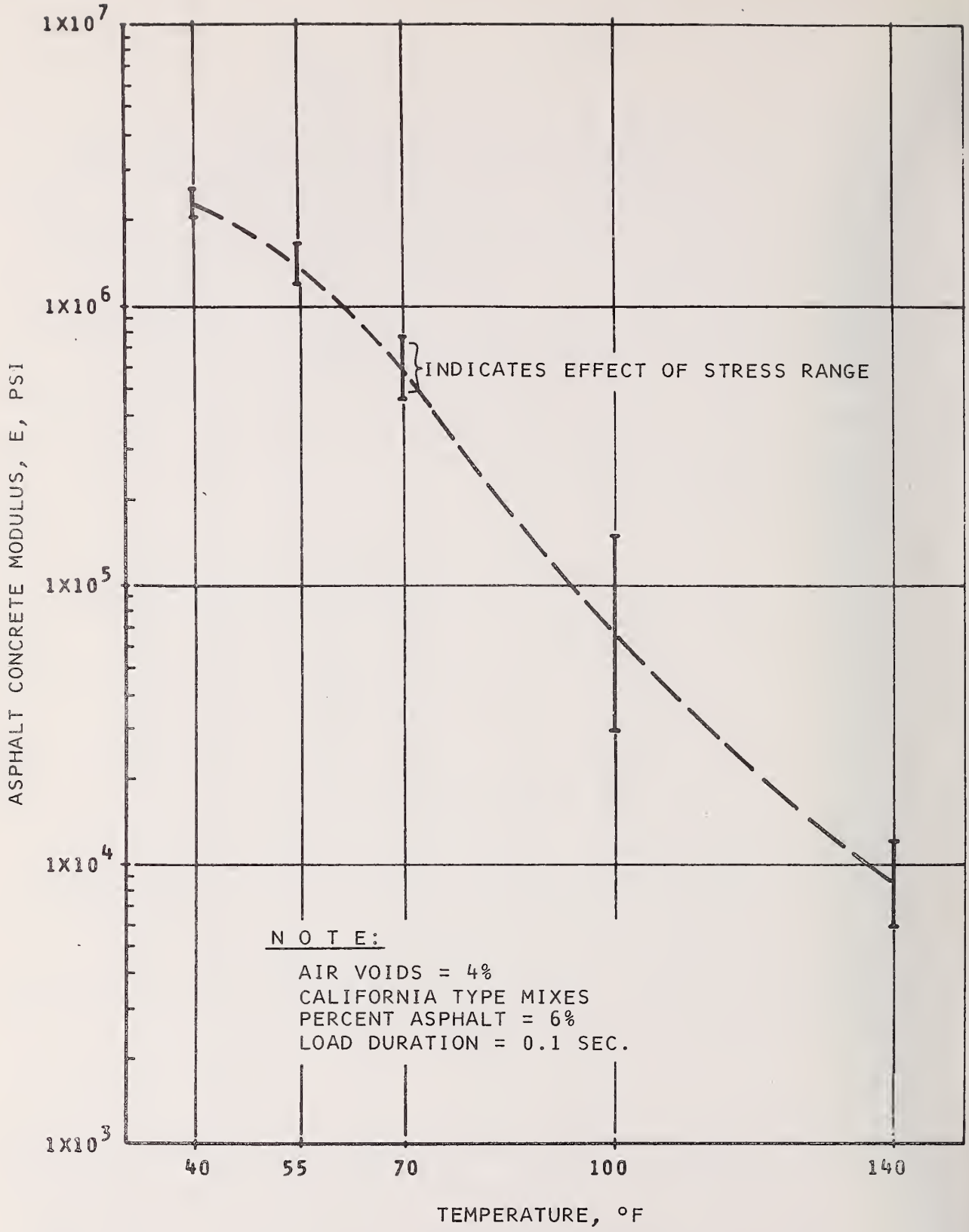

FIGURE 25 - TEMPERATURE DEPENDENCE OF ASPHALT CONCRETE MODULUS (AFTER MR&D (1970))

the structural analysis model selected. The results of this sensitivity analysis will yield the effect of assuming a constant linear elastic modulus and a constant average Poisson's ratio. The average values of modulus and Poisson's ratio selected were based on experimental results and preliminary structural analysis of the pavement section geometries being considered.

To determine a realistic average modular value for the untreated granular base course, a preliminary structural analysis of Sections 2 and 3 was performed using a layered nonlinear elastic computer program. The base course layer was divided into three sublayers, and each was represented as nonlinearly elastic according to one of the following equations:

$$E = 2000\ \theta^{0.6}\ \text{(psi)}$$

$$E = 5000\ \theta^{0.6}\ \text{(psi)}$$

where θ = the first stress variant. These two constitutive equations were selected as representative of lower and upper bounds on nonlinear modular relationships reported in the literature. This form of equation represents a linear relationship between modulus and first stress invariant on a log-log plot. Poisson's ratio has been found to be dependent on the ratio of principal stress, Hicks (1970). The dependence of Poisson's ratio on principal stress ratio was not considered directly in the analysis; however, Poisson's ratio values of 0.3 and 0.5 were investigated.

The asphalt concrete and subgrade were represented as linear elastic. The asphalt concrete modulus was varied from $2,350 \times 10^3$ to 70×10^3 psi, and Poisson's ratio was taken as 0.4. The subgrade was represented by a modulus of 5,000 psi and a Poisson's ratio of 0.4.

Since the base course layer was subdivided into three layers (all with the same properties), the modulus variation through the depth of the base course layer could be found. The modulus varies with depth because the modulus is a function of stress which varies with depth. The average modulus over the depth of the base course layer for each case analyzed was found and are summarized in Table 4.

The base course modulus increases as the asphalt concrete modulus decreases since more stress is transmitted to the base course layer. The higher value of Poisson's ratio also results in higher base course moduli. The average base course modulus for all four asphalt concrete moduli are shown in the last row of the table for each section.

Since the two nonlinear modular relationships used bound the majority of experimental data reported in the literature, modular values between these extremes are more typical. The average base course modulus for all conditions on each section represent these more typical values. These values result in an average modulus of 9,048 psi for Section 2, and 11,824 psi for Section 3. Therefore, a modular value of 10,000 psi was selected as a realistic average modular value for untreated base course material and was used in the sensitivity analysis.

TABLE 4

AVERAGE BASE COURSE MODULI OVER DEPTH OF BASE

BASE COURSE LAYER PREDICTED USING NON-LINEAR ANALYSIS

SECTION 2

	$E_{BC} = 2000\,\theta^{0.6}$		$E_{BC} = 5000\,\theta^{0.6}$	
E_{AC} (KSI)	$\nu_{BC} = 0.3$	$\nu_{BC} = 0.5$	$\nu_{BC} = 0.3$	$\nu_{BC} = 0.5$
2,350	4,372	5,770	10,022	12,806
1,000	4,836	6,392	10,500	13,254
250	5,796	7,565	10,844	13,299
70	6,680	8,548	11,145	12,937
$\bar{E}_{BC}$ =	5,421	7,069	10,628	13,074

AVERAGE E_{BC} FOR ALL CONDITIONS = 9,048 PSI

SECTION 3

	$E_{BC} = 2000\,\theta^{0.6}$		$E_{BC} = 5,000\,\theta^{0.6}$	
E_{AC} (KSI)	$\nu_{BC} = 0.3$	$\nu_{BC} = 0.5$	$\nu_{BC} = 0.3$	$\nu_{BC} = 0.5$
2,350	5,623	7,599	12,362	15,870
1,000	6,368	8,521	13,057	16,399
250	7,472	9,803	14,154	16,954
70	8,514	10,951	15,619	19,925
$\bar{E}_{BC}$ =	6,994	9,219	13,798	17,287

AVERAGE E_{BC} FOR ALL CONDITIONS = 11,824 PSI

($\nu_{AC} = 0.4$, $E_{SG} = 5,000$ psi, $\nu_{SG} = 0.4$)

The purpose of selecting average material properties was to investigate the sensitivity of fatigue life prediction. Fatigue life prediction is basically controlled by the maximum horizontal tensile strain in the asphalt concrete (temperature is also important). The maximum horizontal tensile strain values predicted by the layered nonlinear analysis are shown in Table 5. Comparison of the strain values for the two different Poisson's ratio values analyzed showed minor changes in the strains. Care must be taken not to regard such minor changes in strain as unimportant, since small strain changes can change the predicted fatigue life significantly. However, in comparison to asphalt concrete or base course modulus changes, the effect of Poisson's ratio is small. Therefore, the selection of an average Poisson's ratio value was felt to be of minor importance to the sensitivity analysis. An average Poisson's ratio of 0.3 was selected for the untreated base course material and used in the analysis.

Subgrade

The selection of average properties for the subgrade material is restricted by the geometry of the structural sections chosen for the sensitivity analysis. These structural sections are representative of a pavement constructed on a subgrade with an average modulus of 5,000 psi (CBR $\simeq$ 3, R $\simeq$ 15) for a heavy volume highway. Therefore, the average modulus used for the analysis was 5,000 psi. An average Poisson's ratio of 0.4 was selected as representative of most subgrades.

Failure Characteristics

Since this sensitivity analysis was conducted within the framework of the fatigue subsystem, it was assumed that

TABLE 5

MAXIMUM HORIZONTAL TENSILE STRAINS IN THE ASPHALT CONCRETE PREDICTED USING NON-LINEAR ANALYSIS

SECTION 2

	$E_{BC} = 2000\theta^{0.6}$		$E_{BC} = 5000\theta^{0.6}$	
E_{AC} (KSI)	$\nu_{BC} = 0.3$	$\nu_{BC} = 0.5$	$\nu_{BC} = 0.3$	$\nu_{BC} = 0.5$
2,350	50	50	48	48
1,000	101	100	95	95
250	295	288	257	253
70	648	626	494	478

SECTION 3

	$E_{BC} = 2000\theta^{0.6}$		$E_{BC} = 5000\theta^{0.6}$	
E_{AC} (KSI)	$\nu_{BC} = 0.3$	$\nu_{BC} = 0.5$	$\nu_{BC} = 0.3$	$\nu_{BC} = 0.5$
2,350	139	134	121	117
1,000	258	246	209	201
250	598	564	418	400
70	1,005	957	537	531

($\nu_{AC} = 0.4$, $E_{SG} = 5{,}000$ psi, $\nu_{SG} = 0.4$)

the pavement failed in fatigue. Fatigue failire is further assumed to occur in the asphalt concrete as a function of the maximum tensile strain in the asphalt concrete.

The fatigue failure characteristics of the asphalt concrete used in this analysis were those developed at UCB. This failure criterion was determined from repeated loading tests on asphalt concrete beams. The results are presented in the form of maximum initial tensile bending strain vs. repetitions to failure as shown in Figure 26. The fatigue life (number of repetitions to failure) was determined from this figure for each particular strain and asphalt concrete stiffness.

These curves were developed from typical California-type mixes containing 6% asphalt at an average air void content of 5%. The beams were tested in a controlled stress mode of fatigue with a square wave repeated load of 0.1 second duration and frequency of 20 repetitions per minute. The initial bending strain is considered to be the strain measured on the 200th repetition. The fatigue failure curve is a function of the modulus (temperature) of the asphalt concrete. Initial strain values below 70 μ in/in are considered to cause no fatigue damage and, therefore, result in an indefinitely long fatigue life.

Loading Condition

One loading condition was used for the entire sensitivity analysis. It was recognized that the load magnitudes applied to a pavement are distributed in some random fashion. Normally, the effect on fatigue life prediction of varying load magnitudes are considered through Miner's

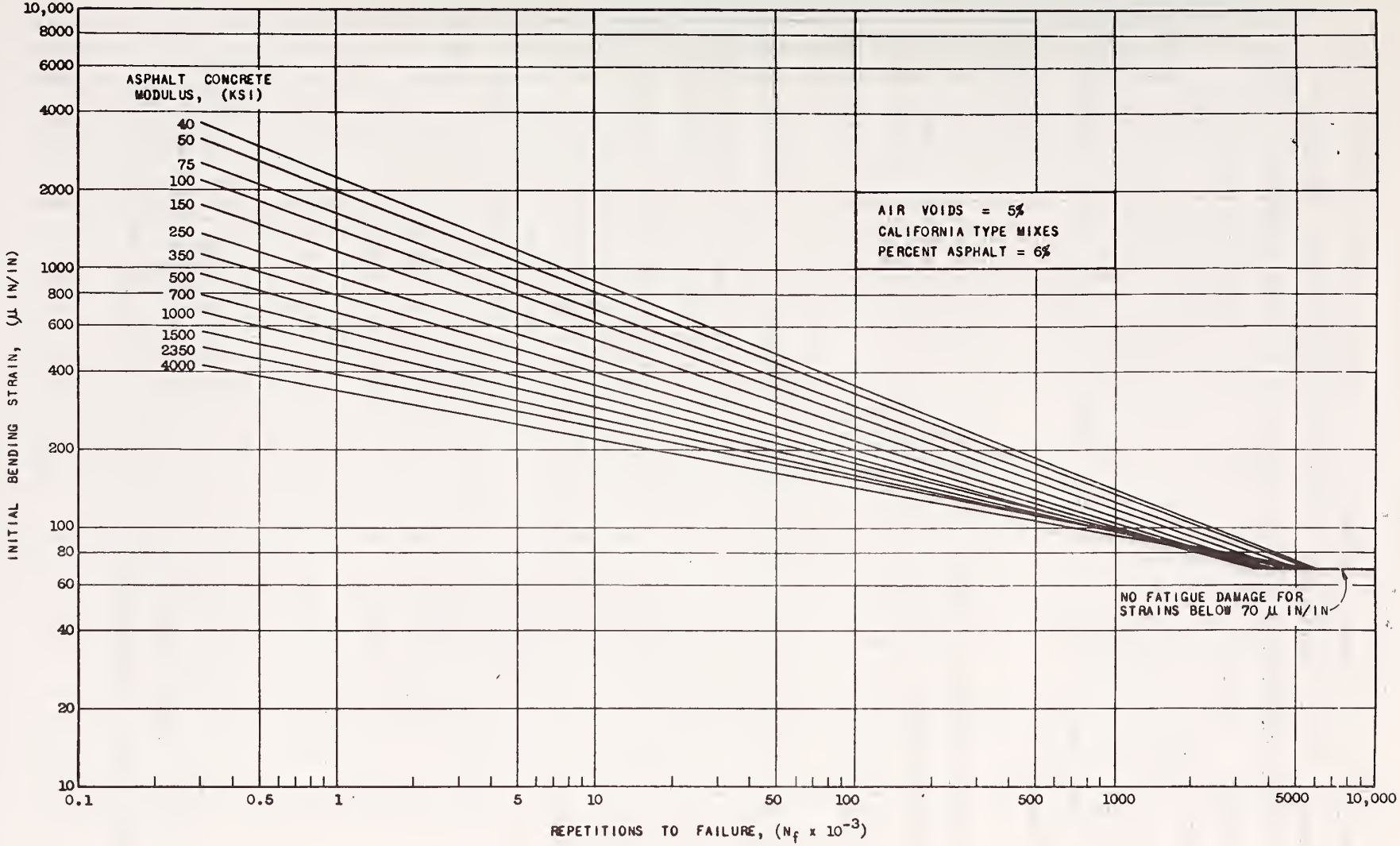

FIGURE 26 - FATIGUE FAILURE CRITERIA (AFTER MONISMITH, ET. AL. (1970))

hypothesis of a linear summation of damage due to each load magnitude. It is strongly recommended that the distribution of load magnitudes be considered in any rational pavement design. However, this sensitivity analysis was not concerned with the design of a specific pavement. Therefore, for the purposes of this sensitivity analysis, it was sufficient to examine one typical loading condition which can be considered equivalent to some varying load magnitude distribution.

The loading condition analyzed was a single 9,000 lb. wheel load with a tire pressure of 70 psi. The load area was assumed to be circular which resulted in a load radius of 6.40 inches.

PARAMETERS INFLUENCING FAILURE PREDICTION

The primary objective of this sensitivity analysis was to examine the effect of inadequacies in materials characterization on the prediction of pavement failure and thereby define an adequate material characterization. Because such effects are only significant in a relative sense, various other parameters were also investigated so that their significance could be determined and compared with those due to any inadequacies in material characterization. The factors considered were selected based on the structural subsystem shown in Figure 21 and are subsequently described in detail.

Traffic

The volume of traffic was not directly considered in the sensitivity analysis for the sake of generality. The fatigue life is expressed in number of load repetitions

and are applicable to relatively heavy volumes which might exist on a main highway, although no particular level was assumed. The general level of traffic volume enters indirectly into the analysis because the representative structural section geometries studied reflect a relatively high traffic volume pavement.

Environment

The environment of a pavement can be characterized by its temperature and moisture regime. Temperature was considered to have a major influence on pavement failure and, therefore, two levels of temperature sensitivity were included in the analysis. One level might be considered the macro effect of temperature, and the other level, the micro effect.

The macro effect of temperature was considered by analyzing each section at four average levels of temperature, 40, 60, 80, and 100°F. These can be thought of as average values representing climates ranging from cold to hot. Within each macro temperature level, a micro temperature uncertainty was considered to represent the difference between the assumed and actual macro temperature environment.

The temperature distribution throughout the pavement section was assumed to be uniform. While it was recognized that field pavements do, in fact, have temperature gradients which vary from location to location, season to season, and night to day, the results of the sensitivity analysis are not restricted by assuming a constant uniform temperature gradient. It was not necessary to consider

such details in conducting this sensitivity analysis because a constant temperature gradient is equivalent, in terms of fatigue life prediction, to some situation where all these temperature gradient variations are accounted for.

The moisture environment of a pavement system can vary throughout the year and was assumed to affect only the untreated granular base course and subgrade properties.

Construction Effects

The construction of the pavement was considered to affect both the pavement geometry and the material properties. The effects are representative of the deviations from design values that can take place during construction due to the limits of control possible in the field.

The geometrical effects of construction control were considered only to affect the thickness of the asphalt concrete layer. While it is recognized that deviations from design thickness will exist for all layers in the pavement system, small thickness variations in the base course were felt to have a relatively small influence on the fatigue life prediction layer in comparison to those in the asphalt concrete layer and, therefore, were not considered.

The other influence of construction control is on material properties. Material properties in the field can vary from those determined in the laboratory and subsequently used for design due to the limited degree of control possible in the field. Consider the deviations of parameters (mix properties) controlling the material properties of each layer that are possible in the field.

The most significant construction parameter affecting the material properties of the asphalt concrete is the percent air voids (degree of compaction). A small variation of void content has a major effect on the constitutive equation and fatigue properties of the asphalt concrete. Furthermore, the effect of deviations in air voids on the constitutive equation and fatigue properties are additive. That is, an increase in air voids causes a decrease in modulus which results in higher maximum tensile strain in the asphalt concrete. Also, increased air voids causes a decrease in fatigue life for any given level of strain. Therefore, the net effect of an increase in air voids is to cause two additive reductions in fatigue life.

The material properties of the asphalt concrete are also affected by such parameters as asphalt content, aggregate gradation, temperature at compaction, etc. However, the effects of small variations in these parameters are either reflected in air void variations, or are of minor influence in comparison.

The material properties of untreated granular base course and subgrade material are most strongly influenced by their dry density and water content. The influence of the limits of field control of these parameters were considered in the analysis.

Material Characterization

Variations in materials characterization in terms of both constitutive equations and failure characteristics were considered in the analysis. These variations were considered to be those that might exist from inadequacies in

the experimental definition of the material properties. Inadequacies in materials characterization most commonly arise because ideal materials only approximately model actual material behavior.

Constitutive Equations

Consider the data on the elastic modulus for asphalt concrete shown in Figure 25. The vertical bars in this figure indicate the total range of values measured for the stress states previously described. If the asphalt concrete were truly a linear isotropic elastic material for a specific load duration, shape of load pulse and temperature, all the experimental stress states tested would have yielded the same value. Variations from a single value represent deviations from ideal linear isotropic elastic behavior and can be thought of as inadequacies in the material characterization. These deviations can arise because the asphalt concrete is, in fact, nonlinearly elastic, anisotropic, and/or from experimental errors. Whatever the reasons, typical inadequacies of a linear isotropic elastic characterization are represented by the vertical bars in Figure 25. These deviations from ideal behavior were considered in the sensitivity analysis.

If the asphalt concrete is characterized as elastic, proper consideration must be given to the temperature, load duration, and shape of the load pulse. For an ideal elastic material, material properties are not a function of these parameters. Therefore, this type of characterization might more properly be considered a pseudo-elastic characterization. The effects of temperature, load duration, and shape of the load pulse are considered indirectly rather than directly in the constitutive equation. This

type of characterization is valid so long as the temperature, load duration, and shape can be positively controlled during laboratory testing and are representative of service conditions.

It was considered that the control of temperature in laboratory testing is precise enough so that no experimental errors exist for this pseudo-elastic characterization variable. The asphalt concrete can also be tested over a range of temperatures representative of field without great difficulty. Under the above conditions, no experimental error in pseudo-elastic characterization of asphalt concrete is introduced by the laboratory control of temperature.

Likewise, the laboratory control of a specific load duration and shape is quite accurate. However, characterization inadequacies can arise if the load duration and shape used in laboratory testing does not agree with typical service conditions. The load shape and duration most commonly used for pseudo-elastic characterization testing of asphalt concrete is a square wave of 0.1 second duration. Recently, Barksdale (1971), has reported theoretical equivalent duration of loads in the field as a function of depth, vehicle speed, and shape of the stress pulse.

A main highway pavement is subjected to some distribution of vehicle speeds whose values may typically range from 1 mph to 60 mph. Since pavement designs are controlled by the volume of the truck traffic, it would seem reasonable that a vehicle speed of 45 mph would be more representative of an average vehicle speed for a main highway. Using an

average speed of 45 mph depth of 4 inches, and sinusoidal shaped principal stress pulses a load duration of approximately 0.03 seconds is predicted from Barksdale's results. Since this load duration differs from that normally used for a pseudo-elastic characterization of asphalt concrete, the influence of this variation in load duration on elastic modulus was investigaged in the sensitivity analysis.

The untreated granular base course in this sensitivity analysis was assumed to have linear elastic properties. As noted previously, the properties of untreated granular materials are more closely represented by nonlinear elasticity. As with the asphalt concrete, the influence of assuming the material to behave linearly when, in fact, it is nonlinear were investigated. The effect of load duration on the properties of untreated granular materials has been reported to be negligible (Hicks, 1970; Moore, et. al. 1970) and was, therefore, not considered in the analysis.

The modulus of typical subgrade soils has been found to depend on the axial stress level for typical in-service stress conditions. Examination of many computer-based structural analyses of well designed pavements has indicated that the traffic induced axial stress pulse in the subgrade rarely exceeds 5 psi. Although the exact shape and modulus magnitude vary with the soil type, the general shape of a decrease in modulus, as axial stress level increases, and then an approximately constant modulus above certain axial stress levels has been found for many subgrade soils. Axial stress level has been found to have no significant effect on Poisson's ratio.

If subgrade soil was linear elastic under a repeated load cycle, the modulus would remain constant for all axial stress levels. The dependence of subgrade modulus on axial stress level represents an inadequacy of a linear elastic characterization. The influence of such deviations from linear elastic behavior on the prediction of fatigue failure were investigated in the sensitivity analysis.

In summary, asphalt concrete, untreated granular base course, and subgrade are not ideal linear elastic materials. Therefore, a linear elastic constitutive equation involves approximations which can be considered as inadequacies of the characterization. The influence of such constitutive equation deviations from ideal behavior on the prediction of fatigue failure were considered in the sensitivity analysis.

Failure Characteristics

A complete characterization of a material involves the definition of both a constitutive equation and failure characteristacs. Thus far, inadequacies which arise in the definition of a linear elastic constitutive equation for pavement materials have been discussed. Now consider deviations from predicted behavior that arise in the definition of failure criteria.

For reasons previously discussed, this sensitivity analysis was conducted with the assumption that the pavement fails through fatigue of the asphalt concrete. Thus, actual material failure was assumed to occur only in the asphalt concrete. However, failure of the asphalt concrete, and thus the pavement, is dependent on the properties of all materials comprising the system. Therefore, although

no failure in the base course or subgrade themselves was considered, failure of the pavement system induced by their constitutive properties was considered.

The fatigue failure criteria for the asphalt concrete used in the analysis have been previously described and was shown in Figure 26. Each fatigue failure line shown represents the best linear regression fit to the experimental data. The standard error of estimate is a measure of that part of the variation in the test results left unexplained by the regression fit. It can be thought of as an estimate of the average standard deviation of the logarithm of the fatigue life around the estimated logarithm of fatigue life.

The scatter of the experimental test results are induced by the stochastic nature of fatigue failure and the limits of control possible in laboratory specimen fabrication and testing. The regression lines represent average material behavior, and the scatter about these lines are variations from predicted behavior. Just as deviations from ideal constitutive behavior of pavement materials was considered, the influence of deviations from the fatigue failure criteria itself were considered in the sensitivity analysis.

RELATIONSHIP BETWEEN SYSTEM INPUTS AND PARAMETERS CONSIDERED

Examination of the structural subsystem (Figure 21) used for this sensitivity analysis reveals that inputs to the system were: (i) constitutive constants for the various materials, (ii) failure criteria, and (iii) geometry. As has been previously discussed, the influence of traffic volume and load magnitude on fatigue life prediction were not directly considered. The fatigue life was examined in terms of number of load repetitions to cause failure for

one loading condition. The parameters influencing fatigue life prediction discussed in the previous section could only be considered if they were system inputs or could be related to the system inputs.

The average constitutive constants, failure criteria, and geometries utilized in this analysis have been described, and the many parameters that can affect these system inputs were discussed. Uncertainty about these parameters will cause uncertainty in the system inputs. Relationships between the system inputs and parameters were utilized to aid in the selection of the range of input values studied in this analysis. The following paragraphs describe these relationships.

Constitutive Constants

All materials considered in this analysis were characterized by isotropic linear elasticity. The two constitutive constants utilized in the analysis were modulus and Poisson's ratio.

Asphalt Concrete

The parameters considered to influence the constitutive constants of the asphalt concrete were temperature, stress conditions, load duration, and air voids content. These parameters represent those that were considered to exert major influence on the constitutive constants for a given mix design. A mix design is considered to fix the aggregate type, gradation, asphalt type, and percent asphalt.

Modulus - Temperature exerts a major influence on the modulus of asphalt concrete. The relationship between

temperature and modulus was shown in Figure 25. A temperature range from 40°F to 100°F results in a modulus change from $2,350 \times 10^3$ psi to 70×10^3 psi. Four macro-temperature levels were considered; 40°F, 60°F, 80°F, and 100°F representative of climates ranging from cold to hot.

Within each macro-temperature level, a micro-temperature uncertainty was considered. This represents uncertainty in predicted temperature within each type of climate. Micro-temperature uncertainties considered were ±1, ±3, and ±6°F. The effect of this range of temperature uncertainty on the modulus at each macro-temperature level was obtained from Figure 25.

The total range of influence of all stress states tested are indicated by the vertical bars shown in Figure 25 at test temperatures of 55, 70, 100, and 140°F. These stress states include both axial tension and compression for unconfined and confined tests. Since the stress state within the asphalt concrete layer in the field varies, the influence of stress state induces uncertainty in the average modulus value and was considered in the analysis.

The effect of load duration of asphalt concrete modulus was determined from the master creep curve and time-temperature equivalency developed for a viscoelastic characterization of asphalt concrete, MR&D (1972). Uncertainty in asphalt concrete modulus due to variation of load duration was considered in the analysis.

The relationship between air void content (for a constant percent asphalt) and asphalt concrete modulus was established from experimental results. Shook and Kallas (1969)

have reported on the effect of air voids on asphalt concrete modulus. There is an approximately linear decrease of modulus with air voids increase on a semi-log plot. Epps (1968) has also shown a similar linear relationship on semi-log plots. These relationships can be expressed in the form

$$\text{Log } E = C_1 - C_2(\text{A.V.})$$

where C_1 and C_2 are constants, E is the modulus, and AV is the air voids.

Examination of both sets of experimental data revealed that a representative value for C_2 was 0.05. This constant represents the slope of the relationship between modulus and air voids and was used to relate changes in air voids to changes in modulus. Air void changes of ±1, ±2, and ±3% were considered in the analysis.

The effects of uncertainty in temperature, stress conditions, load duration, and air voids parameters could then be considered through the asphalt concrete modulus system input.

Variations in these parameters cause changes in the average asphalt concrete modulus. Figure 27 shows asphalt concrete modulus variations of ±20 and ±40 percent which cover the range of variation of modulus as influenced by each parameter considered.

Poisson's Ratio - The relationship between Poisson's ratio of the asphalt concrete and temperature, stress conditions,

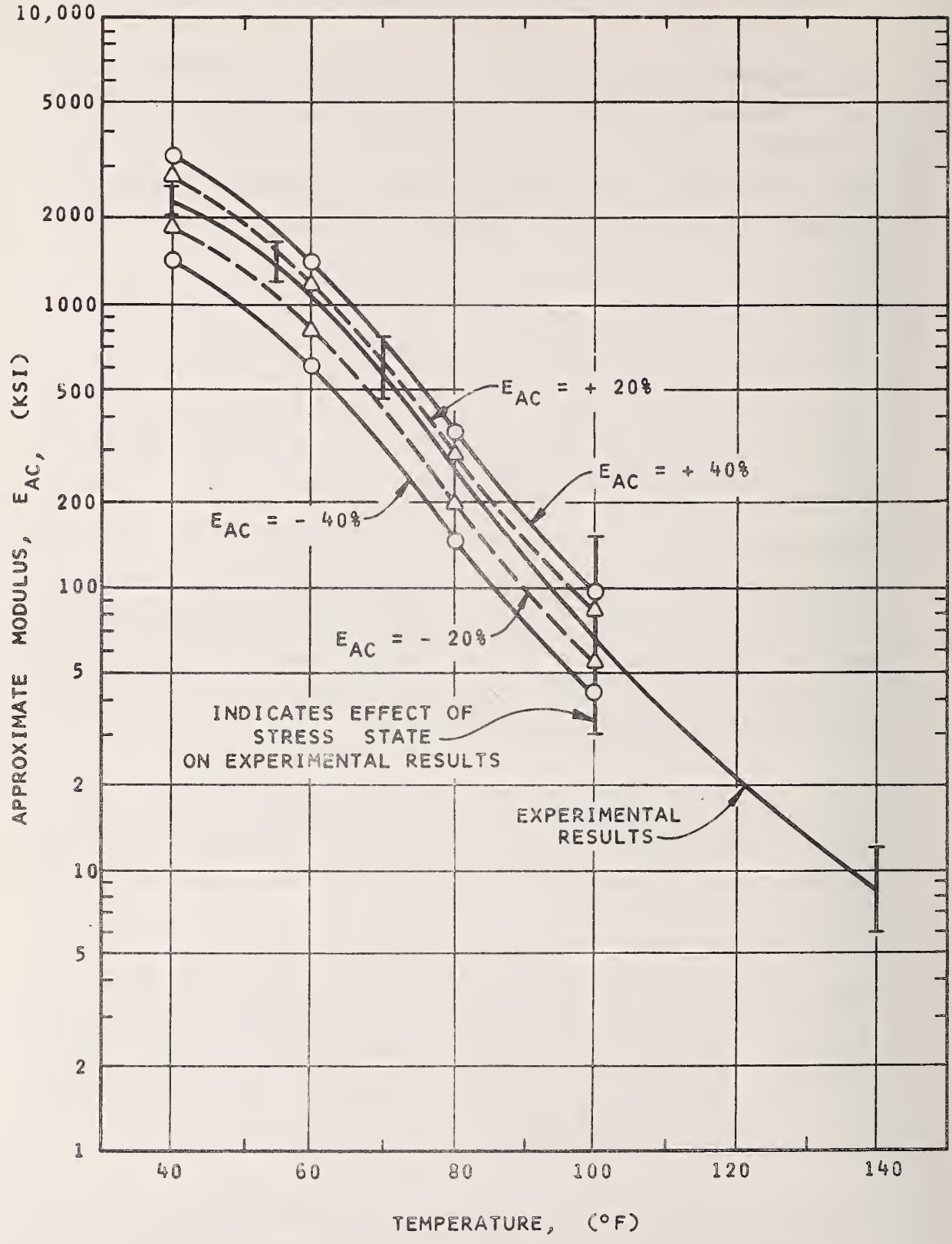

FIGURE 27 - ASPHALT CONCRETE MODULUS CURVES FOR AN ASPHALT CONCRETE MODULUS VARIATION OF ±20° AND ±40%

load duration, and air voids content were more difficult to establish since far less information was available. It was felt that load duration and air void content would have minor effects on Poisson's ratio.

The average value of Poisson's ratio used in the analysis was 0.4 and no dependence of this average value on temperature was considered. Therefore, it was felt that variation of ±0.1 from the average value would be representative of the effects of temperature and stress state. These variations were considered in the sensitivity analysis.

Untreated Base Course

The parameters considered to influence the constitutive constants of the untreated granular base course were dry density, degree of saturation, and stress state. Variations in dry density arise most commonly due to the limits of control possible in the field. Degree of saturation changes are normally associated with seasonal environmental changes.

Modulus - The layered nonlinear elastic analysis described earlier was used to establish the possible range of variation in base course modulus. The two nonlinear elastic modular relationships used bracket the majority of data reported in the literature and were developed for a wide variety of aggregate types, densities, and degrees of saturation. Therefore, the range of modulus values shown in Table 4 represent the range of uncertainty due to stress state, density, and degree of saturation.

These results can be considered as representative of upper and lower bounds on base course modulus. Examination of

Table 4 indicates a range of base course moduli from 4,372 to 19,925 psi. The range of base course moduli utilized in the sensitivity analysis was from 4,000 to 20,000 psi.

Poisson's Ratio - The average value of Poisson's ratio used for the analysis was 0.3. A variation of ±0.1 from this value was considered in the sensitivity analysis.

Subgrade

The parameters considered to influence the constitutive constants of a given subgrade were water content, density, stress state, and number of load repetitions. Even for subgrades with the same average constitutive constants, the influence of each of these parameters is highly dependent on the specific subgrade. Therefore, it was necessary to select typical ranges rather than investigate their influence on a specific subgrade.

Modulus - The average modulus used in the analysis was 5,000 psi. The range of subgrade modulus variation considered in the sensitivity analysis was from 2,000 to 10,000 psi.

Poisson's Ratio - The average value of Poisson's ratio was taken as 0.4. A variation of ±0.1 from this value was considered in the sensitivity analysis.

Failure Characteristics

The only failure characteristics input to the sensitivity analysis were those of the asphalt concrete in fatigue. The parameters considered to influence the fatigue failure characteristics were the maximum tensile strain, temperature

(modulus), uncertainty associated with the fatigue criteria itself, and air void content.

The effects of maximum tensile strain and temperature (modulus) are considered directly in the failure criteria. These effects were shown in Figure 6.

Uncertainty in the failure criteria itself can be measured by the fit of the regression lines to the experimental data. The extent of data scatter can be measured by the standard error of estimate. Examination of the literature (Epps, 1968; Monismith, et. al., 1970) revealed that a representative value for the standard error of estimate was 0.2. The effect of ±1 and ±2 standard errors of magnitude 0.2 were considered in the sensitivity analysis.

The relationship between air voids and fatigue life can be approximated as linear on a semi-log plot, Epps (1968). The slope of the line represents the change of fatigue life with change in air voids for stress controlled fatigue tests. However, since changes in air voids also change the asphalt concrete modulus, the effect of both changes are incorporated in this relationship.

Since the relationship between air voids and both asphalt concrete modulus and fatigue life for a constant stress level have been shown to be approximately linear on a semi-log plot, it was reasonable to assume that the relationship between air voids and fatigue life at a given strain and stiffness would also be linear on a semi-log plot. Fatigue relationships presented by Monismith, et. al (1970) describing fatigue life as a function of strain

and stiffness for air void contents of 5 and 7% were used to define two points on the assumed linear relationship.

Constant strain levels of 200, 300, and 400μ in/in for modulus values of 50, 100, 500, and 1,000 x 10^3 psi were considered. The results of this analysis are shown in Figures 28, 29, and 30.

The slope of these lines relates changes in air voids to changes in fatigue life. Figures 28, 29, and 30 reveal that the slope of the lines was not significantly affected by strain level or modulus value. These lines can be expressed in the form

$$\text{Log } N_f = C_1 - C_2 \text{ (AV)}$$

where C_1 and C_2 are constants, N_f is the fatigue life, and AV is the air void content. Examination of the data revealed that a representative value for the slope constant C_2 was 0.10. This slope value was used in the sensitivity analysis to relate the changes in air voids to changes in fatigue life. Air voids changes of ±1, ±2, and ±3% were considered in the analysis.

Geometry

The overall effect of structural geometry was considered through the investigation of three types of structural sections. Within each type of structural section, variations in the thickness of the asphalt concrete layer were considered. This represents the level of control possible in the field. Thickness variations of ±1/4 and ±1/2 inch were investigated in the sensitivity analysis.

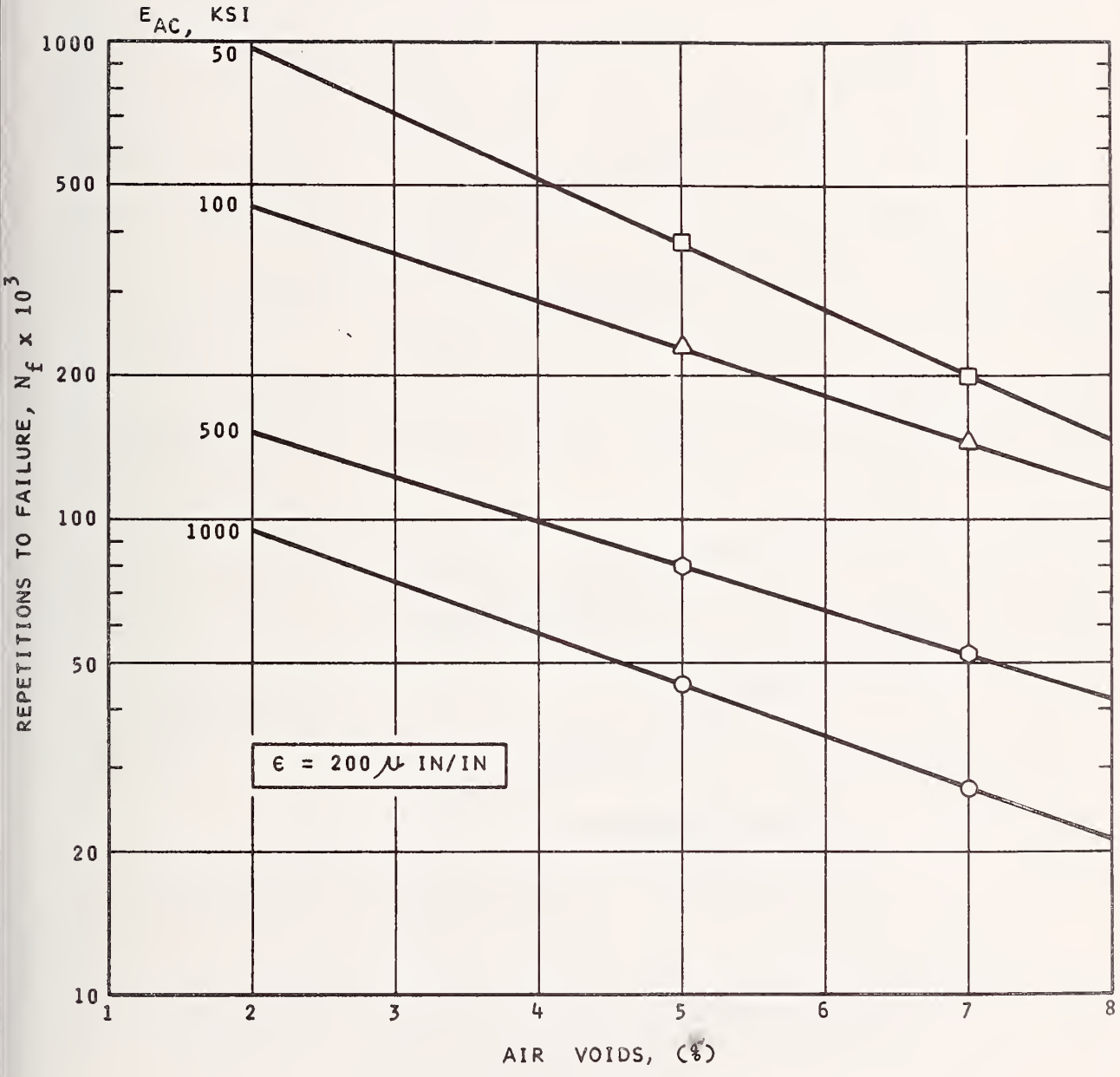

FIGURE 28 - EFFECT OF AIR VOIDS ON FATIGUE LIFE FOR CONSTANT ASPHALT CONCRETE MODULI AND STRAIN LEVEL OF 200 μ IN/IN

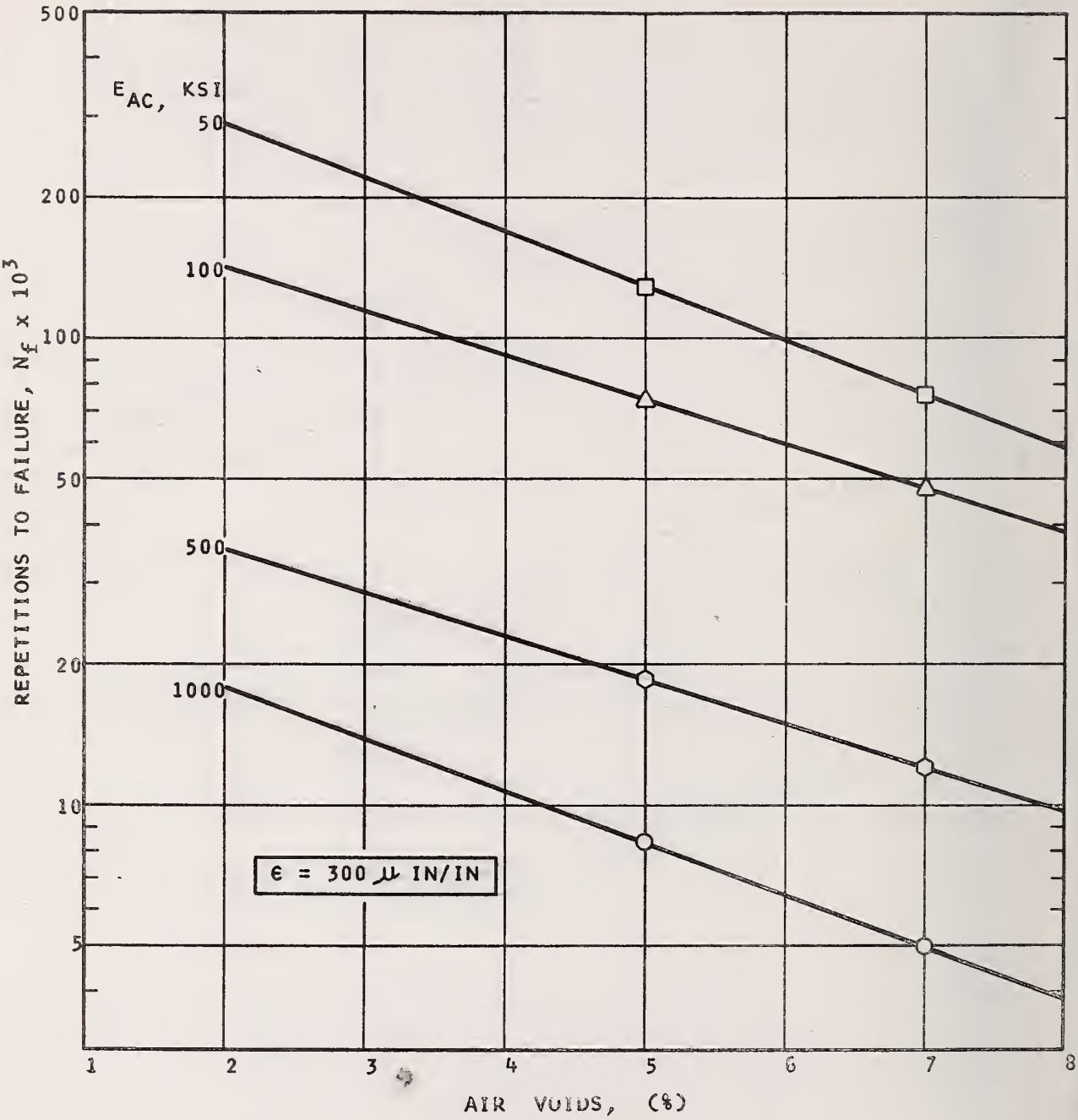

FIGURE 29 - EFFECTS OF AIR VOIDS ON FATIGUE LIFE FOR CONSTANT ASPHALT CONCRETE MODULI AND STRAIN LEVEL OF 300 μ IN/IN

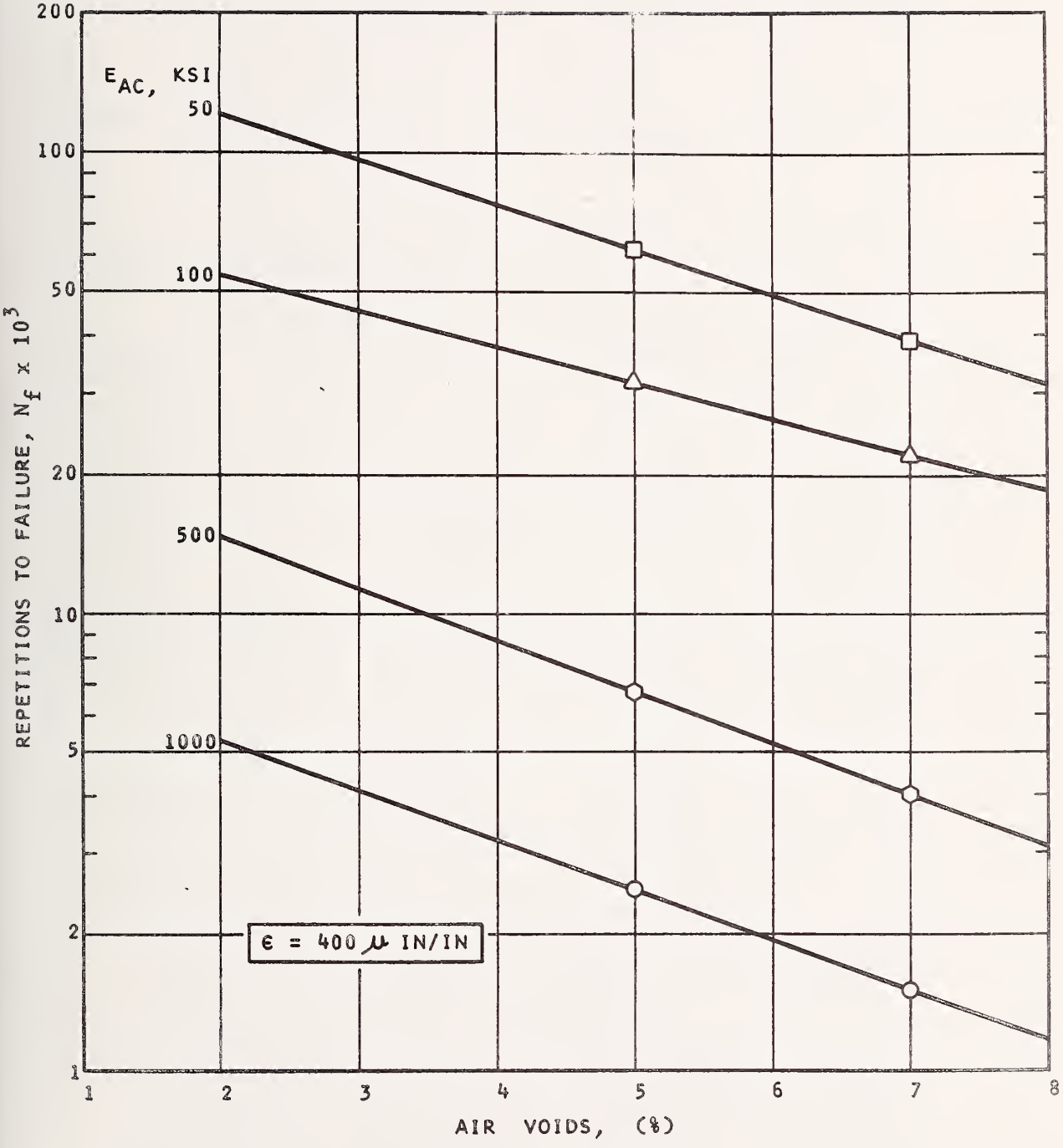

FIGURE 30 - EFFECT OF AIR VOIDS ON FATIGUE LIFE FOR CONSTANT ASPHALT CONCRETE MODULI AND STRAIN LEVEL OF 400 μ IN/IN

CONDUCT OF SENSITIVITY ANALYSIS AND PRESENTATION OF RESULTS

In the previous two sections, the parameters considered to affect the prediction of fatigue life and their relationship to system inputs have been defined. This section describes how this information was utilized to conduct the sensitivity analysis and the results of the analysis.

The variables considered in the sensitivity analysis are summarized in Table 6. This table also indicates the range of uncertainty of each variable and the system inputs affected. Changes in the variables were related to changes in the system inputs utilizing the relationships established in the previous section. The range of uncertainty of each variable shown in Table 6 was investigated for each of the three structural sections and macro-temperature levels of 40, 60, 80, and 100°F.

The sensitivity analysis was conducted by computer simulation of the pavement system as a three-layered linear elastic system.

The computer program CHEV5L) was used to find the maximum horizontal tensile strain at the base of the asphalt concrete for each combination of system inputs considered in the analysis. This strain was then used in conjunction with the fatigue failure criteria shown in Figure 26 to predict the number of repetitions to cause fatigue failure.

The procedure for conducting the analysis was to first predict the fatigue life for each structural section and macro-temperature level using the average values for all system inputs. These fatigue lives are considered to be the average fatigue life for each condition. Once the

TABLE 6

PARAMETERS CONSIDERED IN THE SENSITIVITY ANALYSIS

PARAMETER	RANGE OF VARIATION ABOUT AVERAGE VALUE	SYSTEM INPUT AFFECTED
1. Temperature (T)	±1, ±3, ±6°F	Modulus of AC and Fatigue Criteria
2. Air Voids (AV)	±1, ±2, ±3%	Modulus of AC and Fatigue Criteria
3. Thickness of AC*, (t_{AC})	±¼, ±½ inch	Thickness of Asphalt Concrete
4. Fatigue Criteria*, (N_f)	±0.2, ±0.4 (standard error)	Fatigue Criteria
5. Modulus*		
a. Asphalt Concrete (E_{AC})	±10, ±20, ±40%	Modulus of AC and Fatigue Criteria
b. Base Course (E_{BC})	-20, -40, -60, +25, +50, +100%	Modulus of Base Course
c. Subgrade (E_{SG})	-20, -40, -60, +25, +50, +100%	Modulus of Subgrade
6. Poisson's Ratio*		
a. Asphalt Concrete (ν_{AC})	±0.1	Poisson's Ratio of Asphalt Concrete
b. Base Course (ν_{BC})	±0.1	Poisson's Ratio of Base Course
c. Subgrade (ν_{SC})	±0.1	Poisson's Ratio of Subgrade

*These represent system inputs.

average fatigue life values had been established, the influence of uncertainty in the system inputs caused by uncertainty in the variables listed in Table 6 were considered. The level of uncertainty in each variable was considered independently. Therefore, each fatigue life was determined by changing one variable from its average value while holding all others at their average value. This defined a new fatigue life prediction caused by a change in each variable. The change in fatigue life from the average values could then be expressed as a percentage of the average fatigue life. These percentage changes were utilized to evaluate the sensitivity of fatigue life to uncertainty in each variable.

The basic results of the sensitivity analysis using the above procedure are shown in Tables 7 to 13. Each table was developed for a particular structural section and macro-temperature level. Since all the tables are similar, it is only necessary to explain the contents of one table. Consider the results shown in Table 7 for Section 1 at a macro-temperature level of 80°F. The average material constitutive constants are shown in parentheses under the title. The average system inputs resulted in a maximum tensile strain of 185μ in/in at the base of the asphalt concrete. This value is denoted as $\bar{\varepsilon}$ in the table and remains constant. The fatigue failure criteria shown in Figure 26 was then used to obtain the average fatigue life, $\bar{N}_f$, corresponding to $\bar{\varepsilon}$ and the average asphalt concrete modulus. The remainder of Table 7 shows the effect of the uncertainty levels of each variable on the tensile strain at the base of the asphalt concrete and resulting fatigue life prediction. The following paragraphs describe how these effects were established.

TABLE 7 - SENSITIVITY ANALYSIS OF SECTION 1, T=80°F

($\bar{E}_{AC}$ = 250 x 10^3 psi, $\bar{E}_{BC}$ = ———, $\bar{E}_{SG}$ 5 x 10^3 psi, $\bar{\nu}_{AC}$ = $\bar{\nu}_{SG}$ = 0.4, $\bar{\nu}_{BC}$ = ———)

		ΔTemperature (ΔT)			ΔAsphalt Concrete Modulus (ΔE_{AC})			ΔAsphalt Concrete Thickness (ΔE_{AC})		ΔFatigue Criteria (ΔN_f)[1]		ΔSubgrade Modulus (ΔE_{SG})			ΔBase Course Modulus (ΔE_{BC})			ΔAir Voids (ΔAV)			ΔPoisson's Ratio $\Delta\nu_{AC}$ $\Delta\nu_{BC}$ $\Delta\nu_{SG}$			ΔLoad Duration (ΔLD)
		±1°F	±3°F	±6°F	±10%	±20%	±40%	±¼"	±½"	±1Std error	±2Std error	-20% to +25%	-40% to +50%	-60% to +100%	-20% to +25%	-40% to +50%	-60% to +100%	±1%	±2%	±3%	±0.1	±0.1	±0.1	-0.07 sec.
TENSILE STRAIN (μin/in)	$\bar{\epsilon}$	185	185	185	185	185	185	185	185	-	-	185	185	185	-	-	-	185	185	185	185	-	185	185
	ϵ_{max} to ϵ_{min}	205 to 180	220 to 160	250 to 125	210 to 180	225 to 170	275 to 150	192 to 179	198 to 172	-	-	193 to 176	202 to 169	215 to 158	-	-	-	210 to 175	220 to 165	245 to 150	195 to 170	-	186 to 182	- to 145
FATIGUE LIFE (No. of Repetitions x 10^3)	$\bar{N}_f$	170	170	170	170	170	170	170	170	170	170	170	170	170	-	-	-	170	170	170	170	-	170	170
	$N_f$min to $N_f$max	130 to 180	100 to 230	84 to 440	120 to 170	100 to 190	71 to 260	150 to 190	130 to 210	110 to 270	68 to 430	142 to 190	129 to 230	105 to 280	-	-	-	95 to 235	69 to 332	45 to 540	145 to 225	-	170 to 175	- to 290
	ΔN_f	-40 to +10	-70 to +60	-86 to +270	-50 to 0	-70 to +20	-99 to +90	-20 to +20	-40 to +40	-60 to +100	-102 to +260	-28 to +20	-41 to +60	-65 to +110	-	-	-	-75 to +65	-101 to +162	-125 to +370	-25 to +55	-	0 to +5	- to +120
	$\frac{\Delta N_{fx10^2}}{N_f}$	-24 to +6	-41 to +35	-51 to +159	-29 to 0	-41 to +12	-59 to +53	-12 to +12	-24 to +24	-36 to +59	-60 to +152	-16 to +12	-24 to +35	-38 to +65	-	-	-	-44 to +38	-59 to +95	-73 to +218	15 to +32	-	0 to +3	- to +71

1) One standard error is assumed to be equal to 0.20 on log ϵ - log N_f plot.

TABLE 8 - SENSITIVITY ANALYSIS OF SECTION 1, T= 100°F

($\bar{E}_{AC}$ = 70 x 10^3 psi, $\bar{E}_{BC}$ = ———, $\bar{E}_{SG}$ = 5 x 10^3 psi, $\bar{\nu}_{AC}$ = $\bar{\nu}_{SG}$ = 0.4, $\bar{\nu}_{BC}$ = ———)

		ΔTemperature (ΔT)			ΔAsphalt Concrete Modulus (ΔE_{AC})			ΔAsphalt Concrete Thickness (ΔE_{AC})		ΔFatigue Criteria (ΔN_f)[1]		ΔSubgrade Modulus (ΔE_{SG})			ΔBase Course Modulus (ΔE_{BC})			ΔAir Voids (ΔAV)			ΔPoisson's Ratio $\Delta\nu_{AC}$ $\Delta\nu_{BC}$ $\Delta\nu_{SG}$			ΔLoad Duration (ΔLD)
		±1°F	±3°F	±6°F	±10%	±20%	±40%	±¼"	±½"	±1Std error	±2Std error	-20% to +25%	-40% to +50%	-60% to +100%	-20% to +25%	-40% to +50%	-60% to +100%	±1%	±2%	±3%	±0.1	±0.1	±0.1	-0.07 sec.
TENSILE STRAIN (μin/in)	$\bar{\epsilon}$	475	475	475	475	475	475	475	475	-	-	475	475	475	-	-	-	475	475	475	475	-	475	475
	ϵ_{max} to ϵ_{min}	485 to 465	535 to 425	625 to 370	510 to 440	550 to 415	660 to 370	494 to 464	509 to 448	-	-	511 to 444	553 to 416	611 to 373	-	-	-	510 to 435	550 to 410	585 to 370	495 to 451	-	489 to 464	- to 325
FATIGUE LIFE (No. of Repetitions x 10^3)	$\bar{N}_f$	30	30	30	30	30	30	30	30	30	30	30	30	30	-	-	-	30	30	30	30	-	30	30
	$N_f$min to $N_f$max	30 to 30	26 to 35	24 to 41	28 to 32	24 to 37	19 to 42	26 to 31	24 to 34	19 to 48	12 to 75	25 to 35	20 to 43	15 to 53	-	-	-	21 to 43	16 to 58	12 to 52	27 to 82	- to	27 to 31	- to 56
	ΔN_f	0 to 0	-4 to +5	-6 to +11	-2 to +2	-6 to +7	-11 to +12	-4 to +1	-6 to +4	-11 to +18	-18 to +45	-5 to +5	-10 to +13	-15 to +23	-	-	-	-9 to +13	-14 to +28	-18 to +58	-3 to +4	- to	-3 to +1	- to 26
	$\Delta \frac{N_f x 10^2}{N_f}$	0 to 0	-13 to +17	-20 to +37	-7 to +7	-20 to +23	-37 to +40	-13 to +3	-20 to +13	-36 to +58	-16 to +152	-17 to +17	-33 to +43	-50 to +77	-	-	-	-30 to +43	-47 to +93	-60 to +193	-10 to +13	- to	-10 to +3	- to +87

1) One standard error is assumed to be equal to 0.20 on log ε. - log N_f plot.

TABLE 9 - SENSITIVITY ANALYSIS OF SECTION 2, T=60°F

($\bar{E}_{AC}$ = 1,000 x 10^3 psi, $\bar{E}_{BC}$ = 10 x 10^3 psi, $\bar{E}_{SG}$ 5 x 10^3 psi, $\bar{\nu}_{AC} = \bar{\nu}_{SG}$ = 0.4, $\bar{\nu}_{BC}$ = 0.3)

		ΔTemperature (ΔT)			ΔAsphalt Concrete Modulus (ΔE_{AC})			ΔAsphalt Concrete Thickness (ΔE_{AC})		ΔFatigue Criteria (ΔN_f)[1]		ΔSubgrade Modulus (ΔE_{SG})			ΔBase Course Modulus (ΔE_{BC})			ΔAir Voids (ΔAV)			ΔPoisson's Ratio $\Delta\nu_{AC}$ $\Delta\nu_{BC}$ $\Delta\nu_{SG}$			ΔLoad Duration (ΔLD)
		±1°F	±3°F	±6°F	∓10%	∓20%	∓40%	∓¼"	∓½"	∓1Std error	∓2Std error	-20% to +25%	-40% to +50%	-60% to +100%	-20% to +25%	-40% to +50%	-60% to +100%	±1%	±2%	±3%	∓0.1	±0.1	±0.1	-0.07 sec.
TENSILE STRAIN (μin/in)	$\bar{\varepsilon}$	105	105	105	105	105	105	105	105	-	-	105	105	105	105	105	105	105	105	105	105	105	105	105
	ε_{max} to ε_{min}	110 to 105	125 to 100	155 to 85	115 to 105	125 to 95	165 to 80	112 to 102	118 to 87	-	-	110 to 105	113 to 103	118 to 100	109 to 105	112 to 103	115 to 99	120 to 100	125 to 90	145 to 80	114 to 98	108 to 105	108 to 105	- to 80
FATIGUE LIFE (No. of Repetitions x 10^3)	$\bar{N}_f$	740	740	740	740	740	740	740	740	740	740	740	740	740	740	740	740	740	740	740	740	740	740	740
	N_{fmin} to N_{fmax}	600 to 740	360 to 840	180 to 1900	500 to 740	400 to 1100	150 to 2600	560 to 820	440 to 1500	470 to 1200	300 to 1900	600 to 740	540 to 780	460 to 900	620 to 740	560 to 780	500 to 900	354 to 1070	230 to 2240	115 to 4800	520 to 980	660 to 740	660 to 740	- to 3500
	ΔN_f	-140 to 0	-380 to +100	-560 to +1600	-240 to 0	-340 to +360	-590 to +1860	-180 to +80	-300 to +760	-270 to +460	-440 to +1160	-140 to 0	-200 to +40	-280 to +160	-120 to +0	-180 to +40	-240 to +160	-386 to +330	-510 to +1500	-625 to +4060	-120 to +240	-80 to 0	-80 to 0	- to +1760
	$\frac{\Delta N_f \times 10^2}{N_f}$	-19 to 0	-51 to +14	-76 to +157	-32 to 0	-46 to +49	-80 to +251	-24 to +11	-41 to +103	-37 to +58	-60 to +152	-19 to 0	-27 to +5	-38 to +22	-16 to 0	-24 to +5	-32 to +22	-52 to +45	-69 to +204	-84 to +550	-16 to +32	-11 to 0	-11 to 0	- to - 238

1) One standard error is assumed to be equal to 0.20 on log ε. - log N_f plot.

Table 10 - SENSITIVITY ANALYSIS OF SECTION 2, T = 80°F

($\bar{E}_{AC}$ = 250 x 10^3 psi, $\bar{E}_{BC}$ = 10 x 10^3 psi, $\bar{E}_{SG}$ = 5 x 10^3 psi, $\bar{\nu}_{AC}$ = $\bar{\nu}_{SG}$ = 0.4, $\bar{\nu}_{BC}$ = 0.3)

		ΔTemperature (ΔT)			ΔAsphalt Concrete Modulus (ΔE_{AC})			ΔAsphalt Concrete Thickness (ΔE_{AC})		ΔFatigue Criteria (ΔN_f)[1]		ΔSubgrade Modulus (ΔE_{SG})			ΔBase Course Modulus (ΔE_{BC})			ΔAir Voids (ΔAV)			ΔPoisson's Ratio $\Delta\nu_{AC}$ $\Delta\nu_{BC}$ $\Delta\nu_{SG}$			ΔLoad Duration (ΔLD)
		±1°F	±3°F	±6°F	∓10%	∓20%	∓40%	∓¼"	∓½"	∓1Std error	∓2Std error	-20% to +25%	-40% to +50%	-60% to +100%	-20% to +25%	-40% to +50%	-60% to +100%	±1%	±2%	±3%	∓0.1	±0.1	±0.1	-0.07 sec.
TENSILE STRAIN (μin/in)	$\bar{\epsilon}$	300	300	300	300	300	300	300	300	-	-	300	300	300	300	300	300	300	300	300	300	300	300	300
	ϵ_{max} to ϵ_{min}	315 to 285	335 to 250	385 to 200	320 to 280	345 to 265	420 to 240	312 to 389	326 to 278	-	-	308 to 293	319 to 287	334 to 279	314 to 286	330 to 273	350 to 251	320 to 280	340 to 265	375 to 235	314 to 281	305 to 295	303 to 298	- to 230
FATIGUE LIFE (No. of Repetitions x 10^3)	$\bar{N}_f$	36	36	36	36	36	36	36	36	36	36	36	36	36	36	36	36	36	36	36	36	36	36	36
	$N_f$min to $N_f$max	33 to 38	30 to 52	22 to 84	34 to 40	28 to 42	20 to 54	32 to 41	28 to 46	23 to 57	14 to 90	33 to 38	30 to 42	25 to 46	31 to 44	27 to 48	22 to 64	27 to 53	19 to 75	13 to 116	31 to 44	34 to 38	34.5 to 37	- to 60
	ΔN_f	-6 to +2	-6 to +16	-14 to +48	-2 to +4	-8 to +6	-16 to +18	-4 to +5	-8 to +10	-13 to +21	-22 to +54	-3 to +2	-6 to +6	-11 to +10	-5 to +8	-9 to +12	-14 to +28	-9 to +17	-17 to +39	-23 to +80	-5 to +8	-2 to +2	-1.5 to +1	- to +24
	$\frac{\Delta N_f}{N_f} \times 10^2$	-8 to +5	-17 to +44	-39 to +133	-5 to +11	-22 to +17	-44 to +50	-11 to +14	-22 to +28	-36 to +58	-60 to +152	-8 to +5	-17 to +17	-30 to +28	-14 to +22	-25 to +33	-39 to +78	-25 to +47	-47 to +108	-64 to +222	-14 to +22	-6 to +6	-4 to +4	- to +67

1) One standard error is assumed to be equal to 0.20 on log ε. - log N_f plot.

TABLE 11 - SENSITIVITY ANALYSIS OF SECTION 2, T = 100°F

($\bar{E}_{AC}$ = 70 x 10^3 psi, $\bar{E}_{BC}$ - 10 x 10^3 psi, $\bar{E}_{SG}$ = 5 x 10^3 psi, $\bar{\nu}_{AC} = \bar{\nu}_{SG}$ = 0.4, $\bar{\nu}_{BC}$ = 0.3)

		Δ Temperature (ΔT)			Δ Asphalt Concrete Modulus (ΔE_{AC})			Δ Asphalt Concrete Thickness (ΔE_{AC})		Δ Fatigue Criteria (ΔN_f) [1]		Δ Subgrade Modulus (ΔE_{SG})			Δ Base Course Modulus (ΔE_{BC})			Δ Air Voids (ΔAV)			Δ Poisson's Ratio $\Delta\nu_{AC}$ $\Delta\nu_{BC}$ $\Delta\nu_{SG}$			Δ Load Duration (ΔLD)
		±1°F	±3°F	±6°F	∓10%	∓20%	∓40%	∓¼"	∓½"	∓1Std error	∓2Std error	-20% to +25%	-40% to +50%	-60% to +100%	-20% to +25%	-40% to +50%	-60% to +100%	±1%	±2%	±3%	∓0.1	±0.1	±0.1	-0.07 sec.
TENSILE STRAIN (μin/in)	$\bar{\epsilon}$	635	635	635	635	635	635	635	635	-	-	635	635	635	635	635	635	635	635	635	635	635	635	635
	ϵ_{max} to ϵ_{min}	650 to 625	685 to 590	755 to 530	665 to 610	695 to 585	780 to 530	659 to 617	681 to 598	-	-	650 to 627	667 to 618	692 to 607	698 to 676	771 to 525	868 to 444	665 to 605	690 to 580	725 to 530	643 to 624	662 to 613	645 to 632	- to 485
FATIGUE LIFE (No. of Repetitions x 10^3)	$\bar{N}_f$	14	14	14	14	14	14	14	14	14	14	14	14	14	14	14	14	14	14	14	14	14	14	14
	$N_{f_{min}}$ to $N_{f_{max}}$	12 to 16	13 to 14	14 to 15	13 to 15	13 to 14	13 to 15	12 to 15	11 to 16	9 to 23	6 to 35	13 to 14	12 to 15	11 to 16	11 to 17	8 to 22	6 to 34	10 to 18	8 to 22	7 to 30	13.5 to 14.5	12.5 to 15	13.5 to 14	- to 17
	ΔN_f	-2 to +2	-1 to 0	0 to +1	-1 to +1	-1 to 0	-1 to +1	-2 to +1	-6 to +2	-5 to +8	-8 to +21	-1 to 0	-2 to +1	-3 to +2	-3 to +3	-6 to +8	-8 to +20	-4 to +4	-6 to +8	-7 to +16	-0.5 to +0.5	-1.5 to +1	-0.5 to 0	- to +3
	$\Delta \frac{N_f \times 10^2}{\bar{N}_f}$	-14 to +14	-7 to 0	0 to +7	-7 to +7	-7 to 0	-7 to +7	-14 to +7	-21 to +14	-36 to +58	-60 to +152	-7 to 0	-14 to +7	-21 to +14	-21 to +21	-43 to +57	-57 to +143	-29 to +29	-43 to +58	-50 to +115	-4 to +4	-11 to +7	-4 to 0	- to +21

1) One standard error is assumed to be equal to 0.20 on log ε. - log N_f plot.

TABLE 12 - SENSITIVITY ANALYSIS OF SECTION 3, T = 40°F

($\bar{E}_{AC}$ = 2,350 x 10^3 psi, $\bar{E}_{BC}$ = 10 x 10^3 psi, $\bar{E}_{SG}$ 5 x 10^3 psi, $\bar{\nu}_{AC} = \bar{\nu}_{SG}$ = 0.4, $\bar{\nu}_{BC}$ = 0.3)

		ΔTemperature (ΔT)			ΔAsphalt Concrete Modulus (ΔE_{AC})			ΔAsphalt Concrete Thickness (ΔE_{AC})		ΔFatigue Criteria (ΔN_f)[1]		ΔSubgrade Modulus (ΔE_{SG})			ΔBase Course Modulus (ΔE_{BC})			ΔAir Voids (ΔAV)			ΔPoisson's Ratio $\Delta\nu_{AC}$ $\Delta\nu_{BC}$ $\Delta\nu_{SG}$			ΔLoad Duration (ΔLD)
		±1°F	±3°F	±6°F	∓10%	∓20%	∓40%	∓¼"	∓½"	∓1Std error	∓2Std error	-20% to +25%	-40% to +50%	-60% to +100%	-20% to +25%	-40% to +50%	-60% to +100%	±1%	±2%	±3%	∓0.1	±0.1	±0.1	-0.07 sec.
TENSILE STRAIN (μin/in)	$\bar{\varepsilon}$	140	140	140	140	140	140	140	140	-	-	140	140	140	140	140	140	140	140	140	140	140	140	140
	ε_{max} to ε_{min}	140 to 137	150 to 135	160 to 125	140 to 120	155 to 115	205 to 110	149 to 128	162 to 118	-	-	140 to 132	143 to 127	148 to 118	143 to 132	150 to 127	159 to 118	150 to 125	160 to 120	175 to 105	146 to 127	140 to 136	140 to 137	- to 130
FATIGUE LIFE (No. of Repetitions x 10^3)	$\bar{N}_f$	160	160	160	160	160	160	160	160	160	160	160	160	160	160	160	160	160	160	160	160	160	160	160
	$N_f$min to $N_f$max	160 to 160	130 to 180	95 to 260	130 to 320	100 to 370	36 to 470	120 to 270	80 to 370	99 to 253	64 to 400	160 to 220	150 to 270	130 to 380	150 to 210	120 to 270	90 to 360	99 to 343	58 to 512	32 to 1320	135 to 270	160 to 190	160 to 185	- to 230
	ΔN_f	0 to 0	-30 to +20	-65 to +100	-30 to +160	-60 to +210	-124 to +310	-40 to +110	-80 to +210	-61 to +93	-46 to +240	0 to +60	-10 to +110	-30 to +200	-10 to +50	-40 to +110	-70 to +220	-61 to +183	-102 to +352	-128 to +1160	-26 to +110	0 to +30	0 to +25	- to +70
	$\frac{\Delta N_f}{N_f} \times 10^2$	0 to 0	-19 to +12	-41 to +62	-19 to +100	-37 to +131	-78 to +194	-25 to +69	-50 to +131	-38 to +58	-60 to +151	0 to +37	-6 to +69	-19 to +137	-6 to +31	-25 to +69	-44 to +125	-38 to +114	-64 to +4220	-80 to +730	-16 to +69	0 to +19	0 to +16	- to +44

1) One standard error is assumed to be equal to 0.20 on log ε_t - log N_f plot.

TABLE 13 - SENSITIVITY ANALYSIS OF SECTION 3, T = 60°F

($\bar{E}_{AC}$ = 1,000 x 10^3 psi, $\bar{E}_{BC}$ = 10 x 10^3 psi, $\bar{E}_{SG}$ = 5 x 10^3 psi, $\bar{\nu}_{AC}$ = $\bar{\nu}_{SG}$ = 0.4, $\bar{\nu}_{BC}$ = 0.3)

		ΔTemperature (ΔT)			ΔAsphalt Concrete Modulus (ΔE_{AC})			ΔAsphalt Concrete Thickness (ΔE_{AC})		ΔFatigue Criteria (ΔN_f)[1]		ΔSubgrade Modulus (ΔE_{SG})			ΔBase Course Modulus (ΔE_{BC})			ΔAir Voids (ΔAV)			ΔPoisson's Ratio $\Delta\nu_{AC}$ $\Delta\nu_{BC}$ $\Delta\nu_{SG}$			ΔLoad Duration (ΔLD)
		±1°F	±3°F	±6°F	∓10%	∓20%	∓40%	∓¼"	∓½"	∓1Std error	∓2Std error	-20% to +25%	-40% to +50%	-60% to +100%	-20% to +25%	-40% to +50%	-60% to +100%	±1%	±2%	±3%	∓0.1	±0.1	±0.1	-0.07 sec.
TENSILE STRAIN (μin/in)	$\bar{\varepsilon}$	225	225	225	225	225	225	225	225	-	-	225	225	225	225	225	225	225	225	225	225	225	225	225
	ε_{max} to ε_{min}	140 to 137	150 to 135	160 to 125	140 to 120	155 to 115	205 to 110	149 to 128	162 to 118	-	-	256 to 249	260 to 246	267 to 242	267 to 237	284 to 224	308 to 203	275 to 235	290 to 220	320 to 200	265 to 235	256 to 248	256 to 253	- to 200
FATIGUE LIFE (No. of Repetitions x 10^3)	$\bar{N}_f$	16.5	16.5	16.5	16.5	16.5	16.5	16.5	16.5	16.5	16.5	16.5	16.5	16.5	16.5	16.5	16.5	16.5	16.5	16.5	16.5	16.5	16.5	16.5
	$N_f$min to $N_f$max	160 to 160	130 to 180	95 to 260	130 to 320	100 to 370	36 to 470	120 to 270	80 to 370	99 to 253	64 to 400	16.5 to 18	15.0 to 19	14.0 to 20	14.0 to 24	11.0 to 29	8.0 to 42	12 to 28	7.5 to 43	5 to 80	14.5 to 24.5	16.5 to 20	16.5 to 17.5	- to 40
	ΔN_f	0 to 0	-30 to +20	-65 to +100	-30 to +160	-60 to +210	-124 to +310	-40 to +110	-80 to +210	-61 to +93	-46 to +240	0 to +1.5	-1.5 to +2.5	-2.5 to +3.5	-2.5 to +7.5	-5.5 to +12.5	-8.5 to +25.5	-4.5 to +11.5	-9 to +26.5	-11.5 to +5.35	-2 to +8	0 to +3.5	0 to +1	- to +23.5
	$\frac{\Delta N_f}{\bar{N}_f} x 10^2$	0 to 0	-19 to +12	-41 to +62	-19 to +100	-37 to +131	-78 to +194	-25 to +69	-50 to +131	-38 to +58	-60 to +151	0 to +9	-4 to +15	-15 to +21	-15 to +45	-33 to +76	-52 to +153	-27 to +69	-54 to +160	-69 to +384	-12 to +48	0 to +21	0 to +6	- to +142

1) One standard error is assumed to be equal to 0.20 on log ε. - log N_f plot.

Uncertainty levels in the following variables had no effect on the fatigue failure criteria itself (the actual fatigue prediction using the criteria was, of course, affected): thickness of the asphalt concrete, Δt_{AC}; subgrade modulus, ΔE_{SG}; base course modulus, ΔE_{BC}; and Poisson's ratios, Δv_{AC}, Δv_{BC}, Δv_{SG}. Therefore, the effect of uncertainty levels in these variables could be established solely by their effect on the maximum tensile strain at the base of the asphalt concrete. These variables are also system inputs and the effect of uncertainty in each could be determined directly. Section 1 does not contain base course material so ΔE_{BC} and Δv_{BC} have no meaning for Section 1 but are considered for Sections 2 and 3.

For example, consider the effect of a ±1/4 inch uncertainty in thickness of the asphalt concrete, Δt_{AC}. Since the average asphalt concrete thickness for Section 1 was 12 inches, uncertainty in t_{AC} of ±1/4 inch was investigated by inputing t_{AC} = 11.75 and 12.25 inches, respectively, into structural analysis model (CHEV5L) holding all other variables at their average values. The resulting tensile strains at the base of the asphalt concrete were 192 and 179 (ε_{max} to ε_{min}) μ in/in, respectively. The fatigue failure criteria shown in Figure 26 were then utilized to predict the fatigue life for each strain level for an asphalt concrete modulus of 250 x 10^3 psi ($\overline{T}$ = 80°F).

The resulting fatigue life predictions were 150 and 190 x 10^3 repetitions ($N_{f\ min}$ to $N_{f\ max}$). The change in fatigue life (ΔN_f) from the average fatigue life ($\overline{N}_f$) were then computed and were -20 and +20 x 10^3 repetitions. These changes were then expressed as percentage changes from the average fatigue life ($\Delta N_f/\overline{N}_f$) x 10^2 which

resulted in a -12% and +12% change. Thus, a variation of -1/4 inch in the asphalt concrete thickness for Section 1 at $\overline{T} = 80°F$ resulted in a 12% reduction in the fatigue life.

The influence of uncertainty levels ΔE_{SG}, Δv_{AC}, and Δv_{SG} (ΔE_{BC} and Δv_{BC} for Sections 2 and 3) were obtained in a similar manner. Thus, the effect of uncertainty on the resulting fatigue life prediction for each variable was determined.

As noted in Table 6, uncertainty of temperature, ΔT; asphalt concrete modulus, ΔE_{AC}; air voids, ΔAV; and load duration, ΔLD affect both the modulus of the asphalt concrete and the fatigue criteria. Uncertainty of ΔT, ΔE_{AC} and ΔLD affect the asphalt concrete modulus, and, therefore, change the tensile strain at the base of the asphalt concrete from its average value. In addition to this change, since the asphalt concrete modulus changes, the fatigue failure line utilized to predict failure for the new strain level changes from the $\overline{E}_{AC} = 250 \times 10^3$ psi ($\overline{T} = 80°F$) line. The effect of ΔE_{AC} on both the tensile strain at the base of the asphalt concrete and fatigue prediction could be considered directly. The effect of ΔT was considered in terms of ΔE_{AC} utilizing the relationship between temperature and E_{AC} is shown in Figure 25. Similarly, the effect ΔLD was considered in terms of its effect on E_{AC}.

For example, consider the results shown in Table 7 for $\Delta T = \pm 6°F$. The effect of $\Delta T = \pm 6°F$ on E_{AC} at $\overline{T} = 80°F$ was determined from Figure 25 to result in $E_{AC} = 170$ and 450×10^3 psi, respectively. These two asphalt concrete

moduli values were input into the structural analysis model (CHEV5L) holding all other variables constant at their average values. The resulting tensile strains at the base of the asphalt concrete were 250 and 125μ in/in. Each of these strain values was then used in conjunction with the failure criteria (Figure 26) for the appropriate E_{AC} (170×10^3 and 450×10^3 psi) to determine the fatigue life. The resulting fatigue lives were 84×10^3 and 440×10^3 repetitions. Percent changes from the average fatigue life were determined to be -51% and +159%.

The uncertainty of air voids, ΔAV, also affects both the modulus of the asphalt concrete and the fatigue criteria. However, the effect of ΔAV on the fatigue criteria is not accounted for solely through its effect on E_{AC} as was the case for ΔT, ΔE_{AC}, and ΔLD. For a given E_{AC} (temperature) and resulting strain, it has been shown that ΔAV has an additional effect on the fatigue life (Figures 28, 29, and 30).

For example, consider the results shown in Table 7 for $\Delta AV = \pm 1\%$. Recall the relationship between air voids and both modulus and fatigue life was linear on a semi-log plot. The average slopes of the relationships were $C_2 = 0.05$ for air void effects on modulus and $C_2 = 0.10$ for effects on fatigue life. The slope constant C_2 relates changes in air voids to changes in modulus and fatigue life. First, consider the effect of $\Delta AV = \pm 1\%$ on the modulus, E_{AC}.

The linear relationship on a semi-log plot results in changes being related by $\Delta \log E_{AC} = -C_2 (\Delta AV) = \pm C_2$ for $\Delta AV = \pm 1\%$. Therefore, $\Delta \log E_{AC} = \pm 0.05$. If the logarithm of a number is changed by addition or subtraction,

the number is changed by multiplying and dividing by the antilog. Since antilog (0.05) = 1.12, E_{AC} is changed to $E_{AC}/1.12$ for a 1% increase in air voids and to $1.12\ E_{AC}$ for a 1% decrease in air voids. For $\bar{E}_{AC} = 250 \times 10^3$ psi, the new modulus values for a ±1% change were 223×10^3 psi and 280×10^3 psi, respectively. These modulus values were input into the structural analysis model (CHEV5L) holding all other variables at their average values. The resulting strains were 210 and 175μ in/in. The fatigue criteria shown in Figure 26 were then used to predict the fatigue life for each strain level for the appropriate E_{AC} (223×10^3 and 280×10^3 psi) to determine the fatigue lives. However, these fatigue lives were not those entered in Table 7 because the effect of AV = ±1% on the fatigue life prediction for a given strain and modulus had not been considered.

The slope of the relation between air voids and fatigue life was shown to be independent of strain and modulus magnitudes (Figures 28, 29, and 30). Since this slope was found to be 0.10 and antilog (0.10) = 1.27, the fatigue life predicted for $\Delta AV = +1\%$ due to a ΔE_{AC} change was divided by 1.27, and that for a $\Delta AV = -1\%$ change multiplied by 1.27. The resulting fatigue life predictions for $\Delta AV = \pm 1\%$ were 95×10^3 and 235×10^3 repetitions which represent changes from the average fatigue life, $\bar{N}_f$ of -44% and +38%, respectively.

The effect of data scatter about the fatigue regression line, ΔN_f, is the only variable not yet discussed. The effects of this variable were considered through the standard error of estimate. For example, consider the effect of a ±1 standard error of 0.20. The standard

error represents the average variation of the regression of log ε on log N_f. Therefore, for a given strain level and modulus, log $N_f = \pm 0.20$. Since antilog (0.20) = 1.58, the average fatigue life was divided and multiplied by 1.58 and resulted in fatigue lives of 110×10^3 and 270×10^3 repetitions. This resulted in -36% and +59% changes from the average value.

Each level of uncertainty in each variable was considered, using the techniques described above. This procedure was repeated for each structural section and each macro-temperature level, and the results are shown in Tables 7 to 13.

Sensitivity analysis of Section 1 for macro-temperature levels of 40°F and 60°F, and Section 2 for $\overline{T}$ = 40°F were not possible because the average conditions resulted in an average strain value less than 70μ in/in. Since the fatigue criteria utilized (Figure 26) predicts infinite fatigue life for strains below 70μ in/in, percent changes from the average fatigue life were meaningless.

Sensitivity analysis results for Section 3 at $\overline{T}$ = 80°F and 100°F were also not possible. This was because the strain and modulus value combinations exceeded the range of definition of the fatigue criteria.

The sensitivity of fatigue life prediction to uncertainty in each variable can best be described using the percent changes of fatigue life from the average values ($\Delta N_f \times 10^2/N_f$) shown in Tables 7 through 13. Figure 31 shows a typical plot of the percent decreases in fatigue life caused by uncertainty in each variable for Section 2 at

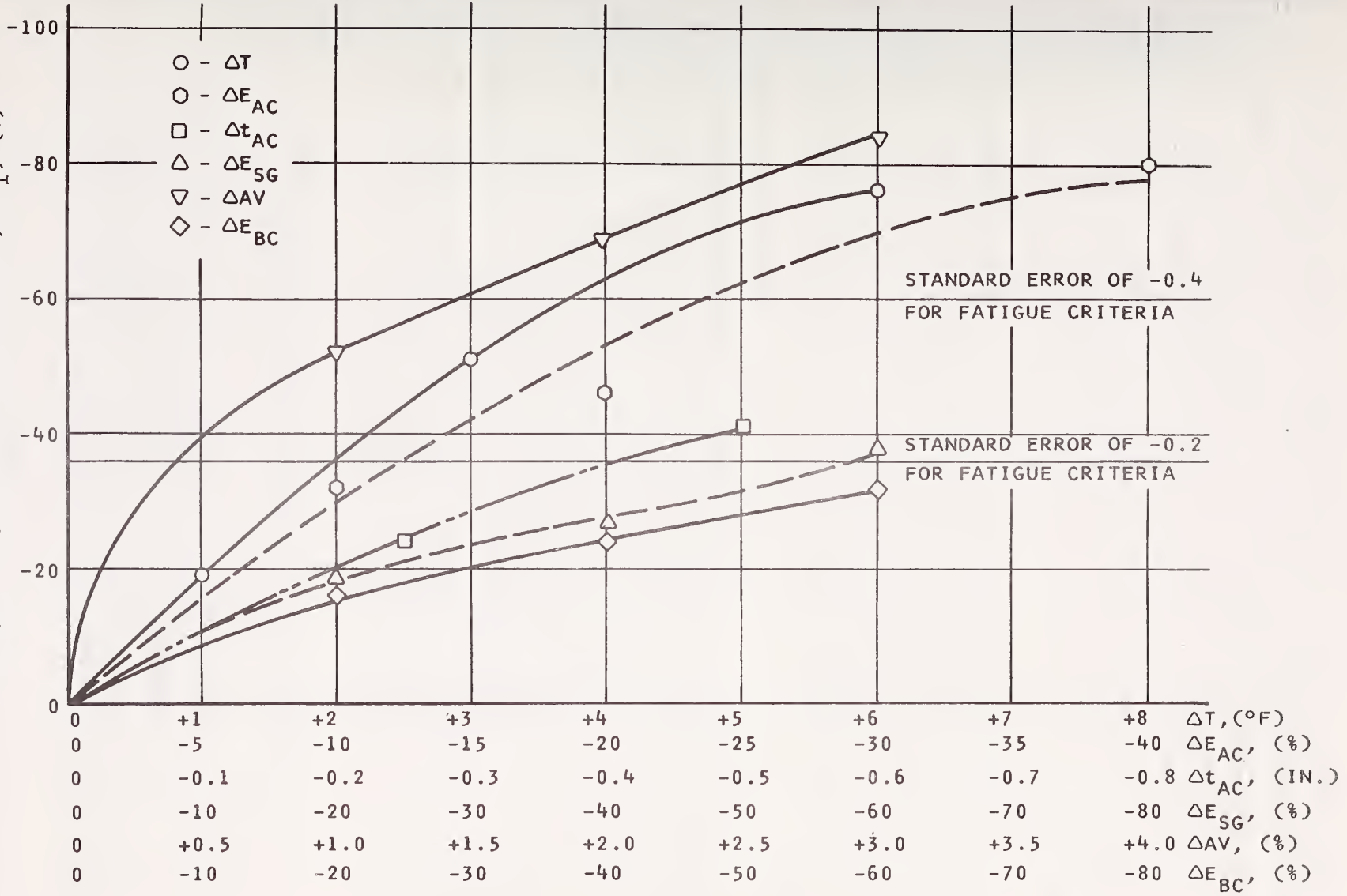

FIGURE 31 - SENSITIVITY OF FATIGUE LIFE TO PARAMETER VARIATIONS FOR SECTION 2, T = 60°F

a temperature of 60°F. The horizontal scales show the magnitude of uncertainty in each variable, and the vertical scale, the percent decreases in fatigue life. The percent decreases due to uncertainty in the fatigue criteria itself (ΔN_f) are shown as horizontal lines for the two values of standard error used. The values are constants for a given standard error (-36 and -60% for standard errors of 0.2 and 0.4).

Similar plots were made for all results shown in Tables 7 through 13. These plots can be used to determine the percent change in fatigue life caused by variable uncertainty, not only at the variable uncertainty levels analyzed, but also at any variable uncertainty level within the analyzed range.

Since the fatigue life uncertainty is dependent on the magnitude of each variable uncertainty, it is difficult to interpret the sensitivity results as typically shown in Figure 31. A more meaningful interpretation of the sensitivity results can be made by comparing percent changes in fatigue life induced by particular values of change in each parameter influencing fatigue life. This type of comparison can be thought of as the relative sensitivity of fatigue life prediction to the selected level of uncertainty in each parameter.

RELATIVE SENSITIVITY OF FATIGUE FAILURE TO PARAMETER VARIATIONS

Normally, when designing a pavement or writing specifications, more effort is taken to prevent a premature failure of the pavement as opposed to having a pavement last longer than anticipated. Therefore, it was felt that the

sensitivity results representing variable uncertainty causing decreases in fatigue life were more critical than those causing increases in fatigue life. Thus, the relative sensitivity analysis was conducted using the results in terms of percent decreases in fatigue life.

The results of a relative sensitivity analysis are only meaningful if compatible levels of uncertainty (variation) are selected for each variable. Realistic variations from the average value of each parameter were selected and utilized to define the relative significance of each parameter on fatigue life. The selection of realistic uncertainties for each variable was based on the scatter of experimental results when possible. Ideally, percent variations from average values (uncertainties) for each parameter should be selected such that each uncertainty has the same likelihood of occurring. This technique eliminates erroneous interpretation of the sensitivity results induced by using incompatible uncertainty levels of the individual variables. The uncertainty levels for each variable were selected such that approximately 70 to 80% of the time the effect of each variable uncertainty level on the decrease in fatigue life would not be greater than that analyzed in the analysis. The following section describes the procedure used to select compatible uncertainty levels for each variable.

Asphalt Concrete Modulus, ΔE_{AC}

This variable represents the uncertainty of asphalt concrete modulus caused by deviations from ideal linear isotropic elastic behavior. Figure 27 showed the experimental results of a linear isotropic elastic characterization for a typical asphalt concrete. The vertical bars at

each temperature tested represents the total range of variation of asphalt concrete moduli for all stress states tested. It can be seen that this range of uncertainty, measured in terms of percentage change from average values, increased with increase in temperature.

Figures 32 through 34 show the actual distribution of asphalt concrete moduli along the range of variation represented by the vertical bars in Figure 27. The probability density (relative frequency) for temperature levels of 40, 55, and 100°F are shown. The distributions represent the uncertainty in asphalt concrete moduli that can be expected from a linear elastic characterization due to stress state effects and variations in laboratory fabricated specimens. This can be thought of as the uncertainty associated with deviations from linear elastic behavior of the asphalt concrete so long as temperature and load duration are properly accounted for.

These figures were used to establish a ΔE_{AC} uncertainty level such that 75% of the time the asphalt concrete modulus would be higher than the selected value. The moduli values at each temperature which 75 percent of the data fall above (Probability = .75) were determined and expressed as percent variations from the average values used in the sensitivity analysis. These percent variations were used as guides to select realistic uncertainty levels for use in the relative sensitivity analysis. The following values were selected:

$T = 40°F$, $\Delta E_{AC} = -2\%$; $T = 60°F$, $\Delta E_{AC} = -10\%$;

$T = 80°F$, $\Delta E_{AC} = -20\%$; $T = 100°F$, $\Delta E_{AC} = -35\%$.

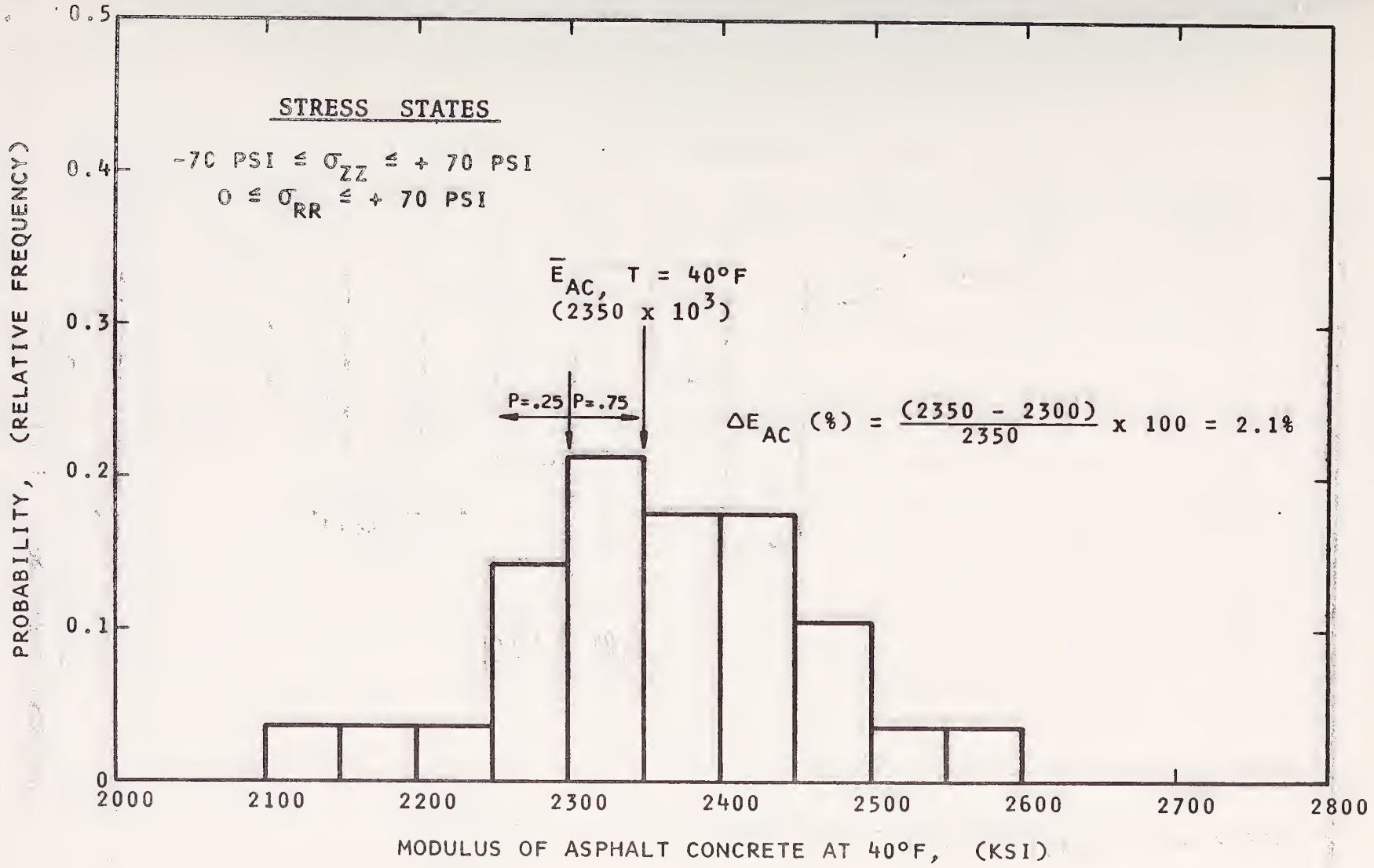

FIGURE 32 - PROBABILITY DENSITY OF E_{AC} AT 40°F FOR ALL STRESS STATES TESTED IN ELASTIC CHARACTERIZATION, (ONE SPECIMEN), AFTER MR&D (1970)

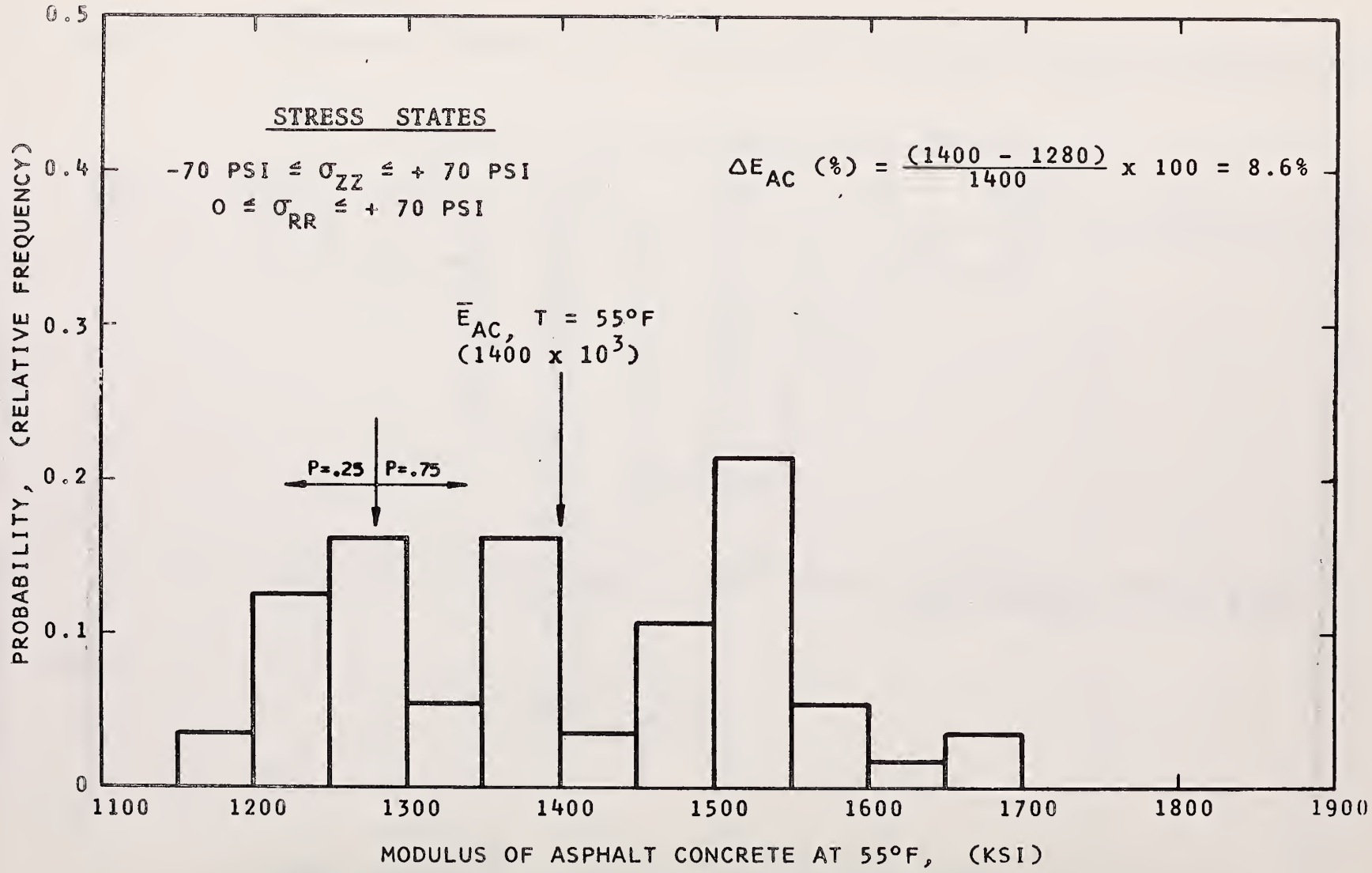

FIGURE 33 - PROBABILITY DENSITY OF E_{AC} AT 55°F FOR ALL STRESS STATES TESTED IN PLASTIC CHARACTERIZATION, (TWO SPECIMENS), AFTER MR&D (1970)

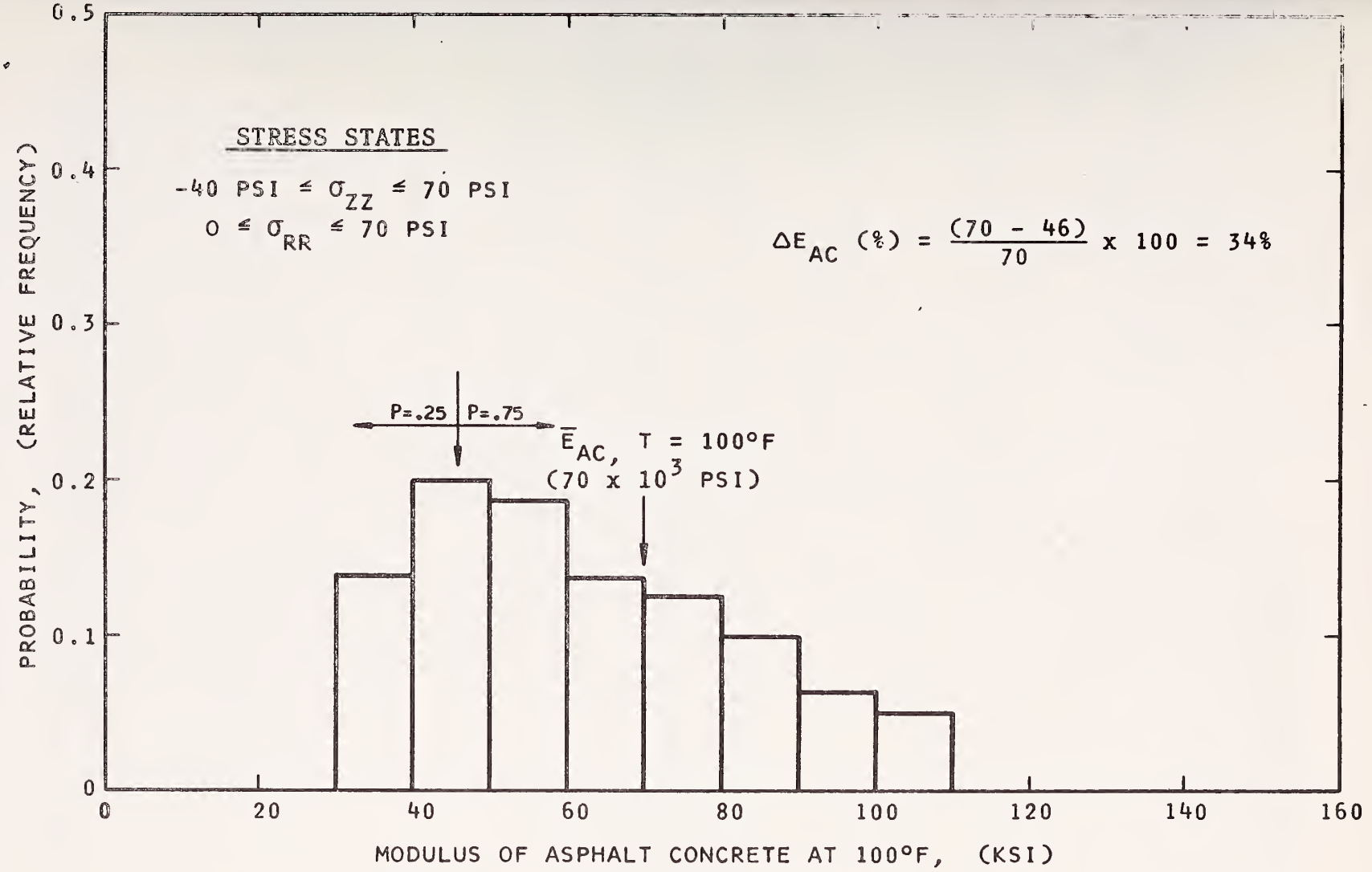

FIGURE 34 - PROBABILITY DENSITY OF E_{AC} AT 100°F FOR ALL STRESS STATES TESTED IN ELASTIC CHARACTERIZATION, (TWO SPECIMENS), AFTER MR&D (1970)

Base Course Modulus, ΔE_{BC}

Two levels of base course modulus uncertainty were evaluated in the relative sensitivity analysis. One level was selected to be representative of uncertainty due to deviations from linear elastic behavior and thus represents uncertainty associated with a linear elastic characterization. The other level of uncertainty was selected to be representative of both linear elastic characterization uncertainty and variations of the properties of in-place base course in the field.

No experimental results were available to establish probability densities for base course moduli values. However, the results of the nonlinear layered elastic analysis used to select a realistic average value for the base course modulus shown in Table 4 proved useful. Recall that these moduli values resulted from two nonlinear elastic modular relationships which bracketed the majority of data reported in the literature. These reported data were developed for a wide variety of aggregate types, densities, and degrees of saturation. Therefore, the range of modulus values shown in Table 4 represent the range of uncertainty due to stress state, density, and degree of saturation.

Consider the results of a Poisson ratio value of 0.3 since this was the average value used in the sensitivity analysis. If we consider that a given pavement will exist under a range of temperatures (asphalt concrete moduli), it can be seen that the change in stress state with temperature results in about a ±1,000 psi difference in the base course modulus from the average values for each constitutive equation. This results in a percent variation

of approximately 10% to 20% depending on the average modulus. Recall that each base course modulus shown in Table 4 was the average value over the total depth of the base course. Therefore, it was felt that a somewhat greater percent variation was needed to represent the uncertainty level due to the effects of stress state.

A $\Delta E_{BC} = -25\%$ was selected as representative of a probability = .75 uncertainty level that might be associated with a reduction in modulus due to the effects of stress state on the assumed average linear elastic modulus. This can be interpreted as an uncertainty level associated with a linear elastic characterization.

The effects of construction control of density and degree of saturation changes throughout the year cause additional uncertainty in the base course modulus. A $\Delta E_{BC} = 50\%$ was selected as representative of a base course modulus uncertainty level representing uncertainty in modulus due to linear elastic characterization uncertainty, field density uncertainty, and variations in degree of saturation.

Subgrade Modulus, ΔE_{SG}

As with the base course modulus, two levels of subgrade modulus uncertainty were investigated in the relative sensitivity analysis. Little information was available to provide guidance in the selection of uncertainty levels for the subgrade material associated with deviations from linear elastic behavior and variations in the properties of in-place subgrades in the field. The effects of stress state, number of load repetitions, water content, and density all cause uncertainty in the subgrade modulus.

The effect of each is dependent on the specific subgrade being considered. Therefore, it was felt that typical uncertainty levels should be selected, rather than uncertainty levels associated with a specific subgrade.

The average subgrade modulus used for the sensitivity analysis was 5,000 psi. It was decided that a modulus value of 3,750 psi would be a typical probability $\simeq .75$ lower bound value on the subgrade modulus due to the effects of deviations from ideal linear elastic behavior (stress state and load repetition effects). Therefore, a $\Delta E_{SG} = -25\%$ was selected as a typical value of uncertainty associated with a linear elastic characterization.

A subgrade modulus value of 2,500 psi was thought to be a typical probability = .75 lower bound on subgrade modulus caused by both deviations from linear elastic behavior and variations of in-place properties in the field (water content and density variations). Therefore, a $\Delta E_{SG} = -50\%$ was selected as a typical uncertainty level associated with both characterization and field variation effects.

Poisson's Ratio, (Δv_{AC}, Δv_{BC}, and Δv_{SG})

Poisson's ratio of the asphalt concrete varies with temperature and stress state. Poisson's ratio values of the base course and subgrade vary with stress state, density, and water content. While it is known that these variations occur, little information is available to establish the statistical properties of variations in Poisson's ratio caused by each. Therefore, it was necessary to select typical uncertainty levels of Poisson's ratio for each material based on subjective judgment.

It was decided that an uncertainty level of $\Delta v = 0.1$ would be a reasonable probability = .75 uncertainty level. Since this relative sensitivity analysis was conducted for variable uncertainties causing a decrease in fatigue life, the following values were selected: $\Delta v_{AC} = -0.1$, $\Delta v_{BC} = +0.1$, and $\Delta v_{SG} = +0.1$.

Temperature, ΔT

The uncertainty in temperature is that representing difference between the predicted and actual temperature regime of a pavement. The selection of a temperature uncertainty level is highly dependent on the degree to which temperature is considered in the design or analysis procedure. If an average yearly temperature is used, the uncertainty level selected for temperature should be quite large. However, if weather records are available and temperature is considered in detail, the uncertainty level associated with temperature would be small. Since most advanced pavement design and analysis techniques consider temperature in great detail, it was felt that uncertainty associated with temperature prediction would be small.

In the sensitivity analysis, each structural section was analyzed for four macro-temperature levels which were assumed to be constant for the life of the pavement and uniform throughout the depth of the asphalt concrete layer.

As discussed previously, these would be unreasonable assumptions if a particular pavement was being designed or analyzed. However, these conditions can be considered equivalent, in terms of fatigue life prediction, to some situation where temperature is considered in detail. The macro-temperature levels can be thought of as average

values representing climates ranging from cold to hot. For each macro-temperature level, the uncertainty level associated with temperature (micro-temperature variations) is the variable of interest.

Since the difference between predicted and actual temperature regime of a pavement would be small if temperature was considered in detail, the uncertainty associated with an equivalent macro-temperature level used in the sensitivity analysis would be even smaller. Therefore, a $\Delta T = +1°F$ was thought to be representative of temperature uncertainty for the conditions considered in this sensitivity analysis.

Thickness of Asphalt Concrete, Δt_{AC}

Uncertainty of the thickness of the asphalt concrete arises due to the limits of construction control possible in the field. The level of uncertainty selected for the relative sensitivity analysis was based on the variation of thickness measured on constructed pavements. At the AASHO Road Test, HRB Special Report 61B (1962), the specified construction tolerance was ±1/4 inch and 98% of the pavements had thicknesses greater than 1/4 inch less than the design thickness. However, quality control standards on the AASHO Road Test cannot be considered typical of the majority of pavement construction. Granley (1969) reported that for average construction control conditions, the standard deviation of thickness was 1/4 inch. Sherman (1970) reported that the standard deviation of 0.4 inch was typical of construction control in California projects from 1962 to 1969. If the distribution of thickness is assumed normal, a thickness one standard deviation less

than average thickness will insure that 84% of the thickness values will be greater. Based on this information, it was decided that an uncertainty level of Δt_{AC} = -1/4 inch would be representative of most pavements. This uncertainty level occurs with a probability of approximately the same magnitude used to select other variable uncertainty levels and was used for the relative sensitivity analysis.

Air Void Content, ΔAV

Uncertainty in the air void content of the asphalt concrete is caused by the limits of construction control in the field. The same three publications mentioned above were utilized to select the uncertainty level for air voids in the relative sensitivity analysis. Data from the AASHO Road Test show a standard deviation of approximately 1.5% for the air void content of asphalt concrete. Granley (1969) reported a standard deviation of approximately 2.25% for research jobs in a number of states. Sherman (1970) reported a standard deviation of about 1.5% for pavements trafficked for 10 to 12 years.

If a normal distribution of air voids is assumed, a +2% uncertainty level of air voids would result in a compatible probability level with all other variable uncertainty levels. Therefore, ΔAV = +2% was used for the relative sensitivity analysis.

Fatigue Criteria, ΔN_f

Uncertainty in the fatigue criteria arises due to the stochastic nature of fatigue failure and test control limitations in the laboratory. Kasianchuk (1968) has

shown the distribution of fatigue life for any given strain level is log normal. This means that the logarithm of fatigue life is normally distributed. The standard error of the regression fit of the fatigue data (log N_f vs. log ε_{AC}) is a measure of the standard deviation of the fatigue criteria. The standard error represents the average standard deviation for the fit of the regression line over all strain levels. Since fatigue life is log normal, one standard error of the logarithm of fatigue life less than the average value will result in 84% of the fatigue lives being greater. Therefore, the level of uncertainty in the fatigue criteria, ΔN_f, selected for the relative sensitivity analysis was -1 standard error of 0.2. Recall that 0.2 was the typical standard error value of the logarithm of fatigue life selected for the sensitivity analysis.

Results of Relative Sensitivity Analysis

The relative sensitivity of fatigue life prediction to the level of uncertainty selected for each variable represent variations from the average values which would cause a decrease in fatigue life. The magnitude of the uncertainty levels were selected such that the probability would be 0.7 to 0.8 that the effect of each variable on decreases in fatigue life would be less than the level analyzed.

The results of the relative sensitivity analysis are presented in Tables 14 through 19. There are two tables for each structural section representing base course and subgrade modulus uncertainties of -25% and -50%. The $\Delta E_{SG} = \Delta E_{BC} = -25\%$ relative sensitivity results can be considered representative of uncertainty in base course and subgrade modulus due to an isotropic linear elastic characterization of each material. The $\Delta E_{BC} = \Delta E_{SG} = -50\%$

RELATIVE SENSITIVITY ANALYSIS SECTION 1

(ΔE_{SG} = -25%)

VARIABLE	T = 40°F(2) ($\bar{\varepsilon}$ = 25 μ"/", $\bar{N}_f$ = >5 x 10^6)		T = 60°F(2) ($\bar{\varepsilon}$ = 60 μ"/", $\bar{N}_f$ = >5 x 10^6)		T = 80°F ($\bar{\varepsilon}$ = 185 μ"/", $\bar{N}_f$ = 170 x 10^3)		T = 100°F ($\bar{\varepsilon}$ = 475 μ"/", $\bar{N}_f$ = 30 x 10^3)	
	$\frac{\Delta N_f}{\bar{N}_f}$ (%)	PERCENT OF TOTAL	$\frac{\Delta N_f}{\bar{N}_f}$ (%)	PERCENT OF TOTAL	$\frac{\Delta N_f}{\bar{N}_f}$ (%)	PERCENT OF TOTAL	$\frac{\Delta N_f}{\bar{N}_f}$ (%)	PERCENT OF TOTAL
ΔE_{AC}(1) (varies)	0	0	0	0	41	20	31	19
ΔT (+ 1°F)	0	0	0	0	24	12	0	0
Δt_{AC} (-.25 in.)	0	0	0	0	12	6	13	8
ΔN_f (-1 std. error)	0	0	0	0	36	17	36	21
ΔE_{SG} (-25%)	0	0	0	0	19	9	20	12
ΔE_{BC} (---)	---	---	---	---	---	---	---	---
ΔAV (+2%)	0	0	0	0	59	29	47	28
$\Delta \nu_{AC}$ (-.1)	0	0	0	0	15	7	10	6
$\Delta \nu_{BC}$ (+.1)	---	---	---	---	---	---	---	---
$\Delta \nu_{SG}$ (+.1)	0	0	0	0	0	0	10	6
Total	0	0	0	0	206	100	167	100

(1) ΔE_{AC}= -2% at T = 40°F, ΔE_{AC} = -10% at 60°F, ΔE_{AC} = -20% at 80°F, ΔE_{AC} = -35% at T = 100°F.

(2) No fatigue damage for strains below 70 μ"/".

TABLE 15

RELATIVE SENSITIVITY ANALYSIS SECTION 1

(ΔE_{SG} = -50%)

	T = 40°F (2) ($\bar{\varepsilon}$ = 25 μ"/", $\bar{N}_f$ = >5 x 10^6)		T = 60°F (2) ($\bar{\varepsilon}$ = 60 μ"/", $\bar{N}_f$ = >5 x 10^6)		T = 80°F ($\bar{\varepsilon}$ = 185 μ"/", $\bar{N}_f$ = 170 x 10^3)		T = 100°F ($\bar{\varepsilon}$ = 475 μ"/", $\bar{N}_f$ = 30 x 10^3)	
VARIABLE	$\frac{\Delta N_f}{\bar{N}_f}$ (%)	PERCENT OF TOTAL	$\frac{\Delta N_f}{\bar{N}_f}$ (%)	PERCENT OF TOTAL	$\frac{\Delta N_f}{\bar{N}_f}$ (%)	PERCENT OF TOTAL	$\frac{\Delta N_f}{\bar{N}_f}$ (%)	PERCENT OF TOTAL
ΔE_{AC} (1) (varies)	0	0	0	0	41	19	31	17
ΔT (+ 1°F)	0	0	0	0	24	11	0	0
Δt_{AC} (-.25 in.)	0	0	0	0	12	6	13	7
ΔN_f (-1 std. error)	0	0	0	0	36	17	36	19
ΔE_{SG} (-50%)	0	0	0	0	29	13	41	22
ΔE_{BC} (---)	---	---	---	---	---	---	---	---
ΔAV (+2%)	0	0	0	0	59	27	47	25
$\Delta \nu_{AC}$ (-.1)	0	0	0	0	15	7	10	5
$\Delta \nu_{BC}$ (+.1)	---	---	---	---	---	---	---	---
$\Delta \nu_{SG}$ (+.1)	0	0	0	0	0	0	10	5
Total	0	0	0	0	216	100	188	100

(1) ΔE_{AC} = -2% at T = 40°F, ΔE_{AC} = -10% at 60°F, ΔE_{AC} = -20% at 80°F, ΔE_{AC} = -35% at T = 100°F.

(2) No fatigue damage for strains below 70 μ"/".

TABLE 16

RELATIVE SENSITIVITY ANALYSIS SECTION 2

($\Delta E_{BC} = \Delta E_{SG} = -25\%$)

PARAMETER	T = 40°F (2) ($\bar{\varepsilon}$ = 50 μ"/", $\bar{N}_f$ = >5 x 10^6)		T = 60°F ($\bar{\varepsilon}$ = 105 μ"/", $\bar{N}_f$ = 740 x 10^3)		T = 80°F ($\bar{\varepsilon}$ = 300 μ"/", $\bar{N}_f$ = 36 x 10^3)		T = 100°F ($\bar{\varepsilon}$ = 635 μ"/", $\bar{N}_f$ = 14 x 10^3)	
	$\frac{\Delta N_f}{\bar{N}_f}$ (%)	PERCENT OF TOTAL	$\frac{\Delta N_f}{\bar{N}_f}$ (%)	PERCENT OF TOTAL	$\frac{\Delta N_f}{\bar{N}_f}$ (%)	PERCENT OF TOTAL	$\frac{\Delta N_f}{\bar{N}_f}$ (%)	PERCENT OF TOTAL
ΔE_{AC} (1) (varies)	0	0	30	12	22	13	7	4
ΔT (+ 1°F)	0	0	19	8	8	4	14	8
Δt_{AC} (-.25 in.)	0	0	24	10	11	6	14	8
ΔN_f (-1 std. error)	0	0	36	14	36	21	36	21
ΔE_{SG} (-25%)	0	0	21	8	10	6	9	5
ΔE_{BC} (-25%)	0	0	18	7	17	10	27	16
ΔAV (+2%)	0	0	69	27	47	27	43	25
$\Delta \nu_{AC}$ (-.1)	0	0	16	6	14	8	4	2
$\Delta \nu_{BC}$ (+.1)	0	0	11	4	6	3	11	7
$\Delta \nu_{SG}$ (+.1)	0	0	11	4	4	2	4	2
Total	0	0	255	100	175	100	169	100

(1) ΔE_{AC}= -2% at T = 40°F, ΔE_{AC} = -10% at 60°F, ΔE_{AC} = -20% at 80°F, ΔE_{AC} = -35% at T = 100°F.

(2) No fatigue damage for strains below 70 μ"/".

TABLE 17

RELATIVE SENSITIVITY ANALYSIS SECTION 2

($\Delta E_{BC} = \Delta E_{SG} = -50\%$)

	T = 40°F(2) ($\bar{\epsilon}$ = 50 μ"/", $\bar{N}_f$ = >5 x 10^6)		T = 60°F ($\bar{\epsilon}$ = 105 μ"/", $\bar{N}_f$ = 740 x 10^3)		T = 80°F ($\bar{\epsilon}$ = 300 μ"/", $\bar{N}_f$ = 36 x 10^3)		T = 100°F ($\bar{\epsilon}$ = 635 μ"/", $\bar{N}_f$ = 14 x 10^3)	
VARIABLE	$\frac{\Delta N_f}{\bar{N}_f}$ (%)	PERCENT OF TOTAL	$\frac{\Delta N_f}{\bar{N}_f}$ (%)	PERCENT OF TOTAL	$\frac{\Delta N_f}{\bar{N}_f}$ (%)	PERCENT OF TOTAL	$\frac{\Delta N_f}{\bar{N}_f}$ (%)	PERCENT OF TOTAL
ΔE_{AC} (1) (varies)	0	0	30	11	22	11	7	3
ΔT (+ 1°F)	0	0	19	7	8	4	14	7
Δt_{AC} (-.25 in.)	0	0	24	9	11	5	14	7
ΔN_f (-1 std. error)	0	0	36	13	36	18	36	18
ΔE_{SG} (-50%)	0	0	31	11	23	11	17	8
ΔE_{BC} (-50%)	0	0	28	10	32	16	51	26
ΔAV (+2%)	0	0	69	25	47	23	43	21
$\Delta \nu_{AC}$ (-.1)	0	0	16	6	14	7	4	2
$\Delta \nu_{BC}$ (+.1)	0	0	11	4	6	3	11	6
$\Delta \nu_{SG}$ (+.1)	0	0	11	4	4	2	4	2
Total	0	0	275	100	203	100	201	100

(1) ΔE_{AC} = -2% at T = 40°F, ΔE_{AC} = -10% at 60°F, ΔE_{AC} = -20% at 80°F, ΔE_{AC} = -35% at T = 100°F.

(2) No fatigue damage for strains below 70 μ"/".

TABLE 18

RELATIVE SENSITIVITY ANALYSIS SECTION 3

($\Delta E_{BC} = \Delta E_{SG} = -25\%$)

	T = 40°F ($\bar{\varepsilon}$ = 140 μ"/", $\bar{N}_f$ = 160 x 10^3)		T = 60°F ($\bar{\varepsilon}$ = 255 μ"/", $\bar{N}_f$ = 16.5 x 10^3)		T = 80°F(2) ($\bar{\varepsilon}$ = -----, $\bar{N}_f$ = -----)		T = 100°F(2) ($\bar{\varepsilon}$ = -----, $\bar{N}_f$ = -----)	
VARIABLE	$\frac{\Delta N_f}{\bar{N}_f}$ (%)	PERCENT OF TOTAL	$\frac{\Delta N_f}{\bar{N}_f}$ (%)	PERCENT OF TOTAL	$\frac{\Delta N_f}{\bar{N}_f}$ (%)	PERCENT OF TOTAL	$\frac{\Delta N_f}{\bar{N}_f}$ (%)	PERCENT OF TOTAL
ΔE_{AC}(1) (varies)	4	3	9	6	---	---	---	---
ΔT (+ 1°F)	0	0	3	2	---	---	---	---
Δt_{AC} (-.25 in.)	25	15	15	10	---	---	---	---
ΔN_f (-1 std. error)	36	23	36	24	---	---	---	---
ΔE_{SG} (-25%)	3	2	2	1	---	---	---	---
ΔE_{BC} (-25%)	11	7	20	13	---	---	---	---
ΔAV (+2%)	64	40	54	36	---	---	---	---
$\Delta \nu_{AC}$ (-.1)	16	10	12	8	---	---	---	---
$\Delta \nu_{BC}$ (+.1)	0	0	0	0	---	---	---	---
$\Delta \nu_{SG}$ (+.1)	0	0	0	0	---	---	---	---
Total	159	100	151	100	---	---	---	---

(1) ΔE_{AC} = -2% at T = 40°F, ΔE_{AC} = -10% at 60°F, ΔE_{AC} = -20% at 80°F, ΔE_{AC} = -35% at T = 100°F.

(2) Definition of fatigue life variations exceed defined range of fatigue curves.

TABLE 19

RELATIVE SENSITIVITY ANALYSIS SECTION 3

($\Delta E_{BC} = \Delta E_{SG} = -50\%$)

	T = 40°F ($\bar{\varepsilon}$ = 140 μ"/", $\bar{N}_f$ = 160 x 10^3)		T = 60°F ($\bar{\varepsilon}$ = 225 μ"/", $\bar{N}_f$ = 16.5 x 10^3)		T = 80°F(2) ($\bar{\varepsilon}$ = -----, $\bar{N}_f$ = -----)		T = 100°F(2) ($\bar{\varepsilon}$ = -----, $\bar{N}_f$ = -----)	
VARIABLE	$\frac{\Delta N_f}{\bar{N}_f}$ (%)	PERCENT OF TOTAL	$\frac{\Delta N_f}{\bar{N}_f}$ (%)	PERCENT OF TOTAL	$\frac{\Delta N_f}{\bar{N}_f}$ (%)	PERCENT OF TOTAL	$\frac{\Delta N_f}{\bar{N}_f}$ (%)	PERCENT OF TOTAL
ΔE_{AC} (1) (varies)	4	2	9	5	---	---	---	---
ΔT (+ 1°F)	0	0	3	2	---	---	---	---
Δt_{AC} (-.25 in.)	25	13	15	8	---	---	---	---
ΔN_f (-1 std. error)	36	19	36	20	---	---	---	---
ΔE_{SG} (-50%)	14	7	12	6	---	---	---	---
ΔE_{BC} (-50%)	34	18	43	23	---	---	---	---
ΔAV (+2%)	64	33	54	29	---	---	---	---
$\Delta \nu_{AC}$ (-.1)	16	8	12	7	---	---	---	---
$\Delta \nu_{BC}$ (+.1)	0	0	0	0	---	---	---	---
$\Delta \nu_{SG}$ (+.1)	0	0	0	0	---	---	---	---
Total	193	100	184	100	---	---	---	---

(1) ΔE_{AC} = -2% at T = 40°F, ΔE_{AC} = -10% at 60°F, ΔE_{AC} = -20% at 80°F, ΔE_{AC} = -35% at T = 100°F.

(2) Definition of fatigue life variations exceed defined range of fatigue curves.

relative sensitivity results are representative of uncertainty in base course and subgrade modulus due to both a linear elastic characterization and field variations.

Tables 14 through 19 show the percent variations in fatigue life from the average fatigue life due to each variable uncertainty level selected for the relative sensitivity analysis. The total of all percent variations in fatigue life was determined, and the percent each variable uncertainty level contributed to the total was calculated. The percent of the total uncertainty for each variable is the value of interest when comparing the relative effect of each variable on the prediction of fatigue life. These values show the relative sensitivity of fatigue life prediction due to uncertainty in each variable.

The relative sensitivity results shown in Tables 14 through 19 are plotted in Figures 35 through 37. These figures summarize the final results obtained from the sensitivity analysis.

Discussion of Relative Sensitivity Results

The relative sensitivity results were derived for constitutive material characterization errors representative of those utilizing isotropic linear elastic theory. However, the temperature dependence of asphalt concrete modulus was recognized and considered. Therefore, the uncertainties induced in fatigue life predictions due to variations in the elastic parameters considered here reflect characterization uncertainties caused by anisotropy and/or nonlinearities and experimental error rather than the difference in viscoelastic or pseudo-elastic characterizations.

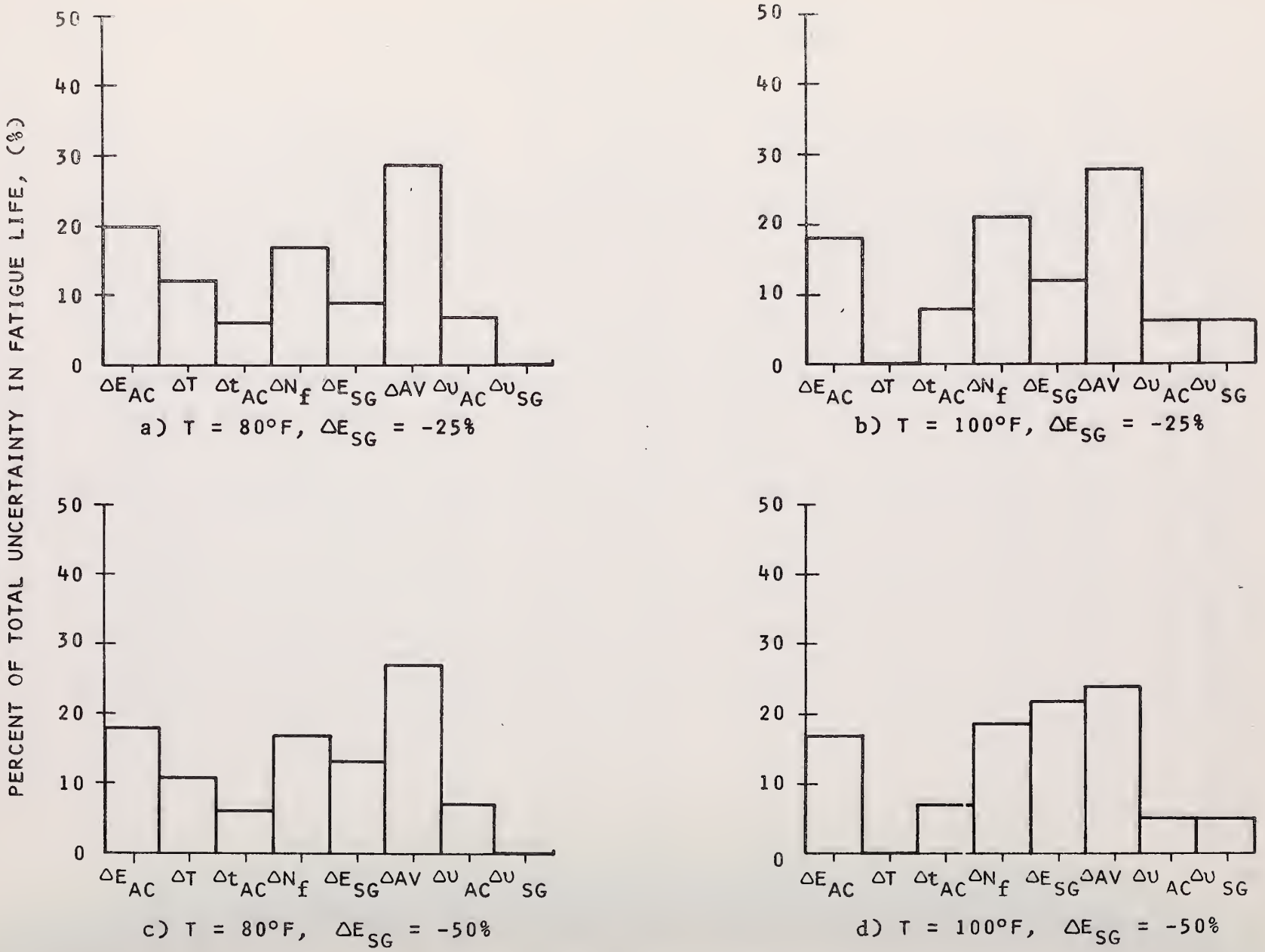

FIGURE 35 - RELATIVE SENSITIVITY OF FATIGUE LIFE TO PARAMETER VARIATIONS FOR SECTION 1

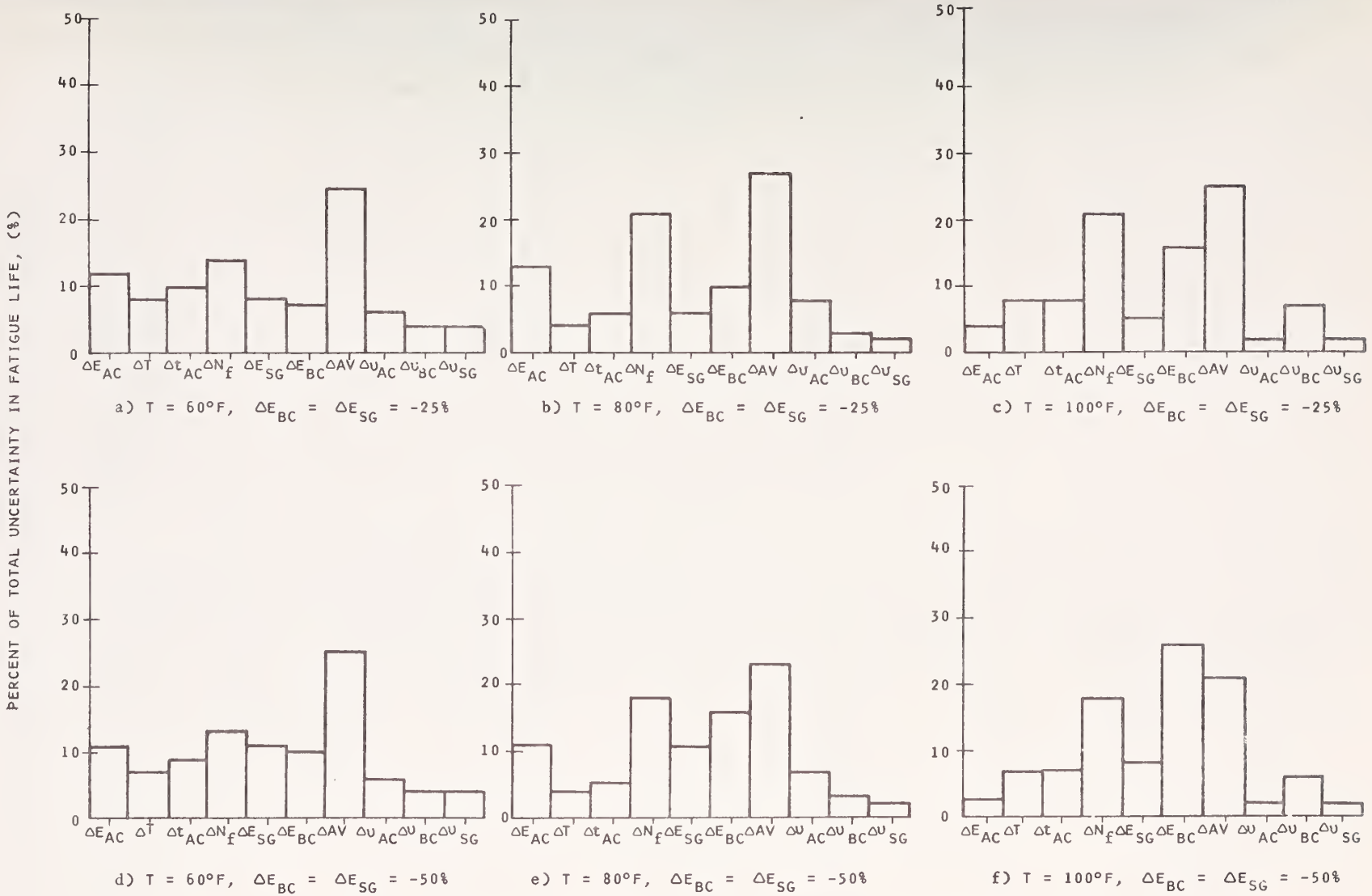

FIGURE 36 - RELSTIVE SENSITIVITY OF FATIGUE LIFE TO PARAMETER VARIATIONS FOR SECTION 2

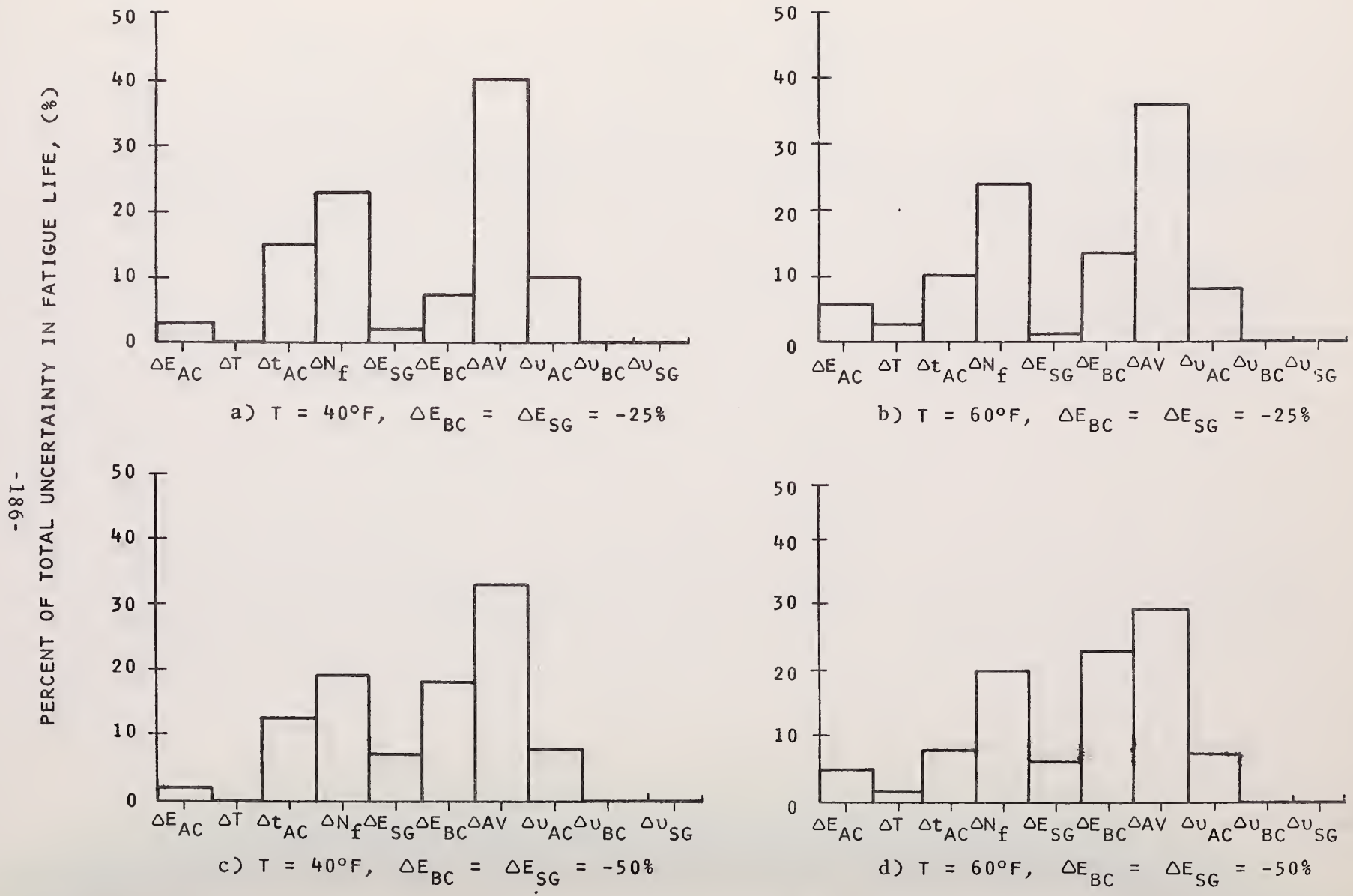

FIGURE 37 - RELATIVE SENSITIVITY OF FATIGUE LIFE TO PARAMETER VARIATIONS FOR SECTION 3

The relative sensitivity analysis was conducted for several macro-temperature levels for each structural section and represents climates ranging from cold to hot. The variation of temperature about some average value influences the interpretation of the relative sensitivity results since a Miner's hypothesis for cumulative fatigue damage is normally used when more than one temperature level is considered.

The fatigue life at a particular strain level increases with temperature increase. However, since the asphalt concrete modulus decreases with increase in temperature, the maximum tensile strain in the asphalt concrete increases. The net results of a temperature increase for pavement sections analyzed is that the effect of the higher strain level dominates and results in a smaller fatigue life. This is according to the criteria developed by Monismith and his associates. It is recognized that there are some fatigue criteria which would not give this result. Since the volume of traffic is normally considered uniformly distributed throughout the year and Miner's cumulative damage hypothesis is used, the majority of the fatigue damage occurs during the warmer months of the year. Therefore, the relative sensitivity of fatigue life to variable uncertainty at the higher macro-temperature levels is more significant than at lower macro-temperature levels for mixed temperature environments.

Note that uncertainty in fatigue life induced by uncertainty of in-situ air voids, asphalt concrete thickness, and fatigue criteria definition can be considered independent of the constitutive parameter uncertainties because of the manner in which each was considered. The

uncertainty induced by these three parameters would exist even if each material was perfectly characterized by linear isotropic elasticity. Therefore, the combined uncertainty due to these three parameters can be used as a measure of the relative significance of constitutive parameter uncertainty.

The relative sensitivity results shown in Figures 35, 36, and 37 provide a quantitative measure of the relative importance of uncertainty induced by non-ideal behavior and experimental errors in materials characterization on fatigue life prediction. Furthermore, the relative sensitivity results can be utilized to select the areas of pavement research which could prove most beneficial in improving our ability to reduce fatigue failure of pavements. Better control or definition of parameters which induce large uncertainties in fatigue life would result in substantial reduction in highway maintenance costs.

With one exception, variation in the air void content of the asphalt concrete was the single most important parameter inducing uncertainty in the fatigue life of a pavement. It should be recognized that influence of air voids was examined through its effect on both the modulus and fatigue characteristics of the asphalt concrete. This dual influence emphasizes the need for better construction control techniques of asphalt concrete air void content.

The results also indicate that generally the second most important parameter variation inducing uncertainty in the fatigue life is that associated with the definition of the fatigue criteria itself. Although much effort has

been spent in developing the currently available fatigue criteria, it appears further work could greatly improve the ability to predict and, therefore, control the fatigue failure of flexible pavements.

The variability in the thickness of asphalt concrete surfacing due to construction practices has a relatively minor influence on the total uncertainty of fatigue life for pavement sections similar to Sections 1 and 2. However, for pavements with thin asphalt concrete surfaces (Section 3) the control of thickness is more critical.

The temperature parameter variation utilized for the relative sensitivity analysis was selected, predicated on accurate consideration of the temperature environment currently used in the more recently developed pavement design and analysis methods. The effect of temperature variation was relatively minor for all cases. Overall, the temperature regime itself has more influence on the fatigue life than any parameter considered in this analysis. This fact is not directly evident from the relative sensitivity analysis because the influence of the temperature regime was considered utilizing several macro-temperature levels. In fact, the two levels (micro and macro) of the temperature parameter utilized in this analysis were motivated by this very fact.

The influence of water content and density variations in the base course and subgrade is revealed by comparison of the upper and lower (-25% and -50%) modular variation relative sensitivity results shown in each of Figures 35, 36, and 37. Examination of these results reveals that the importance of water content and density variations

increases as temperature increases for each structural section. This occurs because the base course and subgrade contribute more to the total strength of the structural section as the temperature increases and the asphalt concrete contribution decreases. Thus, induced base course and subgrade modular variations at higher temperatures become more significant. It appears that measurable improvements in fatigue life could be gained from control and consideration of water content and density variations in the base course and subgrade for pavements in hot climates.

The effect of variations in the asphalt concrete modulus parameter induced by deviations from ideal isotropic linear elastic behavior and experimental errors are more important for full depth sections (Section 1) than for thin-surfaced sections (Section 3). (The uncertainty induced in fatigue life is of major significance for Section 1, but of almost no significance for Section 3. The effect on fatigue life for Section 2 is intermediate except at 100°F where it is of no practical significance.) Generally, the effect of asphalt concrete modular variations decreases with increase in temperature even though the percent variation in modulus used for the relative sensitivity analysis (characterization variations) increased with temperature.

The influence of variation of the base course modulus parameter induced by isotropic linear elastic characterization errors (-25% variation) was of similar magnitude to that associated with asphalt concrete modulus for the lower temperatures for Section 2 and of greater significance at both temperatures for Section 3.

The effect of variation in the subgrade modulus parameter induced by isotropic linear elastic characterization errors (-25% variation) was generally of minor significance. The effect was of most importance for the full depth section (Section 1) and was of practically no significance for Section 3.

The influence of variations in the Poisson's ratio parameter for each material was only of minor significance for all structural sections. In some cases, Poisson's ratio variations showed no measurable effect on fatigue life uncertainty.

It should be recognized that all the sensitivity results were based on only the fatigue mode of pavement distress. A pavement must be designed for all modes of pavement distress to insure that it provides adequate performance. For example, this sensitivity analysis has shown the single most important parameter uncertainty contributing to the total uncertainty in fatigue life was control of air voids in the field. The air void content uncertainty above a specified level can be reduced by increasing the asphalt content of the mix, or by increasing the density. However, this may result in instability of the mix, unacceptable plastic deformations, and hazardous skid resistance conditions due to flushing of the asphalt. Therefore, all modes of pavement distress need to be considered for a complete definition of an adequate characterization of each material.

CONCLUSIONS

The results of the relative sensitivity analysis indicate the following conclusions concerning the improvement of prediction and control of flexible pavement fatigue life:

1. The predominant parameter variation causing uncertainty in fatigue life is that associated with construction control of air voids in the asphalt concrete.

2. A more accurate definition of the fatigue failure criteria for asphalt concrete would be more beneficial than improvement of the constitutive material characterization beyond isotropic linear elasticity.

3. The uncertainty associated with characterization of pavement materials by isotropic linear elasticity can contribute significant uncertainty to the prediction of fatigue life. However, this induced uncertainty in fatigue life is of less significance than that induced by field control of air voids or fatigue criteria definition.

    a) Improved characterization of asphalt concrete would be most beneficial for full depth and thick asphalt concrete surface pavements.

    b) More accurate characterization of untreated granular base course material would also be advantageous, especially for pavements located in hot climates.

c) An isotropic linear elastic characterization of subgrade is adequate if the characterization is performed under stress levels representative of in-service subgrades.

4. Consideration of variations in water content and densities of in-situ base course and subgrade materials would be beneficial for pavements located in hot climates.

5. Within the existing techniques for considering temperature in the analysis, the ability to predict the temperature is sufficiently accurate.

6. Thickness control of the asphalt concrete layer during construction is presently sufficiently accurate.

It should be recognized that the adequacy of a material characterization is a dynamic phenomena. As our ability to describe and control the effects of other parameters influencing the fatigue life of flexible pavements improves, presently adequate characterizations may become inadequate.

A P P E N D I X B

EVALUATION OF BONDED STRAIN GAGE MEASUREMENTS

The epoxy used to bond strain gages to test specimens should have approximately the same stiffness as the test specimens to insure accurate strain measurements. However, most epoxies commonly used to bond strain gages are stiffer than asphalt-treated granular base course material (ATB), especially at high temperatures. The effect of the epoxy on strain measurements is dependent on the strain level and type of test performed. For dynamic tests the effect of differences in stiffnesses of the specimen and epoxy are probably insignificant. However, for creep testing the effect may be more significant. Since creep tests on ATB specimens at temperatures up to 100 °F were planned, it was felt that an evaluation of the accuracy of bonded strain gage measurements was necessary.

An ATB specimen was instrumented with two sets of axial strain gages. One set was bonded with a trial epoxy and the other set with EPY-150 epoxy. EPY-150 has often been used by MR&D in the past; however, there was some evidence suggesting that this epoxy was too stiff for creep testing strain measurements at 100 °F. The trial epoxy was much weaker than EPY-150, and it was felt that its modulus would more closely match that of the ATB specimens at all test temperatures. In addition to the two sets of axial strain gage measurements, platen to platen displacement measurements were made with an LVDT.

Axial strains calculated from platen to platen LVDT measurements are inaccurate because of compression within the test apparatus upon the application of load and the effect of non-uniform stress field near the ends of the specimens. However, inaccuracies due to test apparatus compression upon load application can be approximately compensated for by subtracting the immediate axial deformation from all subsequent values. This technique was applied to all LVDT platen to platen measurements before calculating axial strain values.

Creep tests were performed at three temperatures: 40, 70, and 100°F. The axial strains measured with the two pairs of bonded strain gages over a two-inch length near the mid-height of the specimen and axial strains calculated from platen to platen axial deformation measurements were compared.

The axial strains calculated from platen-to platen deformation measurements were somewhat greater than those measured with strain gages. Moore, et. al. (1969) did a similar evaluation of strain measurement techniques on a material with a modulus similar to ATB at 70°F, and also found that axial strains calculated from platen to platen measurements were higher than those from strain gage measurements.

The difference between the two measurements can probably be attributed to stress and strain non-uniformities caused by end restraint effects and unevenness of contacts between the specimen and end plates.

The results of primary interest from this study are the bonded strain gage measurements. The two axial strain measurements made with strain gages bonded with two different epoxies of widely different stiffnesses yielded almost identical results at all three test temperatures. The trial epoxy stiffness was much less than that of the EPY-150 and was similar to the ATB stiffness at all three temperatures. Therefore, it could be concluded that the stiffness of the EPY-150 had no effect on the strain measurements.

Strain measurement near the mid-height of the specimens essentially eliminates the effects of non-uniform strain field near the ends of the specimens. Therefore, strain gages bonded with EPY-150 epoxy near the mid-height of the specimen could be used with confidence in creep testing planned for ATB specimens.

A P P E N D I X C

DERIVATION OF EQUATIONS (1) AND (2), PAGES 77 AND 78

For an isotropic linear elastic material

$$\left.\begin{aligned} \varepsilon_{zz} &= \frac{1}{E}\left[\sigma_{zz} - \nu\,(\sigma_{xx} + \sigma_{yy})\right] \\ \varepsilon_{yy} &= \frac{1}{E}\left[\sigma_{yy} - \nu\,(\sigma_{xx} + \sigma_{zz})\right] \\ \varepsilon_{xx} &= \frac{1}{E}\left[\sigma_{xx} - \nu\,(\sigma_{yy} + \sigma_{zz})\right] \end{aligned}\right\} \qquad (1)$$

For triaxial conditions when $\sigma_{xx} = \sigma_{yy} = \sigma_r$, Equation (1) can be written as

$$\left.\begin{aligned} \varepsilon_{zz} &= \frac{1}{E}\left[\sigma_{zz} - 2\nu\,\sigma_{rr}\right] \\ \varepsilon_{rr} &= \frac{1}{E}\left[\sigma_{rr} - \nu(\sigma_{zz} + \sigma_{rr})\right] \\ \varepsilon_{\theta\theta} &= \frac{1}{E}\left[\sigma_{rr} - \nu(\sigma_{zz} + \sigma_{rr})\right] \end{aligned}\right\} \qquad (2)$$

From first of Equation (2)

$$\frac{1}{E} = \frac{\varepsilon_{zz}}{\sigma_{zz} - 2\nu\,\sigma_{rr}} \qquad (3)$$

Eliminating E from the first 2 of Equation (2) we get

$$\nu = \frac{\varepsilon_{rr}\,\sigma_{zz} - \varepsilon_{zz}\,\sigma_{rr}}{2\varepsilon_{rr}\,\sigma_{rr} - \varepsilon_{zz}\,(\sigma_{zz} + \sigma_{rr})} \qquad (4)$$

Equations (3) and (4) can be used to get Young's modulus and Poisson's ratio. Analogous equations can be written for Modular Creep Compliance and Poisson's ratio for linear viscoelastic materials. In this case both of these are time dependent.

$$\Psi_{EZ}(t) = \frac{\varepsilon_{zz}\,(t)}{\sigma_{zz} - 2\nu(t)\quad\sigma_{rr}} \qquad (5)$$

(Identical to Equation (1), page 77.)

and

$$\nu(t) = \frac{\varepsilon_{rr}(t)\quad\sigma_{zz} - \varepsilon_{zz}(t)\quad\sigma_{rr}}{2\varepsilon_{rr}(t)\quad\sigma_{rr} - \varepsilon_{zz}(t)\quad\{\sigma_{zz} + \sigma_{rr}\}} \qquad (6)$$

(Identical to Equation (2), page 78, recognizing that $\varepsilon_{rr} = \varepsilon_{\theta\theta}$)

REFERENCES

Barber, E. S. and G. P. Steffens (1958) "Pore Pressures in Base Courses," HRB, Vol. 37.

Barksdale, R. D. (1972 b), "Laboratory Evaluation of Rutting in Base Course Materials," 3rd Intl. Conf. on the Structural Design of Asphalt Pavements.

Barksdale, R. D. (1972 a), "Repeated Load Test Evaluation of Base Course Materials," GHD Research Project No. 7002, Georgia Institute of Technology.

Barksdale, R. D. (1971), "Compressive Stress Pulse Times in Flexible Pavements for Use in Dynamic Testing," HRR No. 345.

Brown, S. F. and P. S. Pell (1967), "An Experimental Investigation of Stresses, Strains, and Deflections in a Layered Pavement Structure Subjected to Dynamic Loads," 2nd Intl. Conf. on Structural Design of Asphalt Pavements.

Coffman, B. S., D. G. Kraft, and J. Tamayo (1964), "A Comparison of Calculated and Measured Deflections for the AASHO Test Road," AAPT.

Coffman, B. S. (1967), "Pavement Deflections from Laboratory Tests and Layer Theory," 2nd Intl. Conf. on Structural Design of Asphalt Pavements.

Davies, J. R. and J. A. Stewart (1969), "An Investigation of the Strength Properties of Sand-Emulsified Asphalt Mixtures," Department of Highways, Ontario, RR 146.

Deacon, J. H. (1965), "Fatigue of Asphalt Concrete," Ph.D. Thesis, University of California, Berkeley.

Dorman, G. M. and C. T. Metcalf (1965), "Design Curves for Flexible Pavements Based on Layered System Theory," HRR 71.

Duncan, J. M. and C-Y Chang (1970), "Nonlinear Analysis of Stress and Strain in Soils," JSMFD, SM5.

Dunlap, W. A. (1963), "A Report on a Mathematical Model Describing the Deformation Characteristics of Granular Materials," Technical Report No. 1, Project 2-8-62-27, Texas Transportation Institute.

Epps, J. A. (1968), "The Influence of Mixture Variables on the Fatigue and Tensile Properties of Asphalt Concrete Mixtures," Ph.D. Thesis, University of California, Berkeley.

Finn, F. N., R. G. Hicks, W. J. Kari, and L. D. Coyne (1968), "Design of Emulsified Asphalt Treated Bases," HRB.

Finn, F. N. (1970), "Observation of Distress in Full-Scale Pavements," HRB Special Report #126.

Granley, E. C. (1969), "Variations in Bituminous Construction," Quality Assurance in Highway Construction, Research and Development Report, BPR (R&D).

Haynes, J. G. and E. J. Yoder (1963), "Effects of Repeated Loading on Gravel and Crushed Stone Base Course Materials Used in the AASHO Road Test," HRR 39.

Heukelom, W. and A. J. G. Klomp (1962), "Dynamic Testing as a Means of Controlling Pavements During and After Construction," 1st Intl. Conf. on Structural Design of Asphalt Pavements.

Heukelom, W. and A. J. G. Klomp (1967), "Consideration of Calculated Strains at Various Depths in Connection with the Stability of Asphalt Pavements," 2nd Intl. Conf. on the Structural Design of Asphalt Pavements.

Hicks, R. G. (1970), "Factors Influencing the Resilient Properties of Granular Materials," Ph.D. Thesis, University of California, Berkeley.

Hicks, R. G. and F. N. Finn (1970), "Analysis of Results from the Dynamic Measurements Program on the San Diego Test Road," AAPT.

Highway Research Board (1962), "The AASHO Road Test, Report 2, Materials and Construction," Special Report 61B.

Highway Research Board (1962), "The AASHO Road Test, Report 5, Pavement Research," HRB Special Report 61E.

Holubec, I. (1969), "Cyclic Creep of Granular Materials," Department of Highways, Ontario, RR 147.

Kallas, B. F. and J. C. Riley (1967), "Mechanical Properties of Asphalt Pavement Materials," 2nd Intl. Conf. on Structural Design of Asphalt Pavements.

Kasianchuk, D. A. (1968), "Fatigue Considerations in the Design of Asphalt Concrete Pavements," Ph.D. Thesis, University of California, Berkeley.

Materials Research & Development (1972), "Characterization of Asphalt Concrete and Cement-Treated Granular Base Course," Final Report FH-11-7319, authored by K. Nair, W. S. Smith, and C-Y Chang.

Materials Research & Development, Inc. (1968), "Systems Approach to Pavement Design," Interim Report, NCHRP Project 1-10, authored by W. R. Hudson, F. N. Finn, F. G. McCullough, K. Nair, and B. A. Vallerga.

McLeod, N. W. (1953), "Some Basic Problems in Flexible-Pavement Design," HRB, Vol. 32.

Mitry, F. G. (1964), "Determination of the Modulus of Resilient Deformation of Untreated Base Course Materials," Ph.D. Thesis, University of California, Berkeley.

Monismith, C. L., J. A. Epps, D. A. Kasianchuk, and D. B. McLean (1970), "Asphalt Mixture Behavior in Repeated Flexure," Report No. TE-70-5, University of California, Berkeley.

Moore, W. M., G. Swift, and L. J. Milberger (1969), Deformation Measuring System for Repetitively Loaded Large Diameter Specimens of Granular Material," Research Report 99-4, Texas Transportation Institute, Texas A&M University.

Moore, W. M., et. al. (1970), "A Laboratory Study of the Relation of Stress to Strain for a Crushed Limestone Base Material," Research Report No. 99-5F, Texas Transportation Institute, Texas A&M University.

Morgan, J. R. (1966), "The Response of Granular Materials to Repeated Loading," 3rd Conf. of Australian Road Research Board, Part 2.

Nair, K. and C-Y Chang (1973), "Flexible Pavement Design and Management--Materials Characterization," NCHRP Report #140.

Ponce, V. M. and J. M. Bell (1971), "Shear Strength of Sand at Very Low Pressures," JSMFD, SM4.

Romain, J. E. (1969), "Rut Depth Prediction in Asphalt Pavements," Centre De Recherches Routieres, Research Report 150/JER/1969, Bruxelles.

Schmidt, R. J., L. E. Santucci, and L. D. Coyne (1973),"Performance Characteristics of Cement Modified Asphalt Emulsion Mixes," AAPT.

Seed, H. B., F. G. Mitry, C. L. Monismith, and C. K. Chan (1967), "Prediction of Flexible Pavement Deflections from Laboratory Repeated Load Tests," NCHRP Report 35.

Sherman, G. B. (1970), "In Situ Materials Variability" HRB Special Report #126.

Shifley, L. G. (1967), "The Influence of Subgrade Characteristics on the Transient Deflections of Asphalt Concrete Pavements," D. Eng. Thesis, University of California, Berkeley.

Shook, J. F. and Kallas, B. F. (1969), "Factors Influencing Dynamic Modulus of Asphalt Concrete," AAPT.

Terrel, R. L. (1967), "Factors Influencing the Resilient Characteristics of Asphalt Treated Aggregates," Ph.D. Thesis, University of California, Berkeley.

Terrel, R. L. and C. L. Monismith (1968), "Evaluation of Asphalt-Treated Base Course Materials," AAPT.

Terrel, R. L. and C. K. Wang (1971), "Early Curing Behavior of Cement Modified Asphalt Emulsion Mixtures," AAPT.

Thompson, O. O. (1969), "Evaluation of Flexible Pavement Behavior with Emphasis on the Behavior of Granular Layers," Ph.D. Thesis, University of Illinois.

Van Der Poel, C. (1954), "A General System Describing the Viscoelastic Properties of Bitumens and its Relation to Routine Test Data," Journal of Applied Chemistry, May.

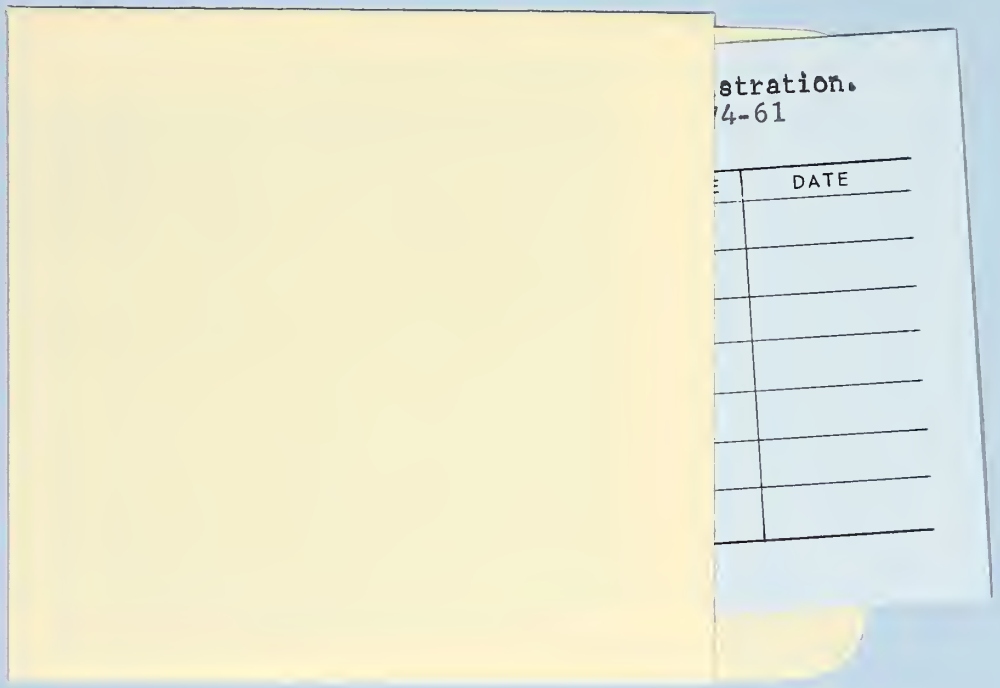
stration.
74-61
DATE